# THE EFFECT OF PHOSPHORYLATION ON OXYSTEROL-BINDING PROTEIN (OSBP) STEROL BINDING ACTIVITY

by

Carolyn-Ann Robinson

Submitted in partial fulfilment of the requirements
for the degree of Master of Science

at

Dalhousie University
Halifax, Nova Scotia
May 2011

DALHOUSIE UNIVERSITY

BIOCHEMISTRY AND MOLECULAR BIOLOGY

The undersigned hereby certify that they have read and recommend to the Faculty of Graduate Studies for acceptance a thesis entitled "THE EFFECT OF PHOSPHORYLATION ON OXYSTEROL-BINDING PROTEIN (OSBP) STEROL BINDING ACTIVITY" by Carolyn-Ann Robinson in partial fulfillment of the requirements for the degree of Master of Science.

Dated: May 10, 2011

Supervisor: _____

Readers: _____

_____

_____

DALHOUSIE UNIVERSITY

DATE: May, 10 2011

AUTHOR: Carolyn-Ann Robinson

TITLE: THE EFFECT OF PHOSPHORYLATION ON OXYSTEROL-BINDING PROTEIN (OSBP) STEROL BINDING ACTIVITY

DEPARTMENT OR SCHOOL: Department of Biochemistry and Molecular Biology

DEGREE: MSc CONVOCATION: October YEAR: 2011



_____

Signature of Author

## DEDICATION PAGE

I would like to dedicate this work to my mother, Anna Robinson, for her unending patience and continual support through every step of my life. She has always encouraged me and provided sound guidance and a positive attitude. I am truly grateful for everything she has given me because without her I would not have made it to where I am today.

## TABLE OF CONTENTS

# LIST OF TABLES

## LIST OF FIGURES

## ABSTRACT

Oxysterol binding protein (OSBP) binds 25-hydroxycholesterol (25OH) and cholesterol, which regulates PH and FFAT domain interaction with the Golgi apparatus and endoplasmic reticulum, respectively. Adjacent to these domains is a phosphorylated serine-rich motif (SRM, T379, S381, S384, S387, S388, S391) that we hypothesize controls sterol transport by OSBP. To test this, OSBP dephospho-mimics or phospho-mimics were expressed in CHO cells. Western blot analysis showed that the S381 is phosphorylated by PKA and is required for phosphorylation of down-stream serine residues. When expressed in OSBP-null CHO cells, there was no difference in the localization of the OSBP mutants, and all mutants restored SM synthesis in response to 25OH. Recombinant OSBP 5S→5E had increased cholesterol binding and extraction, and decreased cholesterol transfer to liposomes compared to OSBP. OSBP 5S→5E also bound VAP more efficiently. A model is proposed wherein SRM phosphorylation facilitates VAP association with the ER and increases cholesterol extraction.

## LIST OF ABBREVIATIONS AND SYMBOLS USED

| | |
|---|---|
| 7αOH | 7α-hydroxycholesterol |
| 7KC | 7-ketocholesterol |
| 22(R)OH | 22(R)-hydroxycholesterol |
| 24(S)OH | 24(S)-hydroxycholesterol |
| 25OH | 25-hydroxycholesterol |
| 27OH | 27-hydroxycholesterol |
| ABC | ATP-binding cassette |
| ACAT | acyl CoA: cholesterol acyltransferase |
| ARF | ATP-ribosylation factor |
| ATP | adenosine triphosphate |
| BA | bile acid |
| BSA | bovine serum albumin |
| cAMP | cyclic adenosine monophosphate |
| cDNA | complimentary DNA |
| CERT | ceramide transport protein |
| CHO | Chinese hamster ovary |
| CK | casein kinase |
| COP | coatamer protein |
| DC | dendritic cell |
| DHE | dehydroergosterol |
| DMEM | Dulbecco's modified eagle medium |

| | |
|---|---|
| ER | endoplasmic reticulum |
| ERC | endocytic recycling compartment |
| ERK | extracellular-signal regulated kinase |
| FCS | fetal calf serum |
| FFAT | two phenylalanines in an acidic tract |
| GAM | goat anti-mouse |
| GAP | GTPase-activating protein |
| GAR | goat anti-rabbit |
| GOLD | Golgi dynamics domain |
| GSK | glycogen synthase kinase |
| GST | glutathione S-transferase |
| HDL | high-density lipoprotein |
| HEK | human embryonic kidney |
| HePTP | haematopoietic tyrosine phosphatase |
| HMG CoA | 3-hydroxy-3-methylglurtaryl-coenzyme A |
| HRP | horseradish peroxidase |
| IFN | interferon |
| IFN-R | interferon receptor |
| LB | lysogeny broth |
| LC | liquid chromatography |
| LDL | low density lipoprotein |
| LDL-R | low density lipoprotein receptor |
| LPS | lipopolysaccharide |

| | |
|---|---|
| MAC | metal affinity chromatography |
| MAPK | mitogen-activated protein kinase |
| MS | mass spectrometry |
| N.A. | numerical aperture |
| NC | nitrocellulose |
| NPC | Niemann-Pick Type C |
| NT | non-targetting |
| OA | okadaic acid |
| OHD | OSBP homology domain |
| ORP | oxysterol-binding protein related protein |
| OSBP | oxysterol-binding protein |
| OSH | OSBP homologue |
| PAGE | polyacrylamide gel electrophoresis |
| PBS | phosphate buffered saline |
| PC | phosphatidylcholine |
| PDK | phosphoinositide-dependent kinase |
| PE | phosphatidylethanolamine |
| PH | pleckstrin homology |
| PI | phosphatidylinositol |
| PI-3,4-$P_2$ | phosphatidylinositol-3,4-bisphosphate |
| PI-3,5-$P_2$ | phosphatidylinositol-3,5-bisphosphate |
| PI-3,4,5-$P_3$ | phosphatidylinositol-3,4,5-triphosphate |
| PI-4-P | phosphatidylinositol-4-phosphate |

| | |
|---|---|
| PI-4,5-$P_2$ | phosphatidylinositol-4,5-bisphosphate |
| PIP | phosphatidylinositol-phosphate |
| PKA | protein kinase A |
| PKC | protein kinase C |
| PKD | protein kinase D |
| PM | plasma membrane |
| PP2A | protein phosphatase type 2A |
| PP2Cε | protein phosphatase 2Cε |
| PS | phosphatidylserine |
| RNA | ribonucleic acid |
| ROS | reactive oxygen species |
| S1P | site 1 protease |
| S2P | site 2 protease |
| SCAP | SREBP cleavage activating protein |
| SCP | sterol carrier protein |
| SCS2 | suppressor of choline sensitivity 2 |
| SDS | sodium dodecyl sulphate |
| shRNA | short-hairpin RNA |
| SM | sphingomyelin |
| SMase | sphingomyelinase |
| SRE | sterol regulatory element |
| SREBP | sterol regulatory element binding protein |
| SRM | serine-rich motif |

| | |
|---|---|
| StAR | steroidogenic acute regulatory protein |
| START | StAR-related lipid transfer |
| TAG | triacylglycerol |
| TBS | tris-buffered saline |
| TLC | thin layer chromatography |
| TLR | toll-like receptor |
| TM | transmembrane |
| VAMP | vesicle-associated membrane protein |
| VAP | VAMP-associated protein |
| VLDL | very low-density lipoprotein |

## ACKNOWLEDGEMENTS

I would like to acknowledge the individuals who have helped with the development and outcome of this project over the course of my Masters degree, without them this work would not have been possible. I would first like to thank my supervisory committee, Drs. Barbara Karten and Roger McLeod for their valued insight and sound advice on my research. I am thankful to Robert Zwicker for his exceptional technical assistance and for always being an excellent sounding board for research ideas. I am grateful to Elden Rowland for all of his technical expertise and knowledge regarding mass spectrometry. I would also like to thank Stephen Whitefield for his assistance on using confocal microscopy. Especially, I would like to thank the Ridgway group and the rest of the ARC for their valuable input on my research, troubleshooting ideas, and for providing a wonderful work environment.

This research was financially supported by grants from the Canadian Institute for Health Research (CIHR) and the Isaac Walton Killam Hospital (IWK).

Finally, I would like to thank my supervisor, Dr. Neale Ridgway, for providing me with a project and lab environment where I could develop as a young researcher. I am appreciative of all of the input I have received over the course of my degree and the challenges that I faced along the way that pushed me to a greater understanding of scientific research.

# CHAPTER 1 INTRODUCTION

## 1.1 Cholesterol

Cholesterol has a planar 27-carbon tetracyclic structure composed of one 5-carbon and three 6-carbon rings, a 3-hydroxyl group and an 8-carbon branched alkyl side chain [1]. Cholesterol is an integral structural component of membranes and an important factor in lipid metabolism and cell signalling. In mammalian membranes, cholesterol preferentially associates with the saturated acyl chains of sphingolipids such as sphingomyelin (SM). The association of cholesterol with membranes comprised of unsaturated fatty acyl chain phospholipids confers rigidity to the membrane while the association of cholesterol with membranes rich in saturated acyl chain lipids confers a more fluid state to the membrane [2]. The cholesterol ring structure aligns with the saturated fatty acyl chains and the hydroxyl group is next to the phospholipid head group, which confers a liquid-ordered domain to disordered membranes [1]. Cholesterol and SM are also involved in the formation of microdomains, sometimes referred to as "lipid rafts", defined as nanoscale dynamic lateral domains that may serve as signalling platforms for proteins within membranes [3]. Cholesterol and SM microdomains have been implicated in Src-family kinase signalling. Src-family kinases are myristoylated and palmitoylated making them preferentially associate with liquid ordered domains containing cholesterol and SM [4]. When cells are depleted of cholesterol through methyl-β-cyclodextrin, Src-family kinases do not associate with the detergent-resistant membranes/lipid rafts and signalling by these kinases is blocked [5]. Lipid rafts provide an important signalling environment for membrane proteins and cholesterol is integral to the composition of these microdomains.

Besides its structural importance, cholesterol has metabolic functions as a precursor in bile acid (BA) synthesis, lipoprotein packaging and secretion, and steroid hormone synthesis. A defect in cholesterol homeostasis is implicated in a number of pathological conditions such as neurological disorders (Alzheimer's and Parkinsons), atherosclerosis, Tangiers disease and lysosomal lipid storage disorders [2,6]. Sterol transport is important in the maintenance of cholesterol content of organelles for proper signalling. Furthermore sterol transport is integral in the regulation of cholesterol synthesis and uptake pathways to keep the intracellular cholesterol content within a narrow range and prevent pathologies associated with defective cholesterol homeostasis. The following study focuses on the role of protein-mediated sterol transport in cholesterol homeostasis responses.

## 1.2 Oxysterols

Oxysterols are a diverse class of molecules involved in lipid metabolism and cell signalling pathways that are obtained from dietary sources or generated through the oxidation of cholesterol [7]. Auto-oxidation or enzymatic peroxidation of cholesterol decreases half-life and increases hydrophilicity allowing it to be exported from the cell more readily [7]. Oxysterols are present in trace amounts in comparison to cholesterol, which is estimated to be 1000-fold more abundant [8]. There are many different oxysterols that act on a wide variety of signalling pathways. Primarily, oxysterols act to regulate gene expression for lipid biosynthesis and reverse cholesterol transport [9-11], and are intermediates in BA synthesis [12].

Oxysterols are formed through auto-oxidation reactions between cholesterol and reactive oxygen species (ROS) and enzymatically by cytochrome P450 monooxygenases

with the substrate oxygen and cofactor NADPH [7,13]. The exception to this is 25-hydroxycholesterol (25OH) which is formed by a microsomal enzyme with a di-iron centre [14]. The enzymes that catalyze the formation of oxysterols are tissue specific, which generates tissue specific oxysterol patterns. Cholesterol 7α-hydroxylase is a liver enzyme that converts cholesterol to 7α-hydroxycholesterol (7αOH) for incorporation into BA for nutrient absorption [15]. 27-hydroxycholesterol (27OH) can also be converted to BA by microsomal oxysterol 7α-hydroxylase 1 (CYP7B1) in extra-hepatic tissues [16]. 24-Hydroxylase converts cholesterol to 24(S)-hydroxycholesterol (24(S)OH) in the endoplasmic reticulum (ER) of neurons in the brain [17]. The conversion of cholesterol to 24(S)OH in the brain allows for rapid export from the neurons to the circulation where 24(S)OH is absorbed and eliminated by the liver [18]. This mechanism prevents the accumulation of excess cholesterol in neurons which could be detrimental to neuronal cell function. This is the major pathway for removal of cholesterol from brain.

25-hydroxylase is not a cytochrome P450 monooxygenase but a ubiquitous microsomal, non-heme iron containing enzyme that [7,14] converts cholesterol to 25OH using molecular oxygen and NADPH [19]. 25OH is a potent inhibitor of cholesterol synthesis through the transcriptional and post-transcriptional suppression of 3-hydroxy-3-methylglutaryl-coenzyme A reductase (HMG CoA reductase), the rate-limiting enzyme in the *de novo* synthesis of cholesterol [20]. However, *in vivo*, 25OH levels are low in comparison to other oxysterols, meaning that it may not play such an important role in cholesterol regulation.

The activation of 25-hydroxylase for production of 25OH is important in the innate and adaptive immune responses. 25OH suppresses differentiation of monocytes to

macrophages in a negative feedback mechanism to prevent accumulation of phagocytic cells where they are not required [21]. In cultured macrophages, 25-hydroxylase gene expression is activated rapidly when a toll-like receptor (TLR) agonist is present, resulting in increased 25OH synthesis and secretion into the media [22,23]. In mice and humans, this response is specific to stimulation of TLR4 by lipopolysaccharide (LPS) [22,23]. Stimulated B cells have increased secretion of 25OH resulting in inhibition of IgA production and decreased proliferation *in vitro* [23]. 25-hydroxylase knockout mice do not produce 25OH in response to TLR stimulation and they have increased IgA levels [23]. Dendritic cell (DC) TLR stimulation had a similar response to macrophages [24]. The response in DCs is induced by TLR3 and TLR4 ligands and is mediated by the TLR adaptor protein TRIF [24], which is supported by the simultaneous increase in interferon (IFN) β [25]. Thus in addition to regulation of cholesterol metabolism, 25OH plays many roles in the signalling and proliferation of immune cells and is an important factor in the response of phagocytic cells to infection [19].

### 1.3 Maintenance of cellular cholesterol distribution

Cholesterol is an important structural component in the plasma membrane, and intracellular organelles. However, cellular membranes have different cholesterol compositions contributing to the fluidity of the membrane. Despite being the site of cholesterol synthesis, the ER is a cholesterol-poor (5 mol%) in comparison with other organelles [26]. There is a gradient of cholesterol within the Golgi apparatus where the *cis*-Golgi is cholesterol-poor and the *trans*-Golgi is more cholesterol-rich [27]. The PM is the most cholesterol-rich membrane, containing approximately 30 mol% cholesterol and 60% of total cellular cholesterol [28,29]. The endocytic recycling compartment

(ERC) is also cholesterol-rich, containing up to 35% of total cellular cholesterol [30]. These membranes form an intracellular cholesterol gradient starting at the cholesterol poor ER, traversing the gradient of cholesterol compositions in the Golgi and ending at the cholesterol-rich PM. The varying cholesterol compositions of organelles could be maintained, in part, by the affinity of cholesterol for SM and sphingolipids. Whether each organelle relies on vesicular transport, protein-mediated transport or a combination of both to maintain the correct cholesterol composition is still under investigation.

### 1.3.1 Cholesterol regulation

Cells obtain cholesterol from two sources, *de novo* synthesis or uptake by receptor-mediated endocytosis using lipoprotein receptors such as the low-density lipoprotein receptor (LDL-R). The synthesis and uptake of cholesterol are highly regulated processes that are necessary to maintain the cellular cholesterol content within a narrow range. Increased or decreased cholesterol content of a cell can have detrimental effects; for example, increased cholesterol in macrophages leads to foam cell development and progression of atherosclerosis [31], and decreased cholesterol in the PM can block signalling by Src-family kinases [4].

*De novo* synthesis of cholesterol occurs in the ER, cytoplasm and peroxisomes and is carried out by approximately 30 enzymatic reactions of which the rate-limiting step is controlled by HMG CoA reductase [3]. The regulation of HMG CoA reductase is carried out by several regulatory proteins located in different compartments of the cell. Up-regulation of HMG CoA reductase transcription occurs when sterol regulatory element binding proteins 1 and 2 (SREBP), membrane anchored transcription factors, are cleaved and enter the nucleus where they bind to sterol regulatory elements (SRE) [32].

SREs activate the expression of genes involved in sterol synthesis and regulation. When cholesterol is increased in the ER, SREBPs remain associated with SREBP cleavage activating protein (SCAP) and Insig, an ER retention protein [33]. Depletion of cholesterol can be sensed by the sterol-sensing domain of SCAP, a cholesterol binding protein, which causes the protein to undergo a conformational change and dissociation from Insig [34]. Upon dissociation from Insig, the SCAP-SREBP complex formed by the interaction of the C-terminus of SREBPs and WD-repeats of SCAP, translocates from the ER to the Golgi by SCAP binding to COPII coat proteins [35]. At the Golgi, site 1 protease (S1P), a serine protease of the subtilisin family [36], and site 2 protease (S2P), a zinc metalloprotease [37], convert SREBP into a soluble transcriptionally active form [32]. Once cleaved, SREBP translocates to the nucleus where it binds to SREs to up-regulate HMG CoA reductase transcription and other genes associated with cholesterol and fatty acid homeostasis such as the LDL-R. Association of oxysterols such as 25OH with Insig cause a tight association with the SCAP-SREBP complex, and prevent movement to the Golgi apparatus [38]. *De novo* synthesis of cholesterol is also regulated through oxysterol-mediated degradation of HMG CoA reductase and 7-dehydrocholesterol reductase through Insig-mediated ubiquitination and proteolysis [39] thus preventing the synthesis of cholesterol.

Uptake of cholesterol from outside the cell is carried out by binding of LDL to the LDL-R in clathrin-coated pits, and rapid internalization and trafficking of LDL to the lysosome where cholesterol is released by hydrolysis of cholesterol esters [40]. Cholesterol released from LDL can promote degradation of HMG CoA reductase and prevent transcription through inhibition of SREBP activation [41]. By inhibiting SREBP

activation, LDL-derived cholesterol also prevents transcription of the LDL-R which is also regulated by a SRE. Furthermore, LDL-derived cholesterol is re-esterified by acyl CoA: cholesterol acyltransferase (ACAT), which is responsible for storing excess cholesterol in cytoplasmic lipid droplets by converting them into cholesterol esters [42]. The regulation of *de novo* cholesterol synthesis and cholesterol uptake by the LDL-R is important for the maintenance of intracellular cholesterol levels for the correct expression of the genes involved in synthesis and uptake of cholesterol.

## 1.4 Pathologies associated with defective sterol transport

There are several diseases that result from deregulation of sterol transport including type II familial hypercholesterolemia, Niemann-Pick Type C disease and Tangier disease. One of the most common of all of these pathologies associated with defective sterol transport is familial hypercholesterolemia, an autosomal dominant disorder that affects about 10 million people worldwide in its heterozygous form [3]. The disease is caused by a mutation in the LDL-R gene which prevents the uptake of LDL from the plasma. Accelerated atherosclerosis and coronary heart disease occur because increased circulating LDL becomes trapped in the intima and is oxidized, accelerating the formation of foam cells [3].

Atherosclerosis is initiated by a build up of cholesterol and oxidized sterols in macrophages due to defects in sterol transport, export and/or storage, resulting in macrophage maturation to foam cells and the formation of a fatty streak in the intima underlying the endothelium of large arteries. When LDL enters the intima of blood vessels by passing through the endothelial gaps, it undergoes chemical modifications such as oxidation, generating oxidized LDL. LDL is thought to pass through endothelial

gaps by an interaction of apoproteins B48 and B100 with the extracellular matrix [43]. Oxidized LDL triggers an inflammatory response involving various cytokines in the macrophage causing it to take up more oxidized LDL, which plays a major role in the conversion of macrophages to foam cells [31]. LDL is oxidized both on the lipid moieties and on the apoproteins; the oxidation of the apoprotein is thought to interfere with the association of LDL with the LDL-R [31]. Oxidized LDL recruits monocytes by inducing the expression of chemokines that causes monocytes to migrate to the area by chemotaxis, they differentiate into macrophages [44,45].

Oxidized LDL is not taken up by the LDL-R but instead is brought into the macrophage by scavenger receptor (SR) class A (SR-A) and CD36, a class B scavenger receptor [46,47]. Oxidized LDL is delivered to the lysosome, where cholesterol can be esterified into cholesterol esters by ACAT for storage or incorporated into the cell membrane [45]. Differentiation of the macrophage to a foam cell occurs due to rapid accumulation of cholesterol and cholesterol esters produced by the uptake of oxidized LDL [31]. Once the macrophage has taken up oxidized LDL, it will secrete cytokines and chemokines to recruit more monocytes to the area of the fatty streak where they take up oxidized LDL and also develop into foam cells. These foam cells recruit T cells to the area of inflammation, which is now an area of chronic inflammation. Smooth muscle cells are also recruited to the fatty streak where they secrete extracellular matrix proteins for the formation of the fibrous cap of the plaque [45]. The formation of foam cells and recruitment of other cells to the site of inflammation continues in the presence of excess cholesterol until the artery is completely obstructed by the plaque. The plaque can eventually rupture and resulting thrombosis causes a myocardial infarction or stroke.

Macrophages efflux excess cholesterol through the reverse cholesterol transport pathway involving ATP-binding cassette transport protein A1 (ABCA1)- and ABCG1-mediated efflux to apoAI and high-density lipoprotein (HDL), respectively. This could be the reason why high levels of HDL are protective against atherosclerosis [3]. ABCA1 mediates the removal of cholesterol from the cell to apoAI, further lipidation by ABCG1 forms mature HDL [48]. The absence of ABCA1 results in Tangier disease, which is characterized by sterol accumulation in macrophages, HDL deficiency and accelerated atherosclerosis [3]. In the absence of ABCA1, accelerated atherosclerosis occurs because macrophages have no way of removing cholesterol through the reverse cholesterol transport pathway, resulting in a build up of intracellular cholesterol and oxidized sterol species and differentiation into foam cells.

Niemann-Pick Type C disease is the result of a mutation in Niemann-Pick Type C protein 1 (NPC1) or NPC2 resulting in a loss of protein function. The loss of either one of the proteins results in the same phenotype, the death of Purkinje cells in the cerebellum and death [49]. Niemann-Pick Type C is an autosomal recessive neurodegenerative disorder that is characterized by the accumulation of cholesterol in the late endosomes and lysosomes. NPC1 is a lysosomal membrane protein and NPC2 is a soluble lysosomal protein involved in export of cholesterol from the endocytic pathway [50]. The defect in cholesterol trafficking also prevents down-regulation of SREBP processing. Cells deficient in NPC1 or NPC2 are cholesterol loaded; however, since this cholesterol remains within the endocytic pathway it does not trigger down-regulation of *de novo* synthesis of cholesterol and LDL-R mediated cholesterol uptake.

These diseases indicate why proper cholesterol homeostasis and trafficking are important for proper cellular function and health. A complete understanding of the maintenance of cholesterol homeostasis and cholesterol trafficking is required in order to better understand and prevent these diseases.

## 1.5 Vesicular and protein-mediated transport of cholesterol

Since the cell has varying concentrations of cholesterol in intracellular organelles, there must be mechanisms to deliver cholesterol to the compartments to maintain the correct composition. The transport of cholesterol between organelle membranes could be occurring through vesicular or non-vesicular transport; however, it is likely that a combination of the two forms of transport is required.

For vesicular transport to occur, sorting of cholesterol may be facilitated in part by sterol binding proteins but is probably primarily based on the physical properties of different lipids [51]. In the case of cholesterol, it may preferentially partition into vesicles containing SM because of its increased affinity for this lipid. Different types of vesicles may also selectively include or exclude cholesterol. SM and cholesterol are excluded from COPI vesicles for retrograde transport from the *trans*-Golgi to the ER [52], which maintains the cholesterol-poor state of the ER and *cis*-Golgi. However, cholesterol and SM both partition preferentially into anterograde vesicles going from the *trans*-Golgi to the PM [53], which would contribute to the cholesterol and SM-rich environment of the PM.

There is evidence supporting both vesicular and protein-mediated transport of cholesterol within the cell. The treatment of cells with brefeldin A, which blocks anterograde vesicular transport through the Golgi, reduces the amount of newly

synthesized cholesterol in the ER from reaching the PM by 20% [54]. This result would imply that there is a non-vesicular pathway(s) for cholesterol from the ER to the PM and that vesicular transport plays a minor role in cholesterol trafficking. The rate at which dehydroergosterol (DHE), a fluorescent cholesterol analogue, is trafficked to the endocytic recycling compartment (ERC) from the PM in the absence of adenosine triphosphate (ATP) is only slightly reduced [55] suggesting that non-vesicular transport of cholesterol is playing a major role in this lipid transport pathway.

Although trafficking of sterols to the PM is important for membrane function, trafficking from the ER to lipid droplets is also required for storage as cholesterol esters. Transport to lipid droplets does not occur through vesicular pathways but instead employs lipid diffusion or protein-mediated transport [56]. Some lipid droplets are thought to have phospholipid monolayers continuous with the outer leaflet of the ER membrane that allows diffusion of cholesterol esters or cholesterol between the two compartments [57]. Any lipid droplets not continuous with the ER would use protein-mediated transport of cholesterol. Trafficking to lipid droplets also occurs from the PM. Using DHE as a probe, it was found that trafficking from the PM to lipid droplets has a half-time of 1.5 minutes and is energy independent [58]. The rapid rate of transfer and energy independence would imply that there is protein-mediated transport of cholesterol occurring between the PM and lipid droplets.

Membrane contact sites may facilitate protein-mediated transport of cholesterol. Membranes within both eukaryotic and prokaryotic cells are found in close proximity, called zones of apposition, and could mediate the formation of membrane contact sites [59]. The ER comes into proximity with many organelles, including the mitochondria,

PM, *trans*-Golgi and the ERC, which allows for the formation of membrane contact sites that could be quite stable [60,61]. These zones of apposition have a different sterol composition than the rest of the ER membrane [62]. Yeast membrane contact sites between the ER and the PM contain phosphatidylserine (PS) synthase and phosphatidylinositol (PI) synthase on the ER side of the contact site. The products of these enzymes, PS and PI respectively, are required in abundance at the PM so it is likely that transport of these molecules is facilitated by the close proximity of the membranes [62]. Since contact sites exist between the ER, the site of cholesterol synthesis, and other membranes, they are good candidates as facilitators of protein-mediated sterol transport.

### 1.5.1 Lipid-binding and transport proteins

Lipid transport proteins need to be able to extract lipids from membranes into a hydrophobic pocket and then insert the lipid into a target membrane [56]. There are numerous proteins that possess this type of hydrophobic binding pocket but proving their role in lipid transport is challenging for technical reasons and due to functional redundancies within large gene families.

Steroidogenic acute regulatory protein (StAR) is the founding member of the StAR-related lipid transfer (START) domain proteins, a 15-member family in mammals with potential roles in trafficking cholesterol and other lipids. StAR transports cholesterol between the outer and inner mitochondrial membranes in steroidogenic cells for steroid biosynthesis [63]. *In vitro* experiments showed that StAR specifically transports cholesterol, but not phospholipids, from liposomes to mitochondria or microsomes [64]. Other members of the START domain family of proteins include MLN64 and ceramide transfer protein (CERT). MLN64 is an integral membrane protein

that binds cholesterol via its START domain and localizes cholesterol to the late endosome [65]. A deletion of the START domain of MLN64 causes an accumulation of cholesterol in the late endosome, similar to NPC-deficient cells [66]. However, mice lacking MLN64 display no phenotype [67] indicating that other proteins can compensate for the loss of MLN64.

CERT contains a pleckstrin homology (PH) domain at its N-terminus, two phenylalanines in an acidic tract (FFAT) motif, and a START domain [68]. The FFAT motif of CERT localizes it to the ER where it binds newly synthesized ceramide using its START domain and then transports this ceramide via an interaction between the PH domain and phosphatidylinositol-4-phosphate (PI-4-P) to the Golgi apparatus [68]. The FFAT motif allows CERT to localize to the ER via its interaction with vesicle-associated membrane protein (VAMP)-associated protein (VAP). Once at the Golgi apparatus, ceramide is a substrate for sphingomyelin synthase using PC as the phosphocholine donor. CERT could be shuttling ceramide between the ER and Golgi perhaps facilitated by membrane contact sites [69,70]. The transport of ceramide is controlled by phosphorylation of CERT and is mediated by oxysterol-binding protein (OSBP), which will be discussed later.

Another group of proteins involved in lipid transport are the ABC gene family, specifically ABCA1 and ABCG1 located at the PM. ABCA1 is responsible for the efflux of cholesterol to apoAI to form a nascent HDL particle. ABCG1 is required for the lipidation of nascent HDL to mature HDL [71]. Both proteins are required for the reverse cholesterol transport pathway that removes excess cholesterol from cells, primarily macrophages [3]. These proteins may flip cholesterol, phospholipids and SM between

the bilayers of the PM by binding to apoAI rather than functioning as actual transport proteins [72].

The NPC proteins, NPC1 and NPC2 are involved in transport of cholesterol from the late endosomes and lysosomes to other compartments. NPC1 is a polytopic membrane protein in the late endosomes and lysosomes that contains a luminal N-terminal cholesterol binding domain [73,74] and a sterol sensing domain within its transmembrane segment [75]. NPC2 is a soluble cholesterol-binding protein in the lumen of lysosomes that is targeted there by post-translational modification with mannose 6-phosphate [2]. NPC2 catalyzes the exchange of sterols with lipid bilayers, specifically those containing acidic phospholipids that are present in the lysosomal membrane [76]. NPC2 also transports sterol to and from NPC1 and based on the orientation of the sterol in the binding pockets of NPC2 and NPC1 the sterol could easily slide from one protein to the other [77,78]. A deficiency in either of these proteins causes Niemann-Pick Type C disease. The disease is characterized by a build up of cholesterol in the late endosomes and lysosomes, suggesting that both of these proteins are required to move cholesterol out of these compartments, perhaps to the outer leaflet of late endosomes, where they are accessible to other transport proteins.

Sterol carrier protein-2 (SCP-2) binds sterols and a variety of other lipids including phospholipids, fatty acids and fatty acyl CoAs [79]. SCP-2 is a non-specific lipid transport protein for a wide variety of lipids *in vitro*, and has also been shown to transport cholesterol between the PM and microsomes [79,80]. SCP-2 contains a peroxisomal targeting sequence but is also found in the cytoplasm where it is implicated in facilitating the transport of newly synthesized cholesterol from the ER to the PM

[81,82]. Cells deficient in SCP-2 have decreased newly synthesized cholesterol appearing at the PM after 10 minutes; however, after 20 minutes there is no apparent difference in the amount of cholesterol at the PM meaning that SCP-2 could be playing a role in the initiation of cholesterol transport [82].

Each of the proteins described above has been identified as a lipid transport protein or is a good candidate as a transporter. Lipid transport proteins must be playing a role in sterol transport since it has been determined that vesicular transport cannot be the sole mechanism by which sterol transport is occurring in the cell.

## 1.6 OSBP gene family

Another large family of putative cholesterol transport proteins is OSBP and 11 OSBP-related proteins (ORPs). Based on sequence similarity, the mammalian family of ORPs is broken up into six subfamilies (Figure 1.1A). Subfamily I is comprised of OSBP and ORP4; subfamily II is ORP1 and ORP2; subfamily III is ORP3, ORP6 and ORP7; subfamily IV is ORP5 and ORP8; subfamily V is ORP9; and subfamily VI is ORP 10 and ORP 11 [83]. These proteins all contain a cholesterol and/or oxysterol binding oxysterol homology (OH) domain that contains the conserved signature sequence EQVSHHPP [84]. Many of the ORPs contain short and long variants due to alternative promoters and splice variations [83,84].

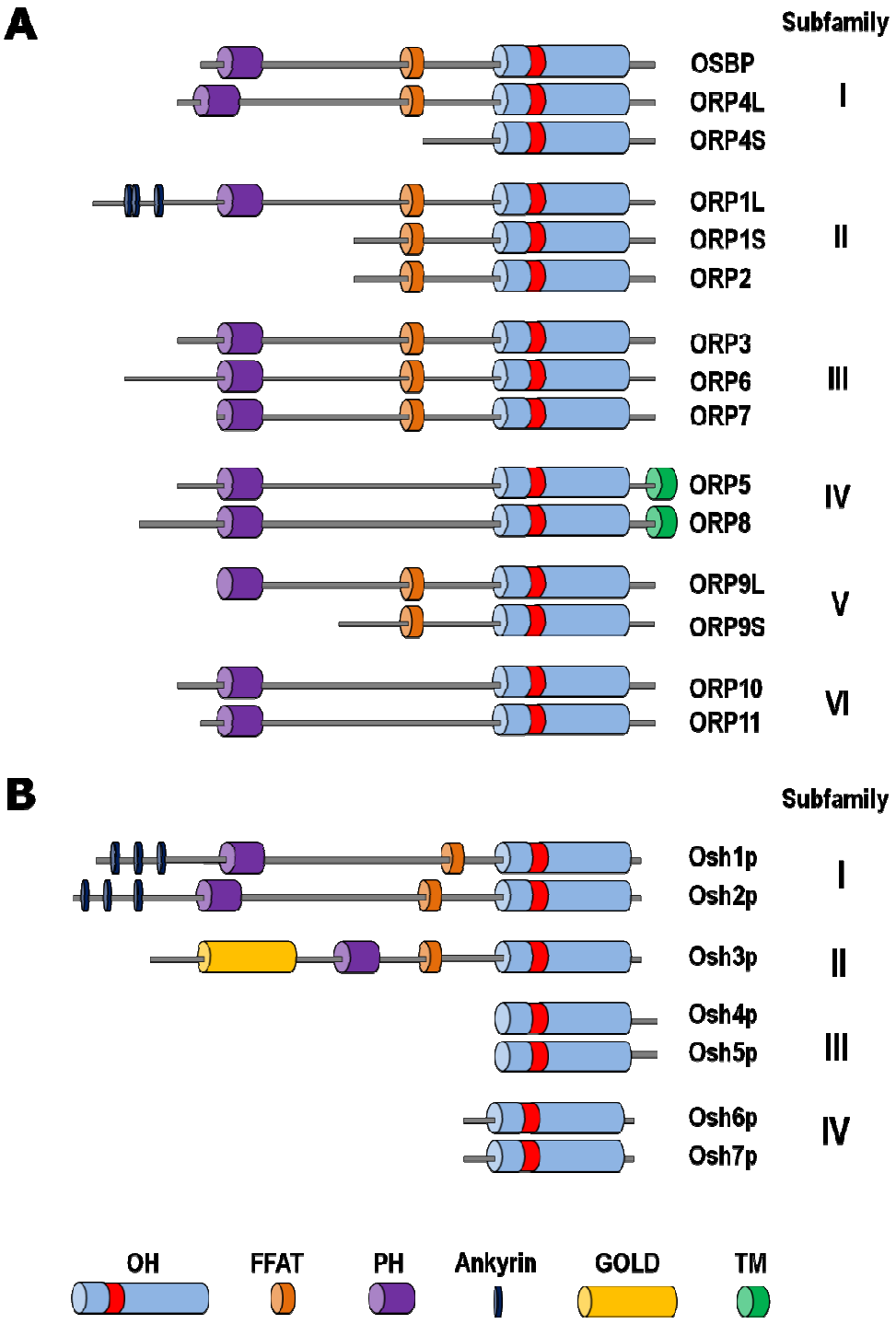


**Figure 1.1. Organization of the mammalian and yeast OSBP gene families.** Mammalian OSBP (A) and yeast OSH (B) family members are organized into subfamilies based on sequence identity. Domains are colour-coded: blue, OH domain; orange, FFAT motif; purple PH domain; black, ankyrin; green, TM domain, yellow, GOLD domain.

With the exception of subfamily IV and VI, all ORPs contain an FFAT motif [84]. Similar to CERT, the FFAT motif allows ORPs to localize to the ER by an interaction with VAP, an integral membrane protein. Other domains of importance are the transmembrane (TM) domain of subfamily IV, which is located at the C-terminus and localizes ORP5 and ORP8 to the ER. All of the long ORPs also contain a PH domain, which binds phosphoinositide phosphates (PIPs) at various membranes in the cell [84].

OSBP and ORPs are not uniformly expressed in all human tissues although the mRNAs for each are expressed at various levels in all tissues [83,85]. OSBP is expressed highly in heart, kidney, liver, and brain and at low levels in other tissues; whereas ORP4L and ORP4S are expressed only in the brain and heart [83,86,87]. Other ORPs with tissue-specific expression are subfamily III: ORP7 is restricted to the gastrointestinal tract, ORP3 is expressed only in the kidney, lymph nodes and thymus, and ORP6 is expressed in the brain and skeletal muscle [88]. OSBP and its related ORPs are excellent candidates for sterol transport proteins since they can bind sterols and localize to different membranes in specific tissues, meaning that they could be moving cholesterol and/or oxysterols between these membranes.

## 1.7 The Osh gene family in yeast

The seven OSBP homologues in yeast, known as OSBP homologue proteins (Osh 1-7), are arranged into four subfamilies (Figure 1.1B) [89]. Yeast requires one of these genes to be viable; deletion of six of the genes with one remaining functional gene results in altered intracellular sterol distribution and slower ergosterol transport from the ER to the PM, but deletion of all seven genes is lethal [89]. The Osh genes contain many similar domains to those found in the mammalian ORPs except that OSH3 has a Golgi

dynamics domain (GOLD). Since only one of these proteins is required for viability in yeast, they must have similar or overlapping functions.

Within yeast subfamily III is Osh4, which is comprised of only an OH domain. The crystal structure for Osh4 has been solved in complex with cholesterol, ergosterol or oxysterols. The binding fold of Osh4 is a hydrophobic β-barrel with an N-terminal α-helical lid that can hold a single sterol ligand with the 3-hydroxy group positioned at the bottom of the barrel [90]. The tunnel is formed by an 180 amino acid β-barrel that is comprised of a 19-strand, anti-parallel β-sheet. The hydrophobic tunnel is plugged by a two-stranded β-sheet and three α-helices opposite the N-terminal lid [90]. Although Osh4 does not contain typical membrane targeting domains, the N-terminal lid contains a membrane curvature-sensing activity that is similar to ATP-ribosylation factor (ARF)-GTPase-activating protein (GAP) that could act to localize it to the Golgi [91]. The C-terminal 125 residues have been shown to mediate membrane binding to anionic lipids and are required for sterol transfer of ergosterol, cholesterol, 7-hydroxycholesterol, 20-hydroxycholesterol and 25OH [92].

The members of subfamily I and II contain PH domains, which in the case of Osh1 and Osh2 bind to PI-4-P and PI-4,5-$P_2$ *in vitro* [84]. Like OSBP, Osh1 localizes to the Golgi in a PI-4-P- and ARF1-dependent manner [93]. Osh2 localizes to the Golgi but also to the PM in a PI-4-P-dependent manner [94,95]. Although Osh4 lacks a PH domain it binds, extracts and transfers PI-4,5-$P_2$ from liposomes *in vitro* using residues 205-314 correlating to β-strands 9-17 of the sterol binding fold [96]. Mutations in residues 205-314 abolished Golgi localization of Osh4 in yeast cells [96,97]. Osh6 also lacks a defined PH domain but binds to various PIPs in a non-specific fashion [98]. The Osh

proteins from subfamily I and II also contain FFAT motifs, which bind to the VAP-homologue, suppressor of choline sensitivity 2 (Scs2) at the ER [99].

OSH proteins play a role in intracellular sterol transport in yeast similar to OSBP and ORPs in mammalian cells. Yeast does not contain START domain proteins, indicating that OSH proteins may have a central role in sterol transport. All of the OH domains of the OSH proteins transfer cholesterol between liposomes *in vitro*. Osh4 increases transfer in the presence of PI-4-P and Osh2, Osh4 and Osh5 have increased transfer in the presence of PS [92,97]. Transfer of ergosterol from the PM to the ER in yeast involves Osh3, Osh4, and Osh5. Even though Osh4 lacks specific localization to either of these membranes it plays a minor role in transport [97]. When the OSH proteins are deleted in yeast, there is a 5-fold reduction in ergosterol transport to the PM [100,101] meaning that OSH proteins are involved in ER to PM nonvesicular transport in addition to PM to ER transport. Collectively, OSH proteins serve as nonvesicular transporters of sterols in yeast.

## 1.8 OSBP and ORPs sterol binding and localization

Although OSBP family members share a C-terminal 400 amino acid OH domain, they do not bind sterols with the same affinity. Results of *in vitro* assays determined that OSBP can bind 25OH ($K_d$ of 10 nM) and cholesterol ($K_d$ of 173 nM) with relatively high affinity but does not bind steroid hormones and binds other oxysterols with greatly reduced affinity [102,103]. ORP4L also binds 25OH ($K_d$ of 10 nM) [87] and ORP4S fused to glutathione-S-transferase (GST) binds 25OH ($K_d$ of 48 nM) and cholesterol ($K_d$ of 267 nM) but this result could not be repeated with ORP4S expressed in Chinese hamster ovary (CHO) cells [87,104]. Furthermore, ORP2 binds 25OH, 22(R)-

hydroxycholesterol (22(R)OH), 7-ketocholesterol (7KC) and cholesterol [105,106], whereas ORP1L binds only 22(R)OH and 25OH [105,107] and ORP8 binds only 25OH [108]. Experiments to measure OSBP and ORP binding of oxysterols and sterols were also conducted in COS cells using photo-activatible 6-azi-cholesterol and 25OH [105]. The OH domains of OSBP, ORP 1-5, ORP7 and ORP10 bound photo-25OH, and all of the OSBP family members bound photo-cholesterol, with the exception of ORP4 and ORP9 [105].

There are differences in the cellular localization of OSBP and ORPs due to the types of domains that they contain. The PH domains of the full-length ORPs are not fully characterized; however, the PH domain of OSBP and ORP9 specifically targets both proteins to the Golgi via an interaction with PI-4-P. The PH domain of ORP3 binds phosphatidylinositol-3,4-bisphosphate (PI-3,4-$P_2$) and phosphatidylinositol-3,4,5-triphosphate (PI-3,4,5-$P_3$) with moderate affinity, which helps localize this protein to the PM [109]. The PH domain of ORP1L also binds to PI-3,4-$P_2$, PI-3,4,5-$P_3$ and phosphatidylinositol-3,5-bisphosphate (PI-3,5-$P_2$) in liposome preparations but this is low affinity and does not localize the protein to a specific membrane [110].

ORPs, with the exception of subfamilies IV and VI, contain an FFAT motif that localizes them to the ER via an interaction with VAP-A and VAP-B, type II integral membrane proteins. The presence of both PH and FFAT domains (or the TM domain in subfamily IV) allows for full-length ORPs to potentially localize to two different organelles. A similar case is observed with CERT, which contains both a PH domain and FFAT motif and shuttles ceramide from the ER to the Golgi.

OSBP localization via its PH domain and FFAT motif is sensitive to cholesterol levels in the cell and the presence of 25OH. When cells are treated with 25OH, OSBP localizes to the Golgi apparatus [103]. Furthermore, when cells are depleted of cholesterol, OSBP is Golgi localized; however, when cells possess excess cholesterol, OSBP localizes to the ER and cytoplasm. In NPC-deficient cells that have cholesterol trapped within the late endosomes and lysosomes, OSBP localizes to the Golgi apparatus [103,111].

### 1.8.1 OSBP and ORPs in sterol transport

Many of the OSBP family members are ideal candidate sterol transport proteins but this is largely unproven for many family members. In the case of OSBP, its PH domain facilitates localization to the Golgi apparatus by an interaction with PI-4-P and ARF1, and the FFAT motif localizes it to VAP at the ER. Thus OSBP could be attached to both membranes simultaneously therefore functioning through a membrane contact site or could shuttle between both membranes (Figure 1.2).

OSBP extracts and transfers cholesterol between liposomes in a PI-4-P-dependent manner [112]. We speculate that this could occur in cells with OSBP transporting newly synthesized cholesterol from the ER to the Golgi apparatus through its interaction with PI-4-P via its PH domain.

ORP9L also localizes to the ER and the Golgi in a similar fashion to OSBP. Furthermore, ORP9L transfers cholesterol between liposomes when the acceptor liposome contains PI-4-P [112]. When ORP9L is silenced, cholesterol builds up in the late endosomes and lysosomes and blockage of ER to Golgi secretion and Golgi fragmentation occurs; ORP9L could be required for the maintenance of the cholesterol

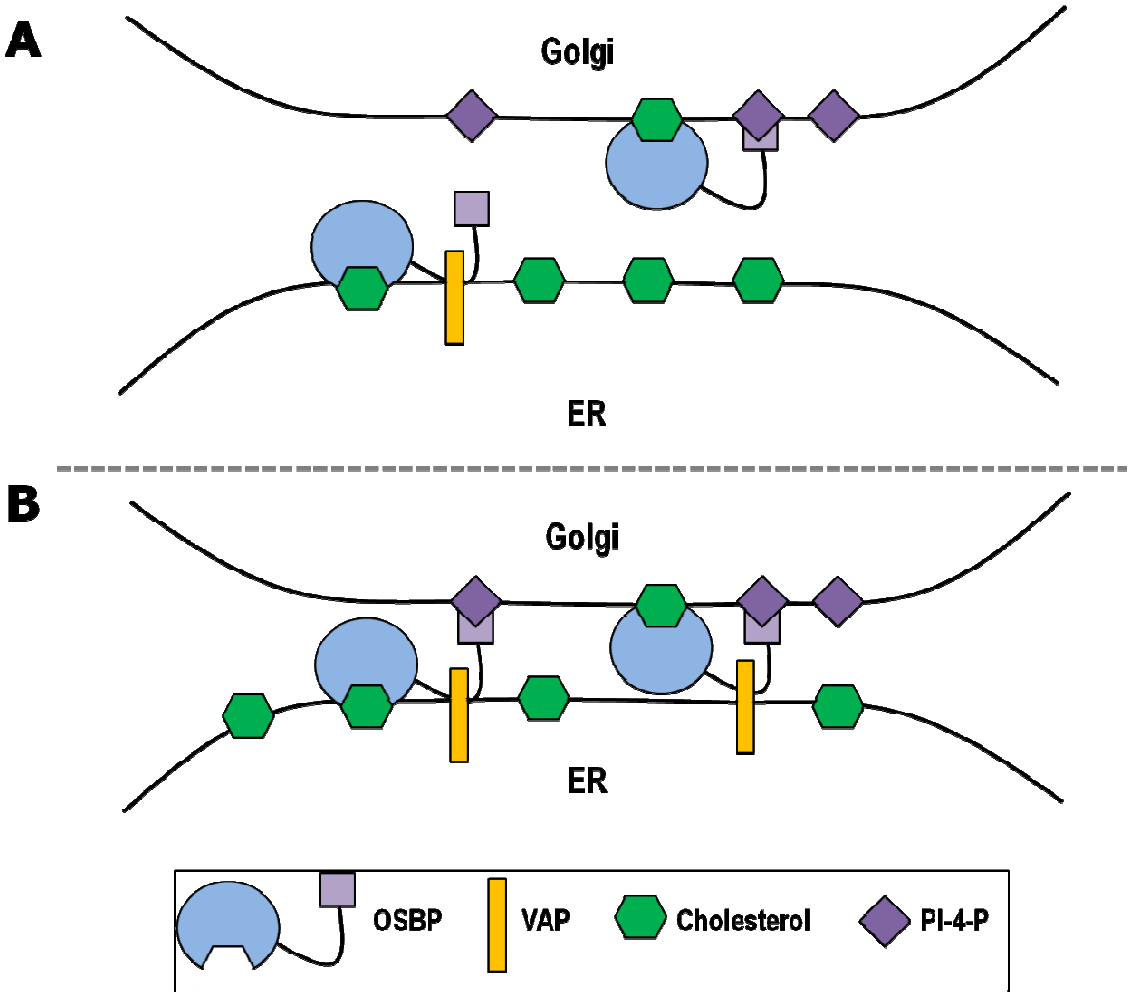


**Figure 1.2. OSBP cholesterol transport.** OSBP could be transferring cholesterol between the ER and Golgi in two possible ways: shuttling between membranes (A) or through membrane contact sites (B). OSBP localizes to the ER via its FFAT domain interaction with VAP and the Golgi using its PH domain interaction with PI-4-P. OSBP can bind cholesterol using its sterol binding domain and transfer it from the ER to the Golgi apparatus.

content in Golgi membranes to ensure proper secretion and organelle structure [84]. When ORP2 is silenced, there is a decrease in triacylglycerol (TAG) hydrolysis and, in the presence of oleate, an increase in cholesterol ester formation, indicating an increase in cholesterol storage in lipid droplets [106]. ORP2 overexpression increases cholesterol synthesis and decreases cholesterol esterification [113]. Furthermore, an ORP2 sterol binding mutant localizes to lipid droplets but disassociates upon treatment with 22(R)OH [106]. These results imply that ORP2 is playing a role in the regulation of cholesterol storage and transfer in lipid droplets.

Further characterization of ORPs is required to fully understand their roles in lipid transport. Since these proteins can bind different sterols and move between cellular organelles it is possible that ORPs are sterol transport proteins.

### 1.8.2 Functions and interactions of OSBP and ORPs

Other than their role in sterol transport, OSBP and ORPs have functions that are not necessarily related to cholesterol homeostasis. OSBP acts as a scaffolding protein that regulates extracellular-signal-regulated kinase (ERK) in a sterol-dependent manner. When OSBP is bound to cholesterol it is a scaffold for the serine/threonine protein phosphatase type 2A (PP2A) and haematopoietic tyrosine phosphatase (HePTP) that deactivate ERK through dephosphorylation [114]. OSBP binds these two phosphatases at its C-terminus [115]. When cholesterol is removed from OSBP or when OSBP is bound to 25OH, the scaffolding complex dissociates and ERK becomes activated through phosphorylation [114].

OSBP is also required for the 25OH- and cholesterol-dependent stimulation of SM synthesis facilitated by ceramide transport from the ER to the Golgi by CERT. When

OSBP is silenced, there is no stimulation of SM synthesis by either 25OH or cholesterol [116,117]. OSBP with a mutated PH or FFAT domain fails to rescue the stimulation of SM synthesis, contact with the ER and Golgi is required for this activity and possibly also the transport of cholesterol from the ER to the Golgi [116]. There is no direct interaction between OSBP and CERT indicating that this mechanism could be a result of sterol-dependent signalling or changes in the lipid environment of the Golgi membrane, making it more favourable for CERT transfer activity. Since OSBP has sterol transport activity *in vitro* it could be localizing to the ER, extracting cholesterol, and then localizing to the Golgi via its PH domain to transfer cholesterol. This would change the lipid composition of the membrane to make CERT binding to the Golgi apparatus more favourable [84]. In this regard, OSBP has been implicated in sterol-dependent activation of PI-4-P synthesis by activation of PI4 kinase IIα in the Golgi apparatus, which would lead to increased CERT localization by its PH domain [118].

The regulation of ABCA1 levels in the cell is integral to the maintenance of the reverse cholesterol transport pathway. Both OSBP and ORP8 play a role in the stability and regulation of ABCA1. When OSBP is silenced the expression of ABCA1 increases 3-fold in CHO cells. However, abolishing cholesterol binding without affecting OSBP localization did not down-regulate ABCA1 [119]. OSBP did not affect ABCA1 expression by down-regulating its transcription but instead decreased ABCA1 protein stability. ORP8 also suppresses ABCA1 protein expression and decreases cholesterol efflux from macrophages [108]. Silencing of ORP8 results in an up-regulation of LXR promoter activity and increased ABCA1 expression [108]. ORP8 and ABCA1 also co-immunoprecipitate showing that the two proteins interact. Since ORP8 is tethered to the

ER via its transmembrane domain, the suppression of ABCA1 could be a result of interacting with the ER [120].

Beyond its involvement in ER-to-Golgi cholesterol transport, ORP9L is involved in the regulation of Akt, an AGC-type kinase [84]. ORP9 contains a phosphoinositide-dependent kinase 2 (PDK2) site that is required for AGC-type kinase activation, and is phosphorylated in a co-ordinated manner with Akt in mast cells [121]. ORP9L has therefore been implied as a negative regulator of Akt phosphorylation and cell proliferation [84].

Four ORPs also affect the cellular cytoskeleton through direct interactions (ORP4 and ORP10) or through signalling (ORP3 and ORP1L) [84]. ORP10 co-localizes with microtubules and has been implicated in TAG synthesis and very low-density lipoprotein (VLDL) secretion [122]. ORP4 binds vimentin [104], an intermediate filament involved in the transport and esterification of LDL-derived cholesterol [123,124]. A leucine repeat, absent in ORP4S, is responsible for the integrity of the vimentin network [104]; overexpressed ORP4S caused a collapse of the vimentin network and inhibited LDL-cholesterol esterification [87].

ORP1L interacts with Rab7 via its ankyrin motifs and recruits microtubule motors to the late endosomes and lysosomes to promote clustering of the compartments [110,125]. This clustering is influenced by the cholesterol content of the late endosomes; high cholesterol content causes ORP1L to bind cholesterol and induce clustering of the late endosomes and lysosomes, apparent in NPC disease [126]. When the endosomal compartment is depleted of cholesterol, ORP1L interacts with VAP and the late endosomes and lysosomes are dispersed [126].

ORP3 co-immunoprecipitates with R-Ras and regulates the actin cytoskeleton [127]. ORP3 overexpression inhibits cell spreading and integrin activity whereas ORP3 silencing increases integrin activity and enhanced cell spreading and adhesion [127].

## 1.9 Post-translational modification of lipid-binding and transport proteins

Post-translational modification is important for localization and function of proteins including lipid transport proteins. One example of post-translational modifications to a lipid transport protein is CERT. CERT localizes to the ER via its FFAT motif or the Golgi apparatus via its PH domain, but the rate and magnitude of transfer could be affected by phosphorylation [116]. Within CERT is a serine-rich phosphorylation motif proximal to its PH domain. Phosphorylation at this motif changes the conformation of CERT to inhibit PH domain interaction with PI-4-P at the Golgi [128]. The first serine residue of this region is phosphorylated by protein kinase D (PKD) at the Golgi apparatus to prime the phosphorylation by casein kinase I (CKI) at eight adjacent serine residues. The phosphorylation of CERT causes Golgi localization to decrease, increases ER localization and decreases the synthesis of SM [129,130]. Furthermore, dephosphorylation of CERT occurs at the ER where protein phosphatase 2Cε (PP2Cε) interacts with VAP. Dephosphorylation of CERT leads to increased Golgi localization and SM synthesis [131]. Dephosphorylation of CERT is triggered by decreased levels of SM and cholesterol which results in the activation of CERT activity [128]. The continual phosphorylation and dephosphorylation of CERT allow it to have controlled localization for the regulated delivery of ceramide from the ER to the Golgi.

### 1.9.1 Post-translational modification of OSBP and ORPs

There are two types of post-translational modification that occur in OSBP: N-acetylation of a lysine residue and phosphorylation at multiple serine and threonine residues. Acetylation on K103 of mouse OSBP has an unknown function [132]. Recently, S238 in mouse OSBP was identified as a PKD phosphorylation site [133]. This phosphorylation site is not similar to that found in CERT since it does not contain downstream CKI phosphorylation sites. However, phosphorylation of this site affects OSBP localization, CERT localization and Golgi structure [133]. Phosphorylation of OSBP by PKD occurs at the Golgi apparatus, decreases localization of OSBP and recruitment of CERT to the Golgi, and causes Golgi fragmentation [133].

Another OSBP phosphorylation site is the serine-rich motif (SRM) that is similar to that found in CERT (Figure 1.3). The site consists of T379, and S381, 384, 387, 388, and 391. Phosphorylation at this site is responsible for the band shift observed when OSBP is analyzed by western blot. The phosphorylated form of the protein is presented in the upper band of the OSBP doublet and the non-phosphorylated form of OSBP at the SRM is presented in the lower band of the doublet [111].

Several studies have been conducted to identify the factors that alter phosphorylation of OSBP at the SRM and the potential kinase(s). When CHO cells were treated with sphingomyelinase (SMase), cholesterol esterification increased and OSBP became dephosphorylated at the SRM and localized to the Golgi [134]. Furthermore, OSBP was re-phosphorylated as the cell recovered after SMase treatment suggesting a link between OSBP phosphorylation and SM synthesis probably through CERT activation. Methyl-β-cyclodextrin treatment affects OSBP phosphorylation at

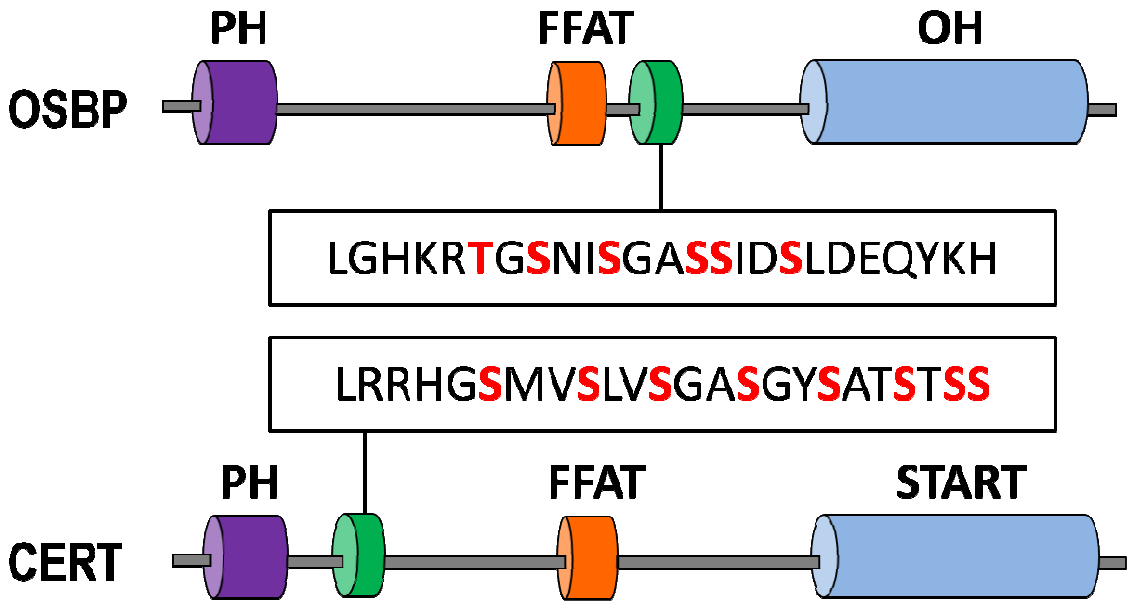


**Figure 1.3. OSBP and CERT serine-rich phosphorylation motifs.** OSBP and CERT both contain a PH domain for Golgi localization and an FFAT motif for ER localization. The START domain of CERT binds ceramide and the OH domain of OSBP binds 25OH and cholesterol. Both proteins contain a serine-rich phosphorylation motif, CERT after its PH domain and OSBP after its FFAT motif. Phosphorylation sites are indicated in red.

the SRM [134]. Decreased dephosphorylation of OSBP is observed when cells are treated with okadaic acid (OA), a PP2A phosphatase inhibitor, resulting in a shift to the upper band when analyzed by western blotting [135]. Treatment of cells with protein kinase C (PKC) inhibitors such as sphingosine or bis-indolylmaleimide does not affect the phosphorylation of OSBP at the SRM [135]. However, treatment of cells with brefeldin A causes OSBP dephosphorylation, suggesting that the kinase responsible for OSBP phosphorylation might be located in the Golgi apparatus [135]. To support this theory, immunoprecipitated OSBP treated with a Golgi-enriched fraction is phosphorylated *in vitro* [135]. The phosphorylation of OSBP could be acting as a switch to regulate intracellular localization similar to the phosphorylation of CERT.

Initially, only S381, 384, and 387 were identified as potential phosphorylation sites [136]; however, through mass spectrometry analysis the phosphorylation of threonine and remaining the two serine residues has been identified [137,138]. By scanning large databases of phosphorylation sites (PHOSIDA, http://phosida.org/, [139]) collected from phospho-proteomic analysis, it is possible to determine whether sequences similar to the OSBP SRM exist in other ORPs; ORP8, ORP9, and ORP11 also contain similar SRMs (Figure 1.4A). These sequences are similar when aligned but also share the same potential kinases when the sequence is analyzed for possible kinase consensus sites (Figure 1.4B). The serine-rich motif of ORP8 occurs between its OH domain and TM domain and probably would not affect its ER localization since the TM domain of ORP8 tethers it to the ER. However, phosphorylation may be affecting the

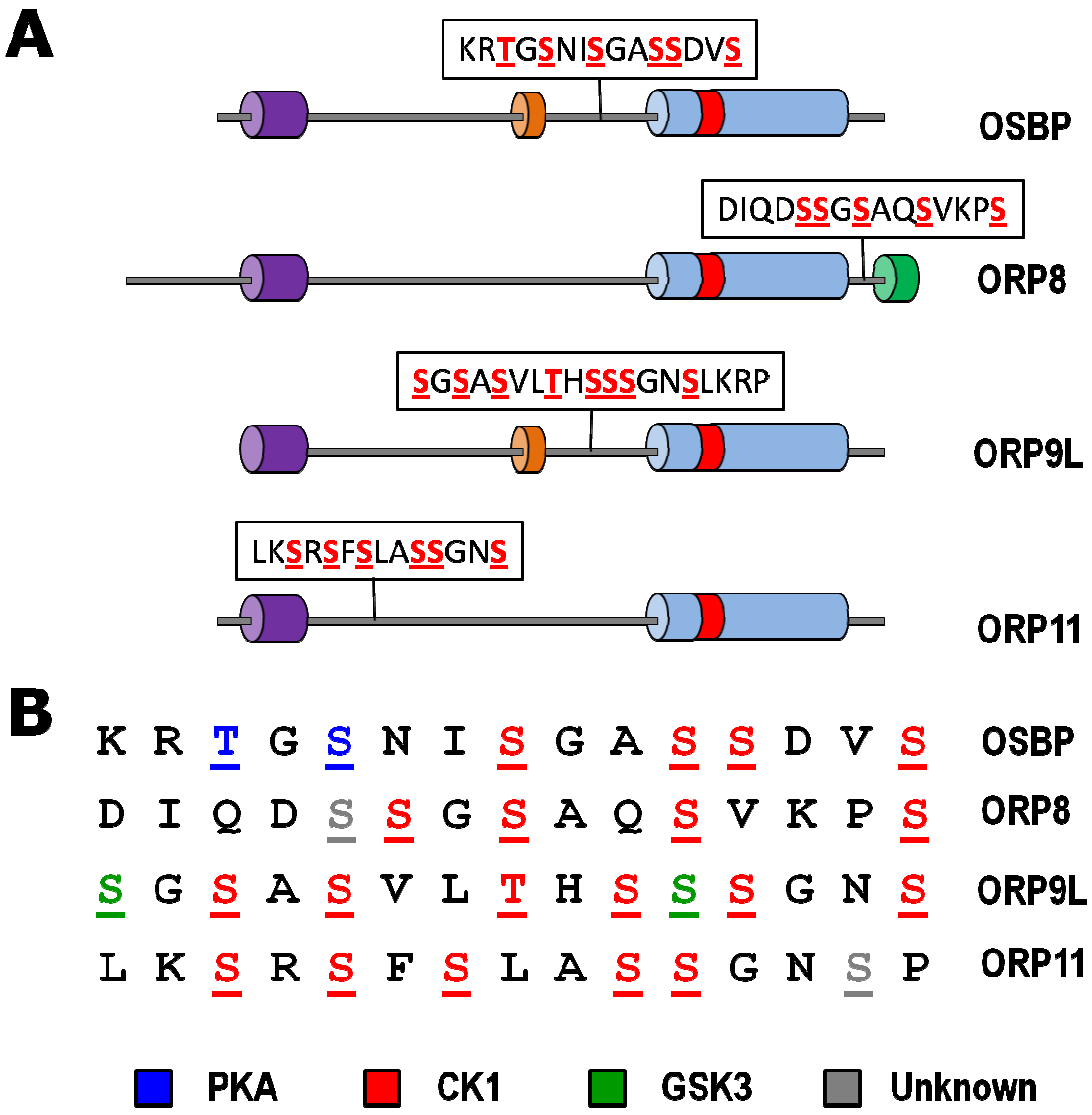


**Figure 1.4. Sequence similarity of OSBP and ORP serine-rich phosphorylation domains.** OSBP, ORP8, ORP9 and ORP11 share a similar serine-rich phosphorylation motif located in different parts of the protein (A). These sequences could serve to regulate protein localization or binding activity. Each of the serine-rich motifs is potentially a site for CKI phosphorylation and PKA may phosphorylate OSBP and ORP11.

conformation of ORP8 and its interaction with the Golgi, sterols or regulation of ABCA1 expression. Similar to OSBP, ORP9 has a serine-rich phosphorylation motif between its FFAT motif and OH domain and several sites have been identified as potential CKI sites. The potential priming kinase in this case is glycogen synthase kinase 3 (GSK3) at S315. Since ORP9 has been shown to transfer sterols *in vitro* in a PI-4-P dependent manner, and the phosphorylation site is similar to OSBP, it is possible that phosphorylation is regulating both of these proteins in the same way. There is also a SRM in ORP11 next to its PH domain. ORP11 does not contain another membrane localization domain but dimerizes with ORP9 at the Golgi and late endosome interface [140]. This interaction involves residues 154 to 219 that encompass the potential phosphorylation sites on serine residues 179 to 189, indicating a potential role for phosphorylation in dimerization.

It is also possible to analyze these sequences for potential kinases based on consensus sequences. There is no identified kinase that phosphorylates T379. However, S381 is a putative protein kinase A (PKA) site and each of the downstream serines is a candidate for CKI phosphorylation. PKA is found in the Golgi apparatus [141] and therefore fits with previous data concerning the Golgi localization of the kinase responsible for OSBP phosphorylation [135]. Therefore, it is possible that OSBP is controlled by a mechanism involving PKA phosphorylation. This form of regulation would make sense due to the similarity of OSBP and CERT function and also the requirement for OSBP in sterol-dependent up-regulation of SM synthesis by CERT.

### 1.10 How phosphorylation affects OSBP

Phosphorylation of OSBP and ORPs could regulate their cholesterol transport activity. We hypothesize that phosphorylation of OSBP affects the sterol binding activity

of OSBP, localization of the protein, interactions with PIPs and VAP, and/or regulation of SM synthesis. Phosphorylation could accomplish this through altering the conformation of OSBP and masking domains such as the PH domain or FFAT motif, therefore modulating localization to the Golgi apparatus or ER.

# CHAPTER 2 MATERIALS AND METHODS

## 2.1 Materials

All radioisotopes ([$^3$H]serine, [$^3$H]cholesterol, [$^3$H]25OH, [3H]PC) were purchased from Perkin-Elmer (Waltham, MA). Restriction enzymes were purchased from New England Biolabs (Mississauga, ON). Plasmid purification kits were purchased from Qiagen (Mississauga, ON). X-B1 blue film for chemiluminescent detection was from Kodak (Toronto, ON). BLOCK-iT™ Lentiviral RNAi Expression System and BaculoDirect™ Baculovirus Expression System, T4 DNA Ligase, ampicillin, kanamycin, Dulbecco's modified Eagle's media (DMEM), Alexa-Fluor® 594 goat anti-mouse, Alexa-Fluor® 488 goat anti-rabbit and Benchmark Protein Ladder were purchased from Invitrogen (Burlington, ON). The QuikChange™ II XL Site-Directed Mutagenesis Kit was purchased from Agilent Stratagene (Santa Clara, CA). The protein kinase A inhibitor Rp-cAMPS was purchased from Santa Cruz Biotechnology Inc. (Santa Cruz, CA). Primers for PCR and mutagenesis were ordered from Integrated DNA Technologies (Coralville, IA). Surfact-Amps® X-100 and GelCode Blue® Stain Reagent were purchased from Thermo Scientific (Rockford, IL). EDTA-free protease inhibitor cocktail tablets were purchased from Roche Applied Science (Laval, QC). All lipids were purchased from Avanti Polar Lipids Inc. (Alabaster, AL) except for glucocerebosides which were purchased from Matreya (Pleasant Gap, PA) and 25OH which was purchased from Steraloids Inc. (Newport, RI). Castor bean agglutinin $RCA_{120}$, bovine serum albumin (BSA) and anti-β-actin monoclonal mouse antibody were purchased from Sigma-Aldrich (St. Louis, MO). Fetal calf serum (FCS) was purchased

from PAA Cell Culture Company (Etobicoke, ON). Talon® Superflow™ Metal Affinity Resin was purchased from Clontech (Mountainview, CA). Glycine, 40% acrylamide, Tween-20, nitrocellulose (NC) membrane, and goat anti-mouse and goat anti-rabbit horseradish peroxidise-conjugated secondary antibodies were purchased from Bio-Rad Inc. (Hercules, CA). IRDye® conjugated goat anti-rabbit and goat anti-mouse secondary antibodies and Odyssey Blocking Buffer were purchased from LI-COR Biosciences (Lincoln, NE). Anti-giantin polyclonal rabbit antibody was purchased from Covance (Emeryville, CA). OSBP 170 polyclonal rabbit antibody and OSBP 11H9 monoclonal mouse antibody are purified in our lab [134]. Immobilon Western Chemiluminescent HRP substrate and Amicon Ultra-15 centrifugal filter units were purchased from Millipore (Billerica, MA). Filter paper and thin layer chromatography (TLC) plates were purchased from Whatman (Kent, UK).

## 2.2 Cell Culture

All mammalian cells were cultured in 37°C in a 5% $CO_2$ atmosphere. CHO cells and CHO cells stably expressing His-tagged OSBP (CHO-OSBP-His) were cultured in DMEM containing 5% FBS and 34 µg/mL proline (Media A). CHO shNT and CHO shOSBP were selected in Media A with 5 µg/mL blasticidin. HEK293FT cells were cultured in DMEM containing 10% FBS, 2 mM L-glutamine, and 1mM sodium pyruvate. HEK293FT cells were selected for after infection in maintenance media with 500 µg/mL Geneticin.

SF21 insect cells were cultured in SF900-II medium containing 5% (v/v) FBS, 10 µg/mL G418 and 0.25 µg/mL fungizone (SF21 Media) in adherent monolayers at 27°C and in suspension at 29°C. Adherent monolayers were passaged at confluency at a 1/5

dilution and suspension cultures were maintained in flasks shaking at 150rpm in log phase growth (0.75-2.5x$10^6$ cells/mL).

### 2.3 Creation of stable CHO shNT and CHO shOSBP cell lines

The BLOCK-iT Lentiviral RNAi Expression System (Invitrogen) was used to generate lentiviral vectors encoding a non-targeting shRNA and an shRNA against OSBP for infection of CHO cell lines. Single-stranded DNA oligos were designed encoding an shRNA targeting OSBP (shOSBP-F, shOSBP-R) and a non-targeting shRNA (shNT-F, shNT-R). The single-stranded oligos were annealed, cloned into the pENTR/U6 vector and transformed into One Shot TOP10 *E. coli*. Colonies were selected on LB plates with kanamycin (50 µg/mL) and cDNAs isolated from resistant colonies were confirmed by sequencing using the U6 Forward primer. The pENTR/U6-OSBP and NT vectors were then used in a LR recombination reaction to insert the shRNAs into pLenti6/BLOCK-iT-DEST and transformed into One Shot Stbl3 *E. coli*. Colonies were selected on LB plates with ampicillin (100 µg/mL) and tested for false positives on LB plates with chloramphenicol (30 µg/mL). DNA from the shNT and shOSBP positive clones was transfected into HEK 293FT cells with Lipofectamine 2000 and ViraPower Packaging Mix (pLP1, pLP2, and pLP/VSVG plasmids lyophilized in TE Buffer, pH 8.0). Media containing virus is collected 72 h post-transfection, cell debris removed by centrifugation and viral stocks were stored at -80°C. CHO cells were infected with virus overnight using Polybrene (6 µg/mL) and cells were selected for two weeks in Media A with blasticidin (5 µg/mL). Stock cultures of CHO shNT and CHO shOSBP cells were maintained in Media A with blasticidin (5 µg/mL).

### 2.4 Mutagenesis

Mutagenesis was performed using the QuikChange™ II XL site-directed mutagenesis kit (Stratagene-Agilent) on pCMV OSBP and pENTR OSBP [112]. Primers were used to mutate threonine 379 to alanine (OSBP T to A), threonine 379 to glutamine (OSBP T to E), and serine residues 388 and 391 to glutamine residues (OSBP 2S to E) (primer sequences are shown in Table 2.1) Mutagenesis reactions were cloned into Top 10 *E. coli*, selected on LB plates with ampicillin (pCMV OSBP) or kanamycin (pENTR OSBP). Plasmids were sequenced to confirm the mutations. Some constructs had additional mutations and were excised from the plasmid with XhoI and PmlI and ligated into a mutation-free vector using T4 DNA Ligase at a 1:5 (insert: vector) ratio.

## 2.5 Analysis of migration of OSBP phosphomutants by SDS-PAGE

CHO shOSBP cells were cultured on 35mm dishes at 200,000 cells/dish in Media A with blasticidin (5µg/mL). Cells were transfected with wild-type OSBP or the OSBP phosphomutants (T379A, S381A, 3S→3E, 5S→5E, 6S/T→6E) using Lipofectamine 2000 for 24 h and then harvested in 137 mM NaCl, 2.7 mM KCl, 10 mM $Na_2HPO_4$, 2mM $KH_2PO_4$ (PBS) and lysed in 100 mM Tris-Cl pH 6.8, 4% w/v SDS, 0.2% w/v bromophenol blue, 20% v/v glycerol, 200 mM β-mercaptoethanol (SDS gel-loading buffer). Samples were analyzed by SDS-PAGE on a 6% polyacrylamide gel (6%-SDS-PAGE) and visualized by western blot with primary monoclonal antibody 11H9 and secondary IRDye® 800CW-conjugated GAM. Samples are visualized using a LI-COR Odyssey IR imaging system.

## 2.6 Analysis of PKA phosphorylation of OSBP

CHO cells were cultured at 400,000 cells per 35mm dish in Media A. When cells reach 80% confluence they were treated with 50µM Rp-cAMPS for up to 8 h. Cells were

harvested in PBS, lysed in SDS gel-loading buffer, proteins resolved by 6%-SDS-PAGE, transferred to NC and detected by western blot using polyclonal antibody 170 and IRDye® 800CW GAR secondary antibody. Samples were visualized and quantified using a LI-COR Odyssey IR imaging system. Total fluorescence of each sample was calculated by measuring the integrated density of both OSBP bands; the amount of protein in the lower band is expressed as a percentage of the total protein fluorescence of each band.

### 2.7 Immunofluorescence and intracellular OSBP localization

CHO shNT and CHO shOSBP cells were cultured at 100,000 cells/coverslip (22 mm x 22 mm) for 24 h and transfected with plasmids encoding OSBP phosphomutants for 48 h (Mock, OSBP WT, OSBP T379A, OSBP S381A, OSBP 3S→3E, OSBP 5S→5E, and OSBP 6S/T→6E). Cells were incubated with either ethanol or 2.5 µg/mL 25OH for 1 h, fixed in 3% formaldehyde in 10 mM $NaPO_4$, 225 mM NaCl, 2 mM $MgCl_2$ pH 7.0 (PBS-IF) for 15 min at room temperature and permeablized in 0.05% Triton X-100 in PBS-IF for 20 min at 4°C. Coverslips were blocked overnight in 1% BSA in PBS-IF and probed with OSBP 11H9 monoclonal mouse antibody and anti-giantin polyclonal rabbit antibody for 1 h. They were then incubated with Alexa-Fluor® 594 goat anti-mouse and Alexa-Fluor® 488 goat anti-rabbit and cells were imaged using a Zeiss LSM 510 Meta laser scanning confocal microscope equipped with a 100x objective (N.A. 1.4). Cells were also imaged with a 40x objective (N.A. 0.6) using a Zeiss Axiovert 200M inverted optical microscope.

### 2.8 Determining phospho-peptides of OSBP using mass spectrometry

CHO-OSBP-His cells stably expressing OSBP with a C-terminal His tag were previously made in our lab (Dr. Ryan Perry). These cells were seeded on 100mm dishes and when 90% confluent, were treated with either 1μM okadaic acid to inhibit PP2A phosphatases and increase the phosphorylation of OSBP or 1mM $H_2O_2$ which was previously found to increase OSBP phosphorylation in our lab (unpublished data) for 2 h before harvesting. Cells were harvested in PBS, subjected to centrifugation at 10,000 rpm for 2 min, resuspended in 20 mM Tris-Cl pH 7.4 with 1X protease inhibitor, left on ice for 1 h to swell, and passed through a 25 G needle and sonicated to lyse the cells. Samples were centrifuged at 45,000 rpm for 1 h at 4°C and the supernatant was bound to Talon resin for 2 h at 4°C. Talon resin was washed with 20 mM Tris-Cl pH 7.4, 150 mM NaCl, and 1X protease inhibitor (Buffer A). OSBP was released from the Talon resin using Buffer A with 150 mM imidazole. Samples were resolved on a 6%-SDS-PAGE and the gels were stained with Gel Code Blue. Both the upper and lower bands of OSBP were excised from the gel, digested with trypsin and peptides were analyzed by nanoflow LC/MS/MS. The disulfide bonds were reduced with dithiothreitol and free cysteines reacted with iodoacetamide. Samples were injected onto a 100 μm I.D. C-18 column with a shallow acetonitrile gradient from 2% to 28% over 35 min. Mass spectrometry analysis was performed on an Applied Biosystems Q TRAP LC/MS/MS system. Predicted mass to charge (m/z) ratios were determined for each of the possible phosphopeptides for the fragment TGSNISGASSIDSLDEQYK (Table 2.2) and used to produce an extracted ion chromatogram of the LC/MS. The extracted ion chromatogram was used to identify MS/MS spectra for detected phosphopeptides for the identification of phosphorylated residues.

## 2.9 Purification of OSBP from SF21 cells

Infected SF21 cells (200 mL) grown for 72 h in suspension at 29°C were collected by centrifugation at 300x g for 10 min. Cell pellets were resuspended in 20 mL of Talon buffer containing 30 mM imidazole and 1X protease inhibitors. Cells were lysed by passage through an 18 G and 25 G needle and sonication. Lysed cells were centrifuged for 1 h at 17,000 rpm to remove cell debris. Supernatants were bound to Talon resin for 2 h at 4°C. Talon resin was washed twice with Talon buffer containing 30 mM imidazole to remove unbound protein. OSBPs were eluted in Talon buffer containing 150mM imidazole. The eluate was diluted 5-fold in 20 mM Tris pH 7.4 and applied to a DEAE Sepharose column, washed with 20 mM Tris-Cl pH 7.4 and 50 mM NaCl, and elution with 20 mM Tris pH 7.4 with 250 mM NaCl. The eluate was concentrated using a 100,000 MWCO Amicon membrane. The concentration of OSBPs was determined using the Lowry method [142]. Purity was confirmed by 6%-SDS-PAGE and staining with GelCode Blue reagent.

## 2.10 Phospholipid overlay assay

Increasing concentrations of PI-4-P, PI-4,5-$P_2$ and PC (dissolved in chloroform: methanol: water (1:2:0.8)) were spotted on nitrocellulose membranes as previously described [112]. Membranes were dried and blocked in TBS containing 3% fatty-acid free BSA and 0.1% Tween-20 for 2 h at room temperature. The membranes were incubated with 200 pmol of purified OSBP WT or OSBP 5S→5E for 1 h and then probed with 11H9 monoclonal antibody and GAM secondary antibody either conjugated to HRP or IRDye® 800CW. Membranes were visualized by exposure to film after applying

Immobilon Western Chemiluminescent HRP substrate or by using the LI-COR Odyssey IR imaging system.

### 2.11 Measurement of sphingomyelin synthesis by [$^3$H]serine labelling

CHO shNT and CHO shOSBP cells were cultured at 500,000 cells/dish for 48 h and transfected with plasmids encoding, OSBP WT, OSBP T379A, OSBP S381A, OSBP 3S→3E, OSBP 5S→5E, and OSBP 6S/T→6E for 48 h. Cells were then incubated in serine-free media A with or without 2.5µg/mL 25-OH for 4 h and then labelled for 2 h with [$^3$H]serine (5 µCi/mL) in serine-free media A with or without 2.5µg/mL 25-OH. Cells were harvested in methanol: water (1:1, v/v) and homogenized by sonication. A sample was taken for Lowry protein quantification [142]. The remaining sample was extracted using chloroform and methanol (1:2, v/v) and 0.58% NaCl, centrifuged to separate the aqueous and organic phases, and the aqueous phase was discarded [143]. Samples were washed twice with methanol, 0.58% NaCl and chloroform (45:47:3, v/v), dried under nitrogen and resuspended in chloroform (1 mL). A 400 µL fraction was used for phospholipid analysis, while a 600 µL fraction underwent base hydrolysis with 0.1N KOH in methanol at 37°C for 1 h and then extraction using chloroform and methanol as described before [143]. Samples are separated by TLC in chloroform: methanol: water (65:31.25:5, v/v) (sphingolipids) and chloroform: methanol: acetic acid: water (60:40:4:1, v/v) (phospholipids). Bands were visualized by incubating the plates in an iodine tank; identification of bands was verified by comparing to the migration of lipid standards. Samples were scraped and radioactivity measured using a Beckmann-Coulter LS 6500 and normalized to total cellular protein.

### 2.12 [$^3$H]25OH binding assay

25OH binding was performed as previously described [103,144]. Purified OSBP WT or OSBP 5S→5E (20 pmol) were incubated overnight at 4°C with increasing concentrations of [$^3$H]25OH in 10 mM HEPES pH 7.4 and 100mM KCl (binding assay buffer) with 2% polyvinyl alcohol and KCl was adjusted to a final concentration of 150 mM. Non-specific binding was determined by adding a 40x excess of unlabelled 25OH to the assay. The next day, 30 µL of charcoal-dextran was added and assays were vortexed at 5 min intervals for 30 min at 20°C. Samples were centrifuged at 13,000 rpm for 10 min at 4°C and 40 µL of the supernatant was measured for radioactivity using a Beckmann-Coulter LS 6500. Specific binding was determined by subtracting the non-specific binding from the total binding. $B_{Max}$ and $K_d$ were calculated by fitting the data to a non-linear regression curve with a one-site binding model using Prism.

### 2.13 [$^3$H]Cholesterol binding assay

Cholesterol binding was performed as previously described [112]. Purified OSBP WT or OSBP 5S→5E (20 pmol) were incubated for 2 h at room temperature with increasing concentrations of [$^3$H]cholesterol in binding assay buffer with 2% polyvinyl alcohol, 300 mM KCl and 0.05% Triton X-100. Non-specific binding was determined by adding a 40x excess of unlabelled cholesterol to the assay. After incubation, 25 µL of a 1:1 slurry of Talon beads was added to the samples for 25 min with shaking at 20°C. Protein was eluted from the Talon beads using binding assay buffer with 150 mM imidazole and assays were measured for radioactivity using a Beckmann-Coulter LS 6500. Specific binding was determined by subtracting the non-specific binding from the total binding. $B_{Max}$ and $K_d$ were calculated by fitting the data to a non-linear regression curve with a one-site binding model using Prism.

## 2.14 Liposome preparation

Liposomes of varying composition were prepared according to the requirements of the experiment. PIPs were dissolved in chloroform: methanol: water (1:2:0.8, v/v) and phospholipids were dissolved in chloroform. Lipids were mixed with 50 µL of chloroform: methanol (2:1, v/v) and dried down under nitrogen. They were resuspended in 25 mM HEPES pH 7.4, 150 mM NaCl and 1 mM EDTA (liposome buffer) and vortexed at 5 min intervals for 1 h. The mixture was extruded through a 400 nm filter 20 times to ensure a liposome population uniform in diameter. Before use, liposomes are centrifuged at 13,000 rpm for 5 min at 4°C to remove aggregates. Liposomes are stored at 4°C for up to 48 h.

## 2.15 Analysis of OSBP phosphomutant affinity for phosphatidylinositols

Liposomes were prepared up to 48 h prior to the experiment and before use were centrifuged at 13,000 rpm for 5 min at 4°C. Stock solutions of liposomes were composed of PC, PE and PI, PI-4-P or PI-4,5-$P_2$ (70:20:10, mol/mol). The liposomes were incubated with 100 pmol of purified protein in liposome buffer for 25 min at 25°C. Samples were centrifuged at 100,000 x g for 30 min to sediment the liposomes and associated OSBP. Both the supernatant and pellet were analyzed by 8%-SDS-PAGE and the protein was visualized by GelCode Blue staining. Bands were quantified by measuring the fluorescence of each band using a LI-COR Odyssey IR imaging system.

## 2.16 [$^3$H]Cholesterol extraction from liposome assays

Liposomes were composed of PC, PE, PS, PI, PI-4-P, or PI-4,5-$P_2$, (49:20:10:10 mol/mol) with 10% lactosyl-PE, 1% cholesterol and [$^{14}$C]PC and [$^3$H]cholesterol. [$^{14}$C]PC was included as a control to ensure that liposomes were not in the supernatant

after centrifugation. Liposomes (0.5 mM) were incubated with increasing amounts of purified protein (25 pmol to 200 pmol) in liposome buffer for 25 min at 25°C. After the incubation, 1 µg of castor bean agglutinin $RCA_{120}$, was added to each sample, the tube was briefly vortexed and incubated on ice for 15 min. Samples were centrifuged at 13,000 rpm for 5 min and a quarter of the supernatant was taken to measure radioactivity using a Beckman-Coulter LS 6500.

### 2.17 [$^3$H]Cholesterol transfer assays between liposomes

Purified OSBP, OSBP S381A or OSBP 5S→5E were incubated with 400 nM [$^3$H]cholesterol in binding assay buffer with 2% PVA, 300 mM KCl and 0.05% Triton X-100 for 2 h at 20°C. After the incubation a 1:1 slurry of Talon beads was added to the mixture at room temperature with shaking for 30 min. The bound OSBP was eluted from the beads using binding assay buffer with 150 mM imidazole and 25 pmol of protein from this solution was used for the transfer assay. The protein was incubated with 13 µM transfer assay liposomes composed of PC, PE, PS, PI, PI-4-P, or PI-4,5-$P_2$, (50:20:10:10; mol/mol) with 10% mol/mol lactosyl-PE, and [$^{14}$C]PC in liposome buffer with 3% FA-free BSA for 10 min at 25°C. After the incubation, 1 µg of castor bean agglutinin $RCA_{120}$ was added to each tube, incubated on ice for 15 min and then centrifuged at 13,000 rpm for 5 min at 4°C. The supernatant was removed and the pellet was resuspended in 1% SDS. Both the supernatant and pellet radioactivity were measured using a Beckmann-Coulter LS 6500.

### 2.18 OSBP-VAP immunoprecipitation assay

CHO shOSBP cells were cultured in Media A with 5 µg/mL blasticidin for 24 h prior to transfection with OSBP, OSBP S381A, or OSBP 5S→5E using Lipofectamine

2000. Cells were harvested 24 h post-transfection in PBS, centrifuged and lysed in 10 mM phosphate pH 7.4, 150 mM NaCl, 5 mM KCl, 2 mM EDTA, 2 mM EGTA and 0.5% Triton X-100. Cells were incubated on ice for 15 min and centrifuged at 13,000 rpm for 10 min at 4°C. The supernatant was transferred to a new tube and 10% of the sample was removed as the input sample. The remaining sample was incubated overnight at 4°C with VAP polyclonal antibody (1:10, v/v). The next day, 60 µL of a 1:1 slurry of Protein A Sepharose CL-4B beads was incubated with each sample for 45 min at 4°C. The beads are washed 3 times with PBS with 0.5% Triton X-100 and resuspended in 50 µL of SDS gel-loading buffer. Samples were resolved by 10%-SDS-PAGE, immunoblotted with OSBP monoclonal antibody and IRDye® 580LT GAM antibody and visualized using a LI-COR Odyssey IR imaging system. Quantification was performed measuring the integrated density of each fluorescent band.

### 2.19 Pull down of OSBP with VAP-GST

CHO shOSBP cells were cultured in Media A with 5 µg/mL blasticidin for 24 h prior to transfection with OSBP, OSBP S381A, or OSBP 5S→5E using Lipofectamine 2000. Cells were harvested 24 h post-transfection in PBS, centrifuged and resuspended in 10 mM phosphate pH 7.4, 150 mM NaCl, 5 mM KCl, 2 mM EDTA, 2 mM EGTA and 0.5% Triton X-100. Cells were incubated on ice for 15 min and centrifuged at 13,000 rpm for 10 min at 4°C. The supernatant was transferred to a new tube and 10% of the sample was removed as the input sample. Half was incubated with 200 pmol VAP-GST and the other half was incubated with 200 pmol GST for 1 h on ice. Samples were incubated with 25 µL of a 1:1 slurry of glutathione Sepharose 4B beads in PBS with 0.5% Triton X-100 for 30 min at 20°C and the beads were washed with PBS with 0.5%

Triton X-100 4 times. The beads were resuspended in 40 µL of 2.5x SDS gel-loading buffer and boiled at 90°C for 5 min. Samples were resolved by 10%-SDS-PAGE and immunoblotted with OSBP 11H9 monoclonal antibody and IRDye 800CW GAM antibody. Protein was visualized by fluorescence using a LI-COR Odyssey IR imaging system.

| Primer/shRNA | Usage | Sequence (5'→3') |
|---|---|---|
| shNT-F | Knockdown | CACCGATAACCAGAATACCATACTTCAAGAGAGTATGGTATTCTGGTTATC |
| shNT-R | Knockdown | AAAAGATAACCAGAATACCATACTCTCTTGAAGTATGGTATTCTGGTTCTC |
| shOSBP-F | Knockdown | CACCGAGAACCAGAATACCATACTTCAAGAGAGTATGGTATTCTGGTTCTC |
| shOSBP-R | Knockdown | AAAAGAGAACCAGAATACCATACTCTCTTGAAGTATGGTATTCTGGTTCTC |
| OSBP-Phos | Sequencing | ACAACCACCTGGAGAGGGC |
| U6 Forward | Sequencing | GGACTATCATATGCTTACCG |
| OSBP T to A-F | Mutagenesis | GGGACACAAACGTGCCGGCAGCAACATCAG |
| OSBP T to A-R | Mutagenesis | CTGATGTTGCTGCCGGCACGTTTGTGTCCC |
| OSBP T to E-F | Mutagenesis | GGGACACAAACGTGAAGGCGAGAACATCG |
| OSBP T to E-R | Mutagenesis | CGATGTTCTCGCCTTCACGTTTGTGTCCC |
| OSBP 2S to E-F | Mutagenesis | CATCGAAGGAGCCGAAGAGGACATCGAGCTTGATGAACAGTAC |
| OSBP 2S to E-R | Mutagenesis | GTACTGTTCATCAAGCTCGATGTCCTCTTCGGCTCCTTCGATG |

**Table 2.1 Table of primers.**

| Potential Phosphopeptide | Calculated m/z ratios (+2) |
|---|---|
| Non-phosphorylated | 986.45 |
| Monophosphorylated | 1026.44 |
| Diphosphorylated | 1066.42 |
| Triphosphorylated | 1106.43 |
| Tetraphosphorylated | 1146.39 |
| Pentaphosphorylated | 1186.37 |
| Hexaphosphorylated | 1226.35 |

**Table 2.2. Expected phosphopeptides and calculated m/z ratios for mass spectrometry analysis.**

# CHAPTER 3 RESULTS

## 3.1 Migration of OSBP phosphomutants

OSBP contains a putative serine-rich phosphorylation motif that starts with T379 and includes S381, 384, 387, 388, and 391 (Figure 3.1). S384, 387, 388 and 391 have been identified as potential CK1 sites that require prior phosphorylation of a serine or threonine at the +2 position for activity of CK1. When resolved by 6%-SDS-PAGE and visualized by western blot, OSBPs migrate as two distinct bands, which correspond to phosphorylated (upper band) and non-phosphorylated (lower band) at this SRM [111]. To examine the function of the SRM, OSBP T379A and OSBP S381A were made as mimics of constitutively non-phosphorylated OSBP and OSBP 3S→3E, OSBP 5S→5E, and OSBP 6S/T→6E were constructed as partially or fully phosphorylated OSBP by site-directed mutagenesis. To determine whether the phosphomutants had the expected migration on SDS-PAGE, CHO shOSBP cells were transfected with plasmids encoding OSBP phosphorylation mutants OSBP, OSBP T379A, OSBP S381A, OSBP 3S→3E, OSBP 5S→5E, and OSBP 6S/T→6E for 24 h (Figure 3.2). Migration of the mutants was analyzed by resolving the protein by 6%-SDS-PAGE, transferring to NC, and immunoblotting with OSBP antibody. Two bands were apparent in the OSBP and OSBP T379A samples, indicating partial phosphorylation of S381 and downstream sites. Only the lower band was present in OSBP S381A expressing cells, indicating that phosphorylation was blocked. Only the upper band was visible in extracts OSBP 3S→3E, OSBP 5S→5E, and OSBP 6S/T→6E expressing cells, indicating that these mutants mimicked the fully phosphorylated state.

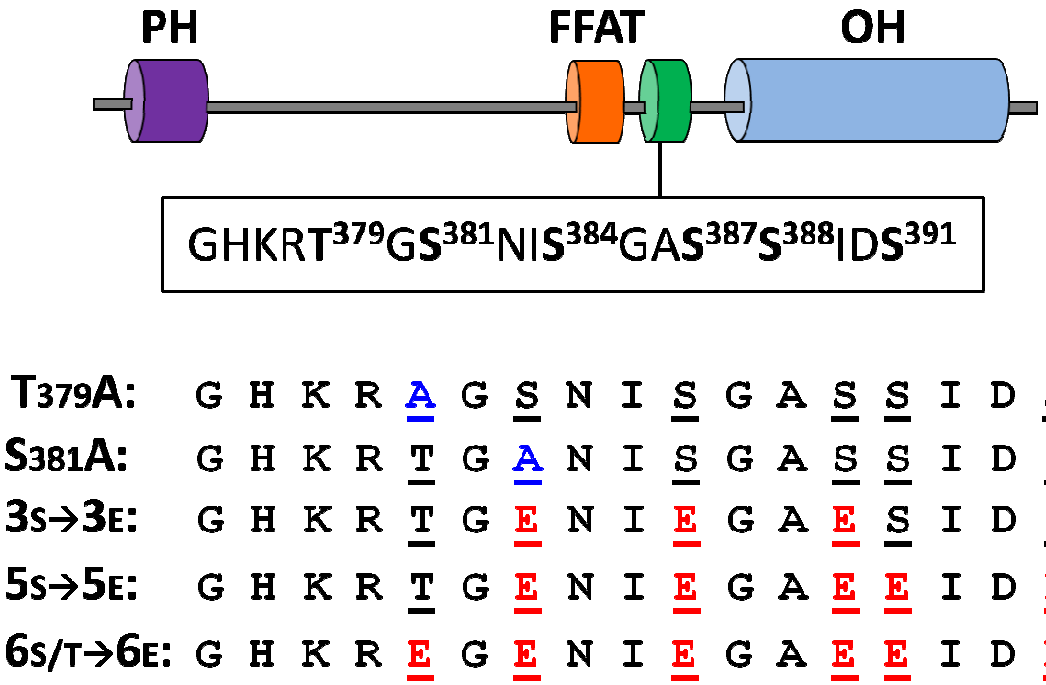


**Figure 3.1. OSBP dephospho- and phospho-mimics.** The serine-rich phosphorylation motif (green) in OSBP is located between the FFAT motif (orange) and OH domain (blue). Different phospho-mimics were generated through site directed mutagenesis: those that mimic constitutive dephosphorylation (T379A and S381A, blue residues) and constitutive phosphorylation (3S→3E, 5S→5E, and 6S/T→6E, red residues).

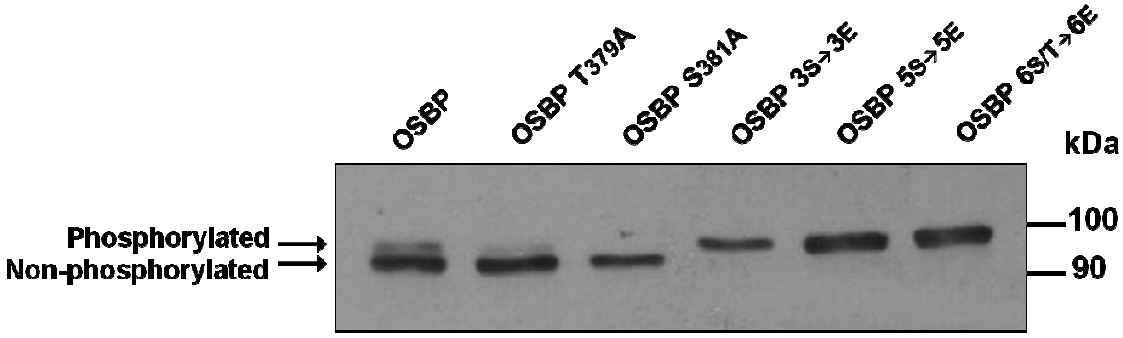


**Figure 3.2. Migration of OSBP phosphorylation mutants.** CHO shOSBP cells were transfected with plasmids encoding OSBP phosphorylation mutants. Cells were harvested after 24 h, lysed, and resolved by 6%-SDS-PAGE. After transfer to NC, the filters were immunoblotted using a monoclonal OSBP antibody and HRP-conjugated goat anti-mouse antibody.

### 3.2 Serine 381 is required for phosphorylation of downstream serine residues

To demonstrate that serine 381 was acting as the priming phosphorylation site for the downstream activity of CK1, determined by phosphor-peptide mapping [111], CHO cells were transfected for 24 h with plasmids encoding OSBP, OSBP T379A or OSBP S381A for 24 h. Cells were then treated with okadaic acid (OA), a PP2A phosphatase inhibitor, for 2 h to prevent dephosphorylation. Cells were harvested, lysed, the proteins were resolved by 6%-SDS-PAGE, transferred to NC and visualized by immunoblotting with an OSBP polyclonal antibody (Figure 3.3). Migration of OSBP and OSBP T379A shifted from the lower band to upper band with increasing concentrations of OA, indicating that the phospho-serine residues downstream of S381 were retained. OSBP S381A appeared as a slower migrating band and displayed no shift to the upper band, indicating that this mutant could not be phosphorylated by CK1 at the upstream sites. These results seem to exclude T379 as the priming phosphorylation site and suggest that serine 381 is required for the phosphorylation of downstream serine residues.

### 3.3 Mass spectrometry analysis of OSBP phosphorylation

To identify phosphorylation residues in the SRM, His-tagged OSBP was purified from stably expressing CHO cells and resolved by 6%-SDS-PAGE (Figure 3.4A). The upper and lower bands were excised, digested with trypsin and analyzed by mass spectrometry. The m/z ratios were calculated for each of the expected peptides produced from the tryptic digest. The peptide of interest was TGSNISGASSDISLDEQYK and contained the complete putative SRM. Three different peaks were identified in the MS spectra corresponding to the expected m/z ratios for the doubly-charged peptide. The

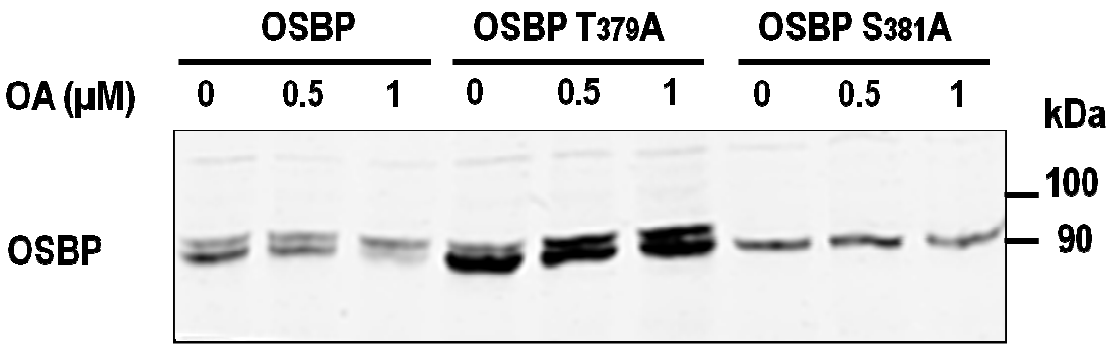


**Figure 3.3. Serine 381 phosphorylation but not threonine 379 is required for downstream phosphorylation of the SRM of OSBP.** CHO cells were transfected with plasmids encoding OSBP, OSBP T379A, or OSBP S381A for 24 h and then treated with the indicated concentrations of okadaic acid (OA) for 2 h prior to harvesting. Cells were lysed and resolved by 6%-SDS-PAGE, transferred to NC and immunoblotted using a polyclonal OSBP antibody and IRDye®-conjugated goat anti-rabbit antibody.

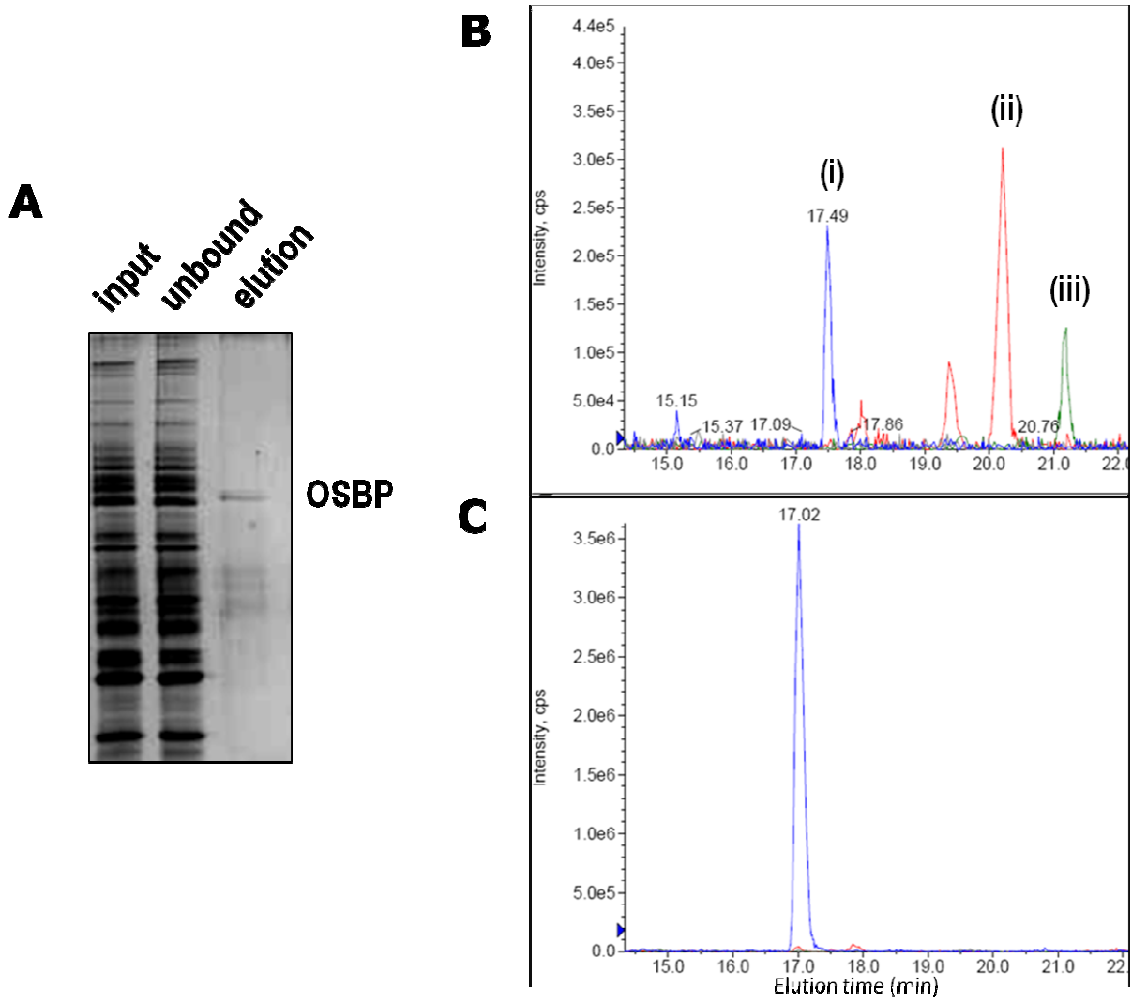


**Figure 3.4. Analysis of OSBP phospho-peptides by mass spectrometry.** CHO cells stably expressing OSBP with a C-terminal His-tag were harvested when confluent and OSBP-His was purified using metal affinity chromatography (MAC). (A) Purified protein was resolved by 6%-SDS-PAGE and stained with GelCode Blue Reagent. The upper and lower band were excised, digested with trypsin and analyzed by LC/MS. Expected m/z ratios calculated for the tryptic peptides were used to identify the TGSNISGASSDISLDEQYK peptide containing the serine-rich phosphorylation motif. (B) Extracted ion chromatogram of the upper band of OSBP. The blue peak (i) represents the non-phosphorylated peptide, the red peak (ii) represents the monophosphorylated peptide, and the green peak (iii) represents the diphosphorylated peptide based on the expected m/z ratios. (C) Extracted ion chromatogram of the lower band of OSBP. The peak represents the m/z ratio expected for the non-phosphorylated peptide.

non-phosphorylated peptide peak was located at 986.45 Da in both the upper and lower band spectra but was much more prominent in the lower band spectra (Figure 3.4C). The monophosphorylated peptide peak (1026.44 Da) and the diphosphorylated peptide peak (1066.42 Da) were both found only in the upper band spectra (Figure 3.4B). MS/MS analysis was performed on the non-phosphorylated peptide (Figure 3.5A) and the monophosphorylated peptide (Figure 3.5B). The diphosphorylated peptide did not produce a signal strong enough for MS/MS analysis. Fragmentation of the non-phosphorylated peptide produced a $b_5$ ion (TGNSI) with a peak at 473.3 Da and a corresponding $y_{14}$ ion (SGASSDISLDEQYK) with a peak at 1499.5 Da. Both of these values are the expected m/z ratios for the fragments without a phosphate group. MS/MS analysis of the monophosphorylated peptide produced two peaks for the $b_5$ ion; one at 525.2 Da, indicative of a phosphate residue present on the ion, and one at 455.2 Da indicating the loss of a phosphate residue to produce a dehydroalanine, the product when a phosphorylated serine residue loses a phosphoric acid. The monophosphorylated peptide also had a $y_{14}$ ion at 1499.5 Da, meaning that the peptide was not phosphorylated in this part of the peptide. From the MS/MS data it can be concluded that the monophosphorylated peptide observed is phosphorylated at serine 381.

### 3.4 Protein kinase A inhibition results in dephosphorylation of OSBP

After confirming through both mass spectrometry and western blotting that serine 381 phosphorylation initiated phosphorylation at downstream serine residues, it was of

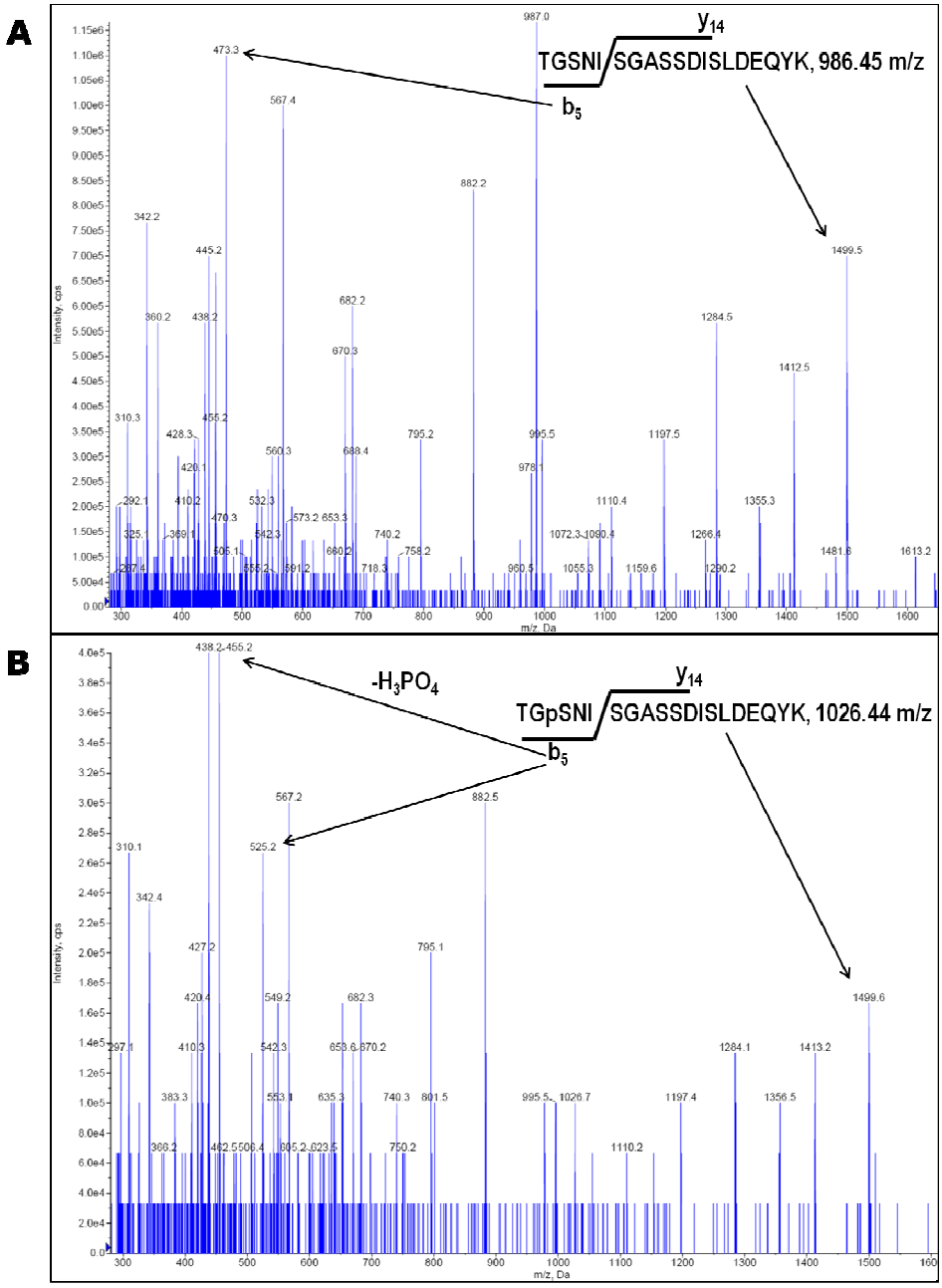


**Figure 3.5. Serine 381 is phosphorylated in the monophosphorylated peptide detected by mass spectrometry.** Phosphopeptides identified by LC/MS were fragmented to produce MS/MS spectra. (A) The non-phosphorylated peptide had a $y_{14}$ ion and a $b_5$ ion both of which had masses indicative of a peptide fragment with no phosphate moiety. (B) The mono-phosphorylated peptide had an identical $y_{14}$ ion to the non-phosphorylated MS/MS with no phosphate group attached. There were two peaks representing the $b_5$ ion, one at the expected mass of the $b_5$ ion with the addition of a phosphate and one peak indicating that the $b_5$ ion had lost phosphoric acid within the mass spectrometer producing a dehydroalanine residue instead of a serine.

interest to identify the potential kinase that phosphorylates this site. Using the PHOSIDA website (http://phosida.org/) [139], PKA was identified as a potential kinase for S381 of OSBP. PKA sites have a consensus sequence RRXS/TY, where X is a small residue and Y is a hydrophobic residue, an arginine may be replaced by a lysine residue [141]. To determine whether PKA does phosphorylate OSBP at this site, CHO cells were treated with the PKA-specific inhibitor Rp-cAMPS, which is a cyclic adenosine monophosphate (cAMP) analogue that prevents dissociation of PKA from the regulatory subunit [145], for up to 8 h. Cells were harvested at different time points, lysed in SDS gel-loading buffer and resolved by 6%-SDS-PAGE. The samples were transferred to NC, immunoblotted for endogenous OSBP using a polyclonal antibody, and visualized using a LI-COR Odyssey (Figure 3.6A). The fluorescence intensity of the upper and lower bands were quantified and used to calculate the percentage of protein in the lower band (Figure 3.6B). PKA inhibition caused a gradual increase of 20% over time in the amount of OSBP in the lower band indicating that PKA inhibition decreased OSBP phosphorylation at the SRM.

### 3.5 Stable silencing of OSBP in CHO cells using lentiviral shRNA

CHO cells that do not express OSBP were created to characterize the function of OSBP phosphomutants with respect to localization, stimulation of SM synthesis, and interaction with VAP. CHO cells were infected with lentiviral constructs encoding shNT or shOSBP and were selected with blasticidin for 2 weeks to produce a stable knockdown cell line. Cells were harvested, lysed, resolved by 6%- SDS-PAGE, and OSBP

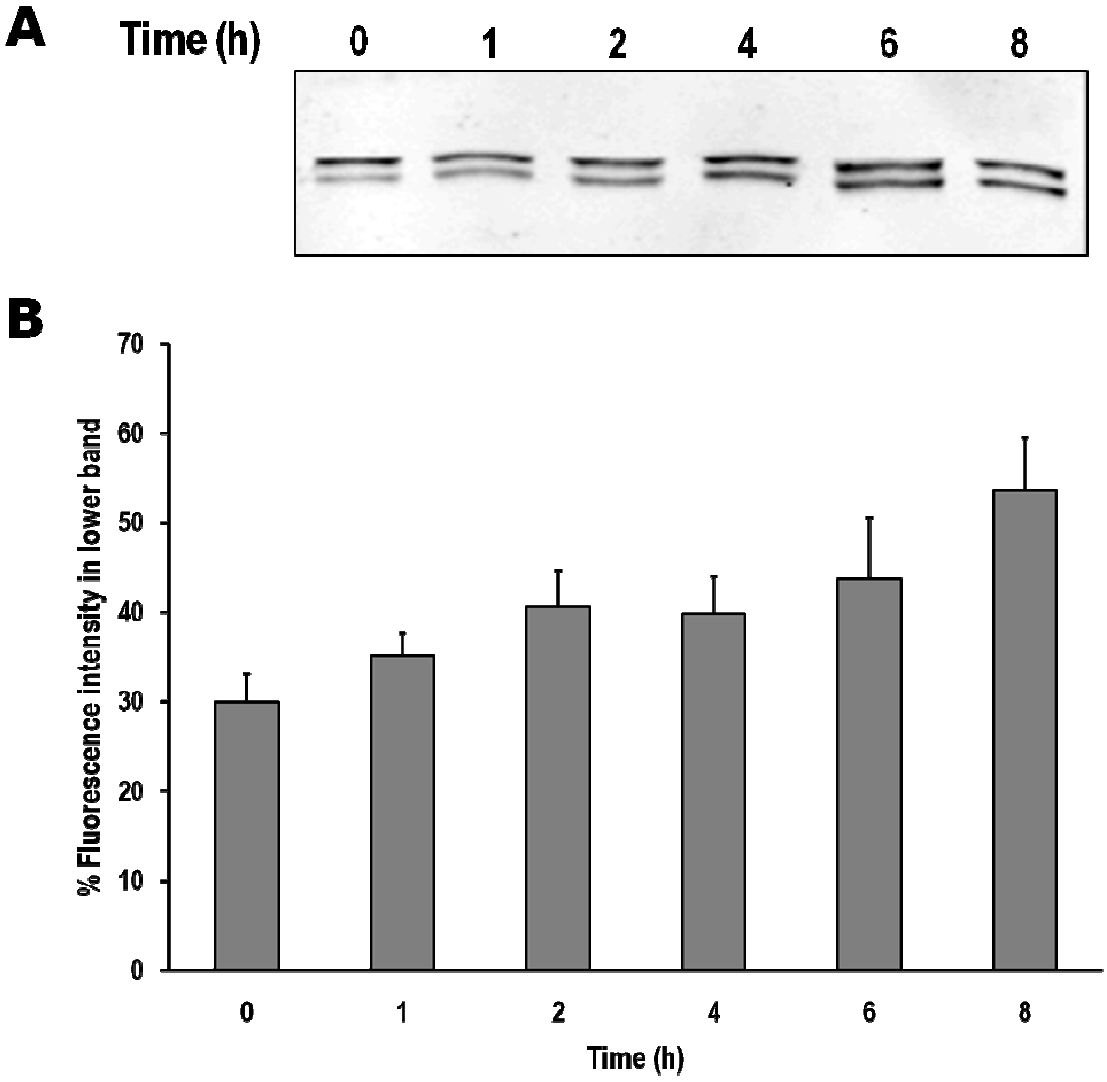


**Figure 3.6. Inhibition of PKA activity decreases OSBP phosphorylation.** CHO cells were treated with 50 μM Rp-cAMPS for the indicated time prior to harvest. (A) Samples were resolved by 6%-SDS-PAGE, transferred to NC and immunoblotted for OSBP using a polyclonal antibody and IRDye®- conjugated GAR 800CW antibody with a LI-COR Odyssey. (B) Fluorescence intensity of each of the bands to quantify the percentage of fluorescence in the lower band. Results are the mean and range of two independent experiments.

was identified by immunoblotting with an OSBP polyclonal antibody and compared to an actin control (Figure 3.7). The lentiviral constructs stably reduced OSBP protein by approximately 90% in CHO cells.

### 3.6 OSBP phosphorylation does not affect localization in response to 25OH treatment

OSBP translocates from the cytoplasm/ER to the *trans*-Golgi network upon treatment with 25OH [133]. Phosphorylation of OSBP may play a role in localization between the Golgi and the ER [133,146] by altering OSBP conformation and inhibiting the association of the PH domain with PI-4-P or the FFAT domain with VAP. To test whether OSBP localization was affected by phosphorylation, CHO shOSBP cells were transfected with plasmids encoding OSBP, OSBP S381A, or OSBP 5S→5E for 24 h and treated with 25OH or ethanol vehicle for 2 h prior to harvest. Cells were probed with an OSBP monoclonal antibody and a Golgi-specific giantin polyclonal antibody, and visualized using confocal microscopy (Figure 3.8). With no treatment, OSBP is localized primarily in the cytoplasm and ER, and upon 25OH treatment, OSBP translocates to the Golgi. OSBP S381A was localized more in the Golgi apparatus than the wild-type protein, and upon treatment with 25OH there was no increase in Golgi localization compared to the untreated cells. The OSBP phosphorylation mimic, OSBP 5S→5E, was localized to the cytoplasm and ER without 25OH treatment, similar to wild-type OSBP. When cells transfected with OSBP 5S→5E were treated with 25OH, OSBP still translocated to the Golgi, however, this localization seemed to be somewhat less than the wild-type protein.

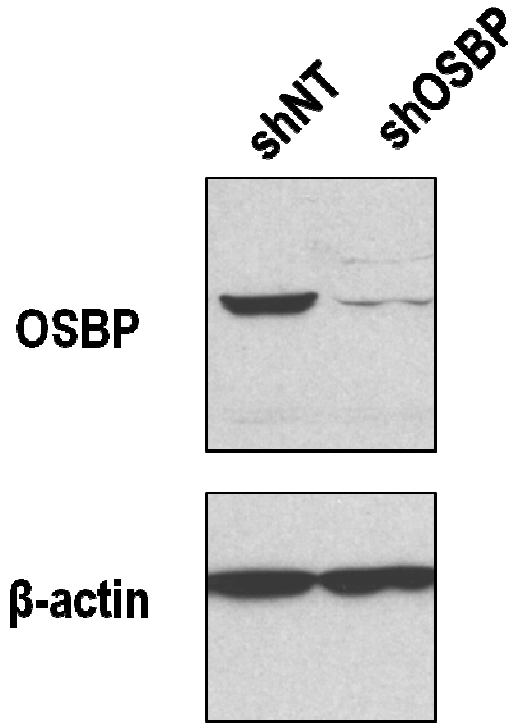


**Figure 3.7. Lentiviral knockdown of OSBP in CHO cells.** CHO cells were infected with lentiviral constructs encoding a non-targeting shRNA (shNT) or an shRNA specific for OSBP (shOSBP). Cells were selected in media A with 5 µg/mL blasticidin for 2 weeks and then maintained in the same media. CHO shNT and CHO shOSBP cells were harvested, lysed and resolved by SDS-PAGE, transferred to NC and visualized by immunoblotting using polyclonal OSBP and monoclonal β-actin antibodies and HRP-conjugated GAR and GAM antibodies.

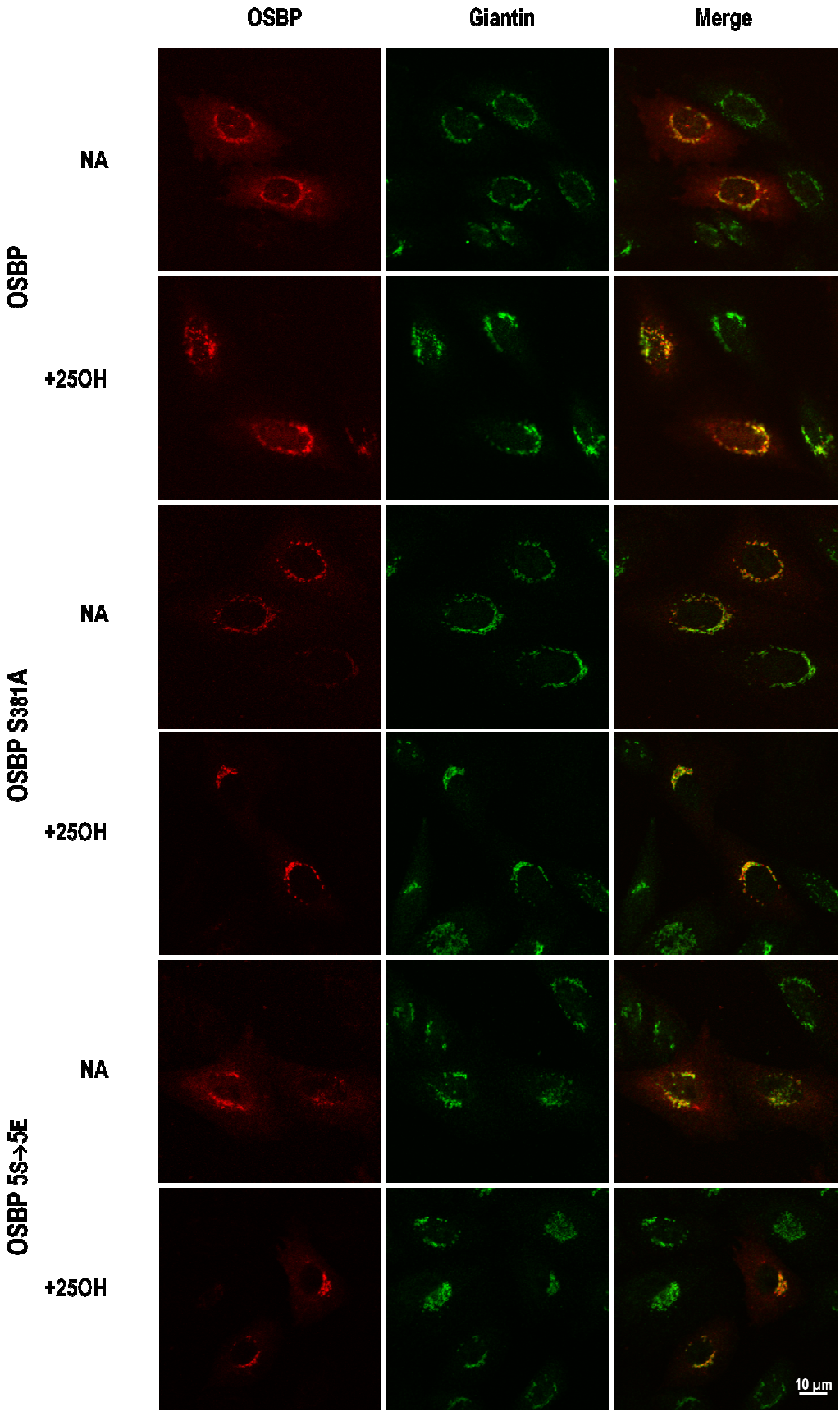
OSBP
Giantin
Merge
OSBP
NA
+25OH
OSBP S381A
NA
+25OH
OSBP 5S→5E
NA
+25OH
10 µm

**Figure 3.8. OSBP phosphorylation does not affect Golgi localization.** CHO shOSBP cells were transfected with plasmids encoding OSBP, OSBP S381A, or OSBP 5S→5E for 48 h and treated with ethanol or 25OH for 1 h prior to fixing in 3% formaldehyde and permeablization in 0.05% Triton X-100. Cells were probed with a monoclonal OSBP antibody and a polyclonal giantin antibody followed by an AlexaFluor GAM 594 and GAR 488. Microscopy was performed on a Zeiss LSM 510 Meta laser scanning confocal microscope with a 100x objective. Images are single optical sections of 0.6 µm.

However, phosphorylation does not appear to effect the intracellular localization of OSBP.

### 3.7 OSBP phosphorylation does not affect stimulation of SM synthesis by 25OH

It has been previously found that OSBP is required for the stimulation of SM synthesis when cells are treated with 25OH, and that both the FFAT and PH domains of OSBP are needed for this effect [116]. Since there appeared to be a small change in the localization of OSBP 5S→5E to the Golgi apparatus, phosphorylation may have a role in the stimulation of SM synthesis. In order to observe the effects of OSBP phosphorylation on the stimulation of SM synthesis CHO shNT and shOSBP cells were transfected with empty vector, or plasmids encoding OSBP or the OSBP phospho-mutants for 48 h. Cells were incubated with ethanol or 25OH for 4 h in serine-free media A and then labelled with [$^{3}$H]serine for 2 h. Cells were harvested and lipids were extracted and resolved by TLC. Radioactivity was measured in SM (Figure 3.9A), glucosylceramide (Figure 3.9B), ceramide (Figure 3.9C), PS (Figure 3.10A) and PE (Figure 3.10B). Knockdown of OSBP resulted in no response to 25OH treatment however transfection of the CHO shOSBP cells with wild-type OSBP restored activation of SM synthesis with 25OH. However, there was no significant difference between OSBP and the phospho-mutants in SM, glucosylceramide, ceramide, PS or PE. A slight attenuation of SM synthesis by OSBP 5S→5E and OSBP 6S/T→6E was apparent but not significant when cells were treated with 25OH. No change in ceramide levels indicates that it was being converted to SM. Glucosylceramide increases with 25OH treatment with OSBP and the phospho-mutants indicating that ceramide is also being converted to glucosylceramide normally. The lack

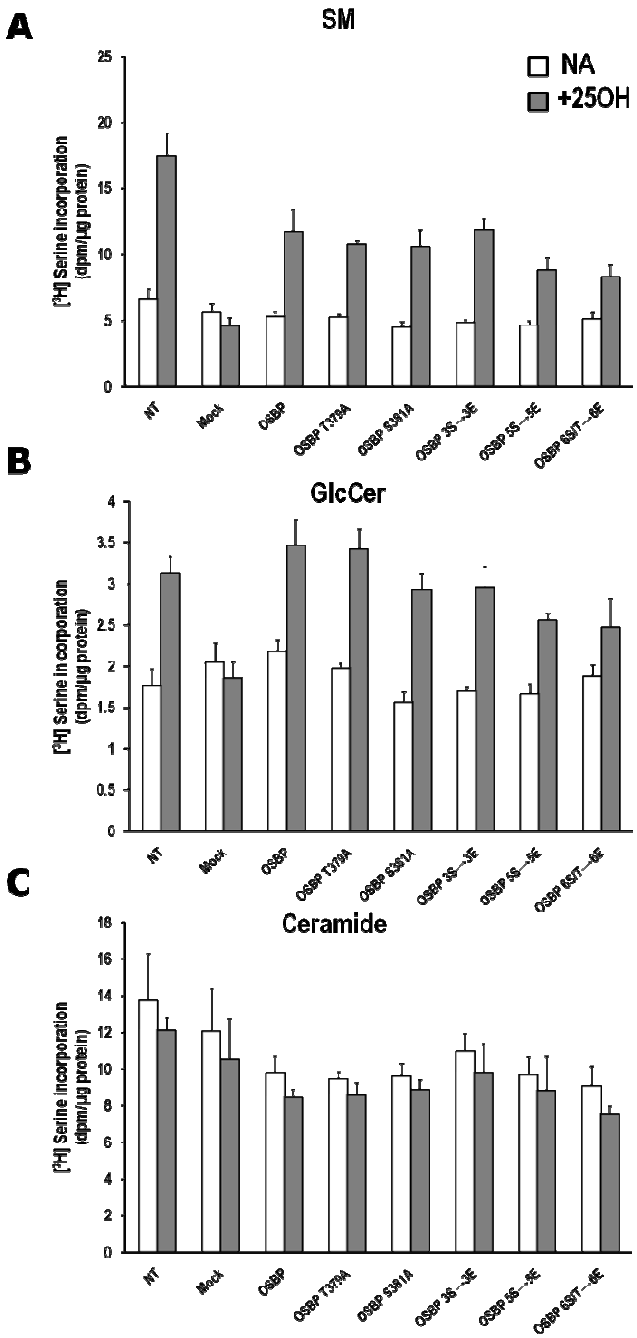


**Figure 3.9. OSBP phosphorylation has no effect on 25OH-stimulated SM synthesis.** CHO shNT and shOSBP cells were transfected with empty vector, or plasmids encoding OSBP or the phospho-mutants for 48 h. Cells were incubated for 4 h with ethanol or 2.5 µg/mL 25OH in serine-free media A and then labelled for 2 h in serine-free media A with 5 µCi/mL [$^3$H]serine. Cells were harvested as described in Materials and Methods and resolved by TLC. Incorporation of [$^3$H] serine into (A) SM, (B) glucosylceramide (C) ceramide was quantified by measuring the radioactivity of each sample and normalizing to total cell protein. Results are the mean and standard error of the mean (SEM) for 4 independent experiments.

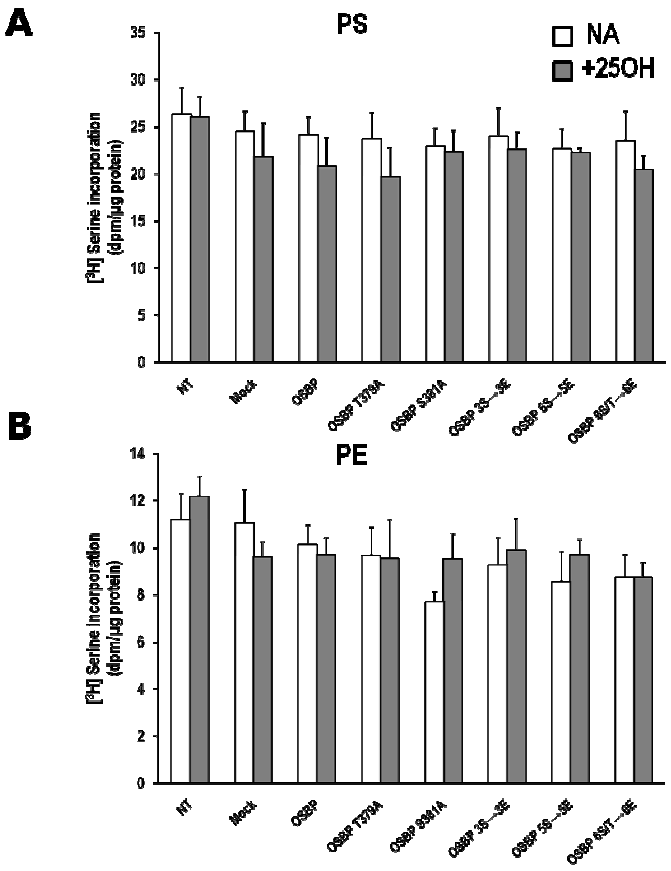


**Figure 3.10. OSBP phosphorylation has no effect on serine incorporation into PS or PE.** CHO shNT (NT) and shOSBP cells were transfected with empty vector (Mock), or plasmids encoding OSBP or the phospho-mutants for 48 h. Cells were incubated for 4 h with ethanol or 2.5 µg/mL 25OH in serine-free media A and then labelled for 2 h in serine-free media A with 5 µCi/mL [$^3$H]serine. Cells were harvested as described in Materials and Methods and resolved by TLC. Incorporation of [$^3$H] serine into PS (A) and PE (B) were quantified by measuring the radioactivity of each sample and normalizing to protein. Results are the mean and SEM for 4 independent experiments.

of change among PS and PE indicated that there was no effect on serine uptake by the cells.

### 3.8 OSBP protein purification from Sf21 insect cells

To measure the binding, extraction and transfer activities of OSBP in comparison to the phospho-mutants, His-tagged OSBP, OSBP S381A, and OSBP 5S→5E were each expressed in Sf21 cells by infection of baculovirus encoding these proteins. After a 72 h infection, proteins were purified from the cells by MAC, resolved by 6%-SDS-PAGE, and visualized by GelCode Blue staining (Figure 3.11). Each of the proteins was purified successfully and the difference in mobility between OSBP and OSBP 5S→5E was apparent.

### 3.9 Phosphorylated OSBP has a higher binding capacity for 25OH and cholesterol than non-phosphorylated OSBP

The serine-rich phosphorylation motif is adjacent to the sterol binding motif of OSBP, therefore it is important to establish whether phosphorylation has an effect on the sterol binding activity of OSBP. Purified OSBP and OSBP 5S→5E were incubated with increasing concentrations of [$^3$H]25OH or [$^3$H]cholesterol in ethanol in the presence or absence of a 40x excess of unlabelled 25OH or cholesterol, respectively. For 25OH binding assays, samples were incubated with charcoal-dextran, centrifuged, and radioactivity was measured in the supernatant (Figure 3.12A). For cholesterol binding assays, samples were incubated with MAC resin, eluted with 150 mM imidazole, centrifuged and the supernantant radioactivity was measured (Figure 3.12B). Specific binding was determined by subtracting the non-specific binding (in the presence of 40X unlabelled ligand) from the total binding. $B_{Max}$ and $K_d$ were calculated by fitting the data

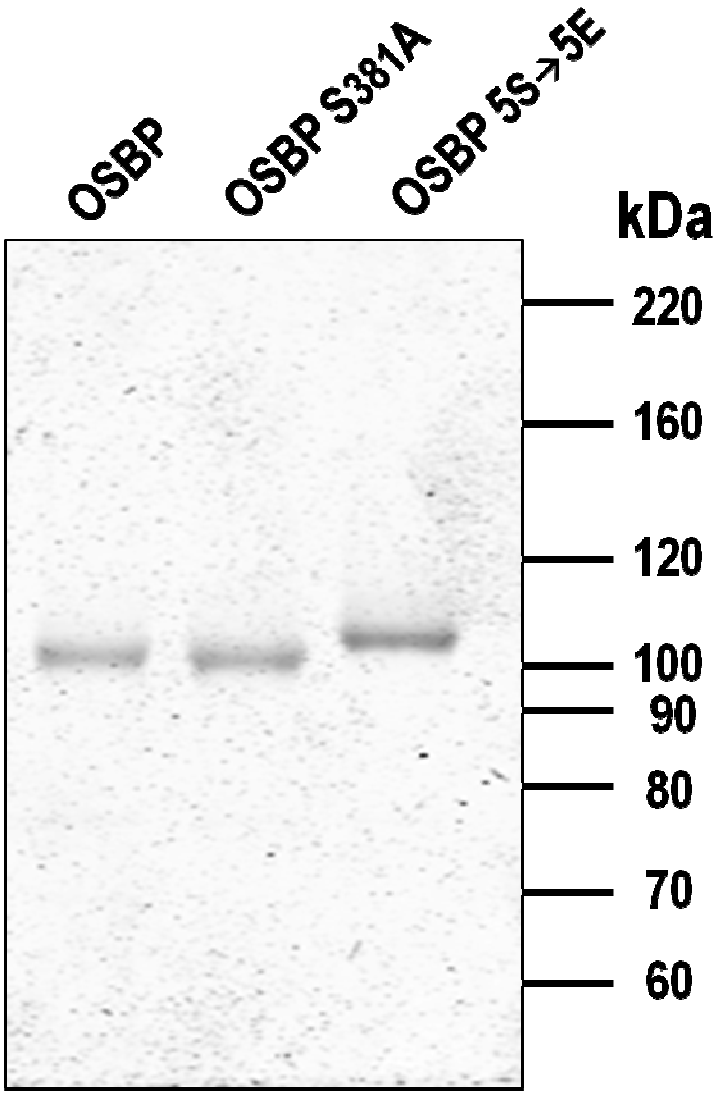


**Figure 3.11. Purified OSBP and phosphomutants.** SF21 insect cells grown in suspension were infected with baculovirus encoding His-tagged OSBP, OSBP S381A or OSBP 5S→5E**.** After 72 h, proteins were purified using MAC and DEAE-Sepharose ion-exchange chromatography. Proteins were analyzed for purity by 6%-SDS-PAGE and staining with GelCode Blue Reagent.

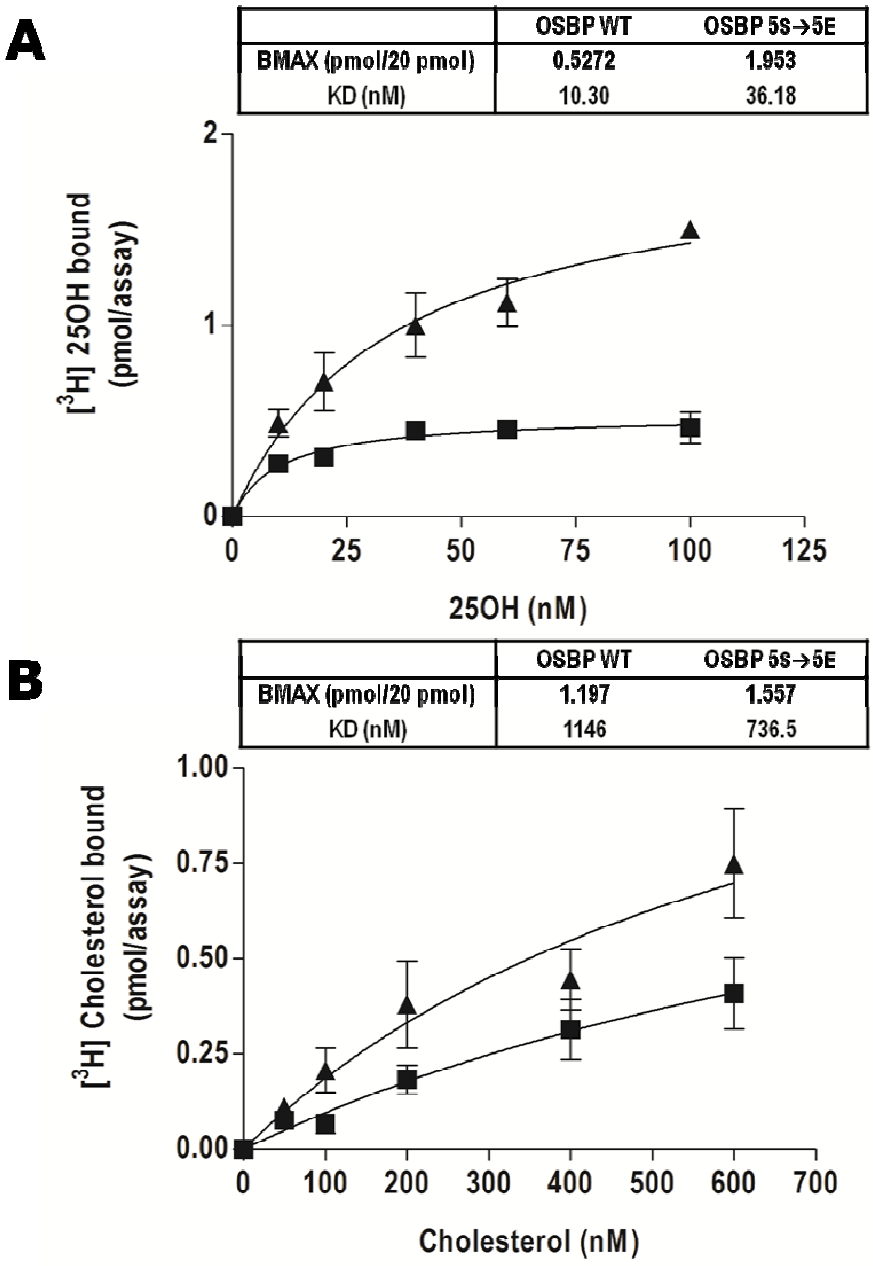


**Figure 3.12. Sterol binding activity of wild type OSBP and OSBP 5S→5E.** Purified OSBP WT and OSBP 5S→5E (20pmol) were incubated with radiolabeled sterol to obtain total sterol binding curves. (A) Proteins were incubated with [$^3$H] 25OH or a 40X excess of 25OH overnight at 4°C. Samples were incubated with charcoal-dextran, centrifuged and supernatants were measured for radioactivity. (B) Proteins were incubated with [$^3$H]cholesterol or a 40X excess of cholesterol for 2 h at room temperature. OSBP was bound to Talon Resin, eluted with imidazole, and radioactivity was measured in supernatants. Specific binding was calculated by subtracting non-specific binding from total binding. Results are the mean and SEM of three independent experiments.

to a non-linear regression curve with a one-site binding model using Prism. For 25OH binding, both the $K_d$ and $B_{Max}$ increased for OSBP 5S→5E in comparison to OSBP, indicating a decreased binding affinity and increased binding capacity. For cholesterol, the $B_{Max}$ increased for OSBP 5S→5E but the $K_d$ decreased in comparison to OSBP, indicating an increase in binding capacity and an increase in affinity for cholesterol.

### 3.10 Phosphorylated OSBP extracts more cholesterol from liposomes

*In vitro*, OSBP 5S→5E had a higher binding capacity for cholesterol than wild-type OSBP meaning that it also might also extract more cholesterol from liposomes. To test this, increasing amounts of purified OSBP, OSBP S381A, or OSBP 5S→5E were incubated with liposomes containing PC, PE, PS and PI (49:20:10:10 mol/mol) with 10% lactosyl-PE, 1% cholesterol and [$^{14}$C]PC and [$^{3}$H]cholesterol for 25 min at 25°C, 1 µg of lectin was added and samples were incubated for 15 min at 4°C and centrifuged for 10 min at 13,000 rpm at 4°C (Figure 3.13). The radioactivity in the supernatant was measured to determine the amount of cholesterol extracted from the liposomes. OSBP and OSBP S381A extracted cholesterol from the liposomes to a similar extent. OSBP 5S→5E extracted approximately two-fold more cholesterol than both OSBP and OSBP S381A. Cholesterol extraction increased in response to the increase in protein amount for each of the OSBPs.

### 3.11 OSBP S381A and OSBP 5S→5E mutations do not affect association with PIPs

Immunofluorescence microscopy indicated that the phosphorylation of OSBP did not affect Golgi localization in response to 25-OH therefore possibly not

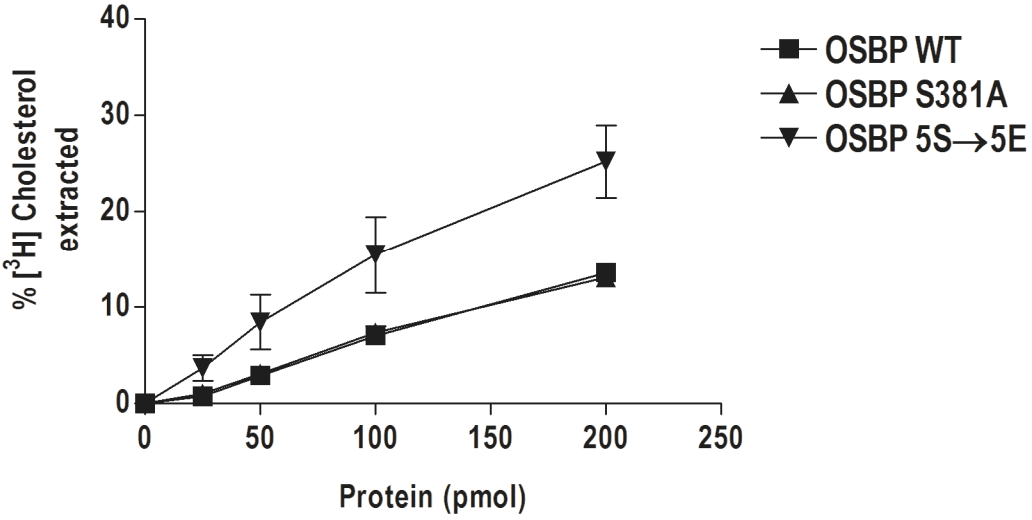


**Figure 3.13. Cholesterol extraction activity of wild-type OSBP, OSBP S381A and OSBP 5S→5E.** Liposomes containing 1 mol% [$^3$H]cholesterol were incubated with the indicated amounts of purified OSBP, OSBP S381A, or OSBP 5S→5E for 30 minutes at 25°C. Liposomes were incubated with 1 µg of lectin, centrifuged at 13,000 rpm for 10 min at 4°C and radioactivity of the supernatants was measured to obtain the amount of cholesterol extracted by OSBP. Results are the mean and SEM of three independent experiments.

influencing the association of OSBP with PI-4-P. To determine whether phosphorylation affected the interaction between OSBP and PIPs, liposomes were made containing 10 mol% PI, PI-4-P, or PI-4,5$P_2$. Purified OSBP, OSBP S381A, or OSBP 5S→5E were incubated with liposomes for 30 min at 25°C, sedimented at 100,000x g for 1 h at 4°C, and both the pellet and supernatant fractions were resolved by 6%-SDS-PAGE and visualized using GelCode Blue reagent (Figure 3.14A). The results were quantified by measuring the fluorescence of each of the bands and calculating the amount of protein located in the pellet and supernatant of each sample (Figure 3.14B and C). OSBP, OSBP S381A, and OSBP 5S→5E bound to each of the PIPs to the same extent; approximately 50% of the protein bound to the PI liposomes, 60% bound to the PI-4-P liposomes, and 85% bound to the PI-4,5-$P_2$ liposomes.

### 3.12 OSBP phosphomutants have similar binding to immobilized PIPs

Determination of the binding of OSBP and OSBP 5S→5E was performed to establish whether phosphorylation of OSBP had an effect on binding of PH domain to PIPs immobilized on NC. Purified OSBP and OSBP 5S→5E were incubated with NC membranes that had been spotted with increasing amounts of PI-4-P, PI-4,5-$P_2$ and PC. The membranes were probed with an OSBP monoclonal antibody and visualized using a IRDye®-GAM secondary antibody (Figure 3.15). OSBP and OSBP 5S→5E both bound to PI-4-P but not PI-4,5$P_2$ or PC. However, OSBP 5S→5E did not have any apparent changes in PI-4-P binding in comparison to wild-type OSBP.

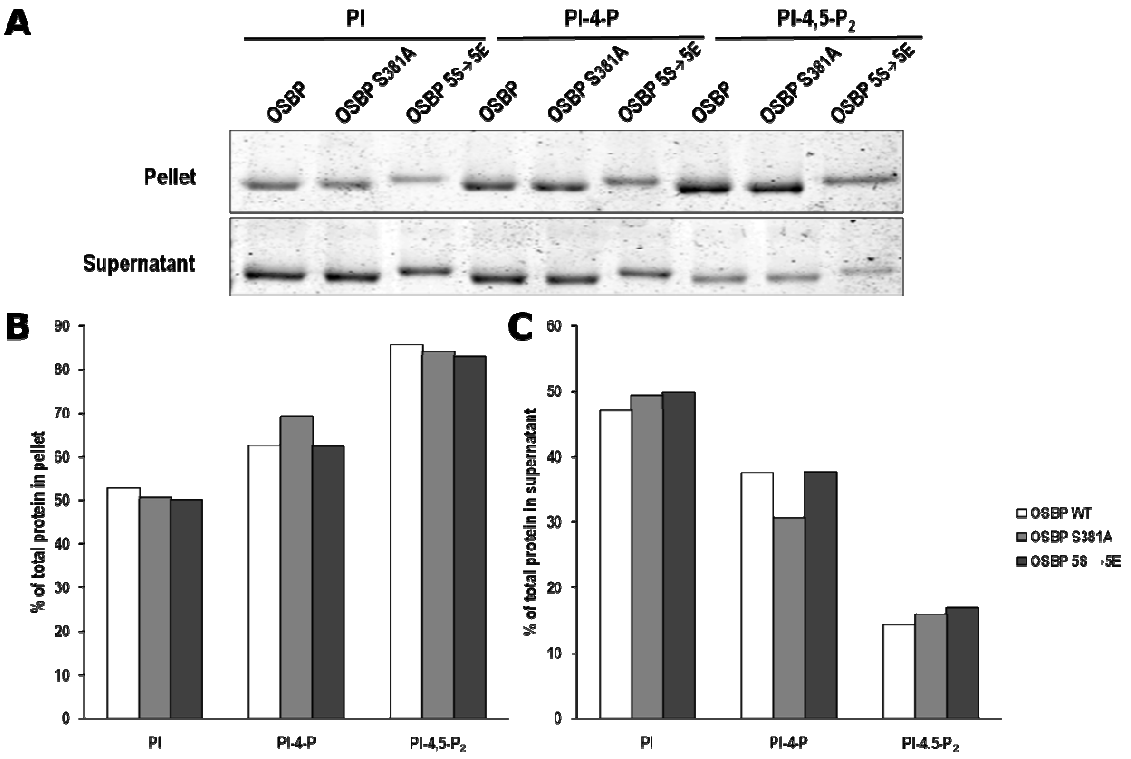


**Figure 3.14. OSBP phosphorylation does not affect affinity for phosphotidylinositol phosphates.** Purified OSBP, OSBP S381A, and OSBP 5S→5E were incubated with liposomes containing 10 mol% PI, PI-4-P, or PI-4,5$P_2$ for 25 min at 25°C. Liposomes were centrifuged at 100,000x g for 1 h at 4°C. (A) The pellet and supernatant fractions were solublized in SDS loading buffer and resolved by 6%-SDS-PAGE. Gels were stained with GelCode Blue Reagent and protein quantified using a LI-COR Odyssey to measure the fluorescence intensity of each band. (B) Percent of total protein measured in the pellet fraction of each sample. (C) Percent of total protein measured in the supernatant of each sample.

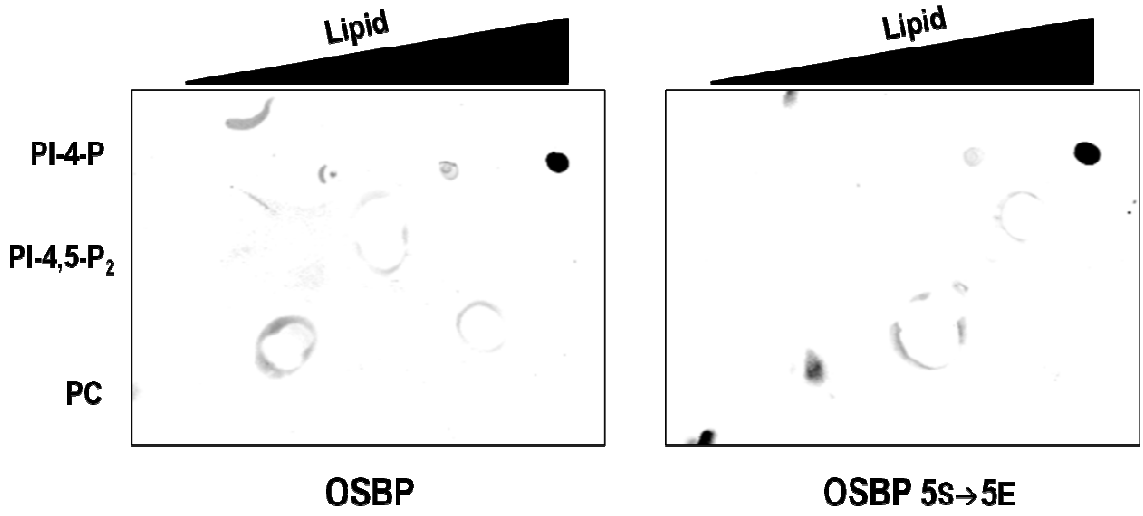


**Figure 3.15. OSBP phosphorylation does not affect PIP binding affinity.** NC membranes were spotted with increasing amounts of PI-4-P, PI-4,5-$P_2$ and PC (0, 100, 200 and 500 pmol), dried and blocked in TBS with 3% FA-free BSA. Membranes were incubated with 200 pmol of purified OSBP or OSBP 5S→5E for 1 h, probed with OSBP monoclonal antibody and visualized with IRDye® conjugated GAM secondary antibody. Membranes were visualized using a LI-COR Odyssey.

### 3.13 OSBP 5S→5E has decreased transfer of cholesterol to liposomes

OSBP 5S→5E binds to and extracts more cholesterol than OSBP but has normal binding to PIPs in liposomes or on NC (Figure 3.14 and 3.15). To determine if the transfer of cholesterol via PH domain localization to liposomes is affected, purified OSBP, OSBP S381A and OSBP 5S→5E were incubated with [$^3$H]cholesterol for 2 h at 20°C, bound to MAC resin, and eluted with 150 mM imidazole. Sterol-loaded OSBPs were then incubated with liposomes containing 10 mol% concentration of PI, PI-4-P, or PI-4,5$P_2$ for 5 min at 25°C. Liposomes and bound protein were incubated with lectin, centrifuged and radioactivity in the supernatant and pellet fractions were measured. The percentage of transfer from the sterol-labelled OSBPs to the pellet fraction (Figure 3.16) showed there was no significant difference in transfer between PI, PI-4-P or PI-4,5-$P_2$. OSBP and OSBP S381A transferred approximately 50% of the total cholesterol for each of the different liposomes; however, OSBP 5S→5E transferred 10% less cholesterol to liposomes with each PIPs compared to OSBP or S381A.

### 3.14 VAP immunoprecipitates more OSBP 5S→5E than wild-type OSBP

OSBP contains a FFAT motif that localizes it to the ER by an association with VAP [146]. Extraction and transfer assays showed that OSBP 5S→5E had increased uptake of cholesterol from liposomes but a slight decrease in cholesterol transport to liposomes. Since OSBP likely extracts cholesterol from the ER while associated with VAP, OSBP phosphorylation could be causing an increase in binding of OSBP to the ER, via VAP, to increasing sterol loading. . To determine if OSBP 5S→5E had increased binding to VAP, CHO shOSBP cells were transfected with plasmids expressing OSBP, OSBP S381A or OSBP 5S→5E for 24 h. Cells were harvested, extracted with Triton X-

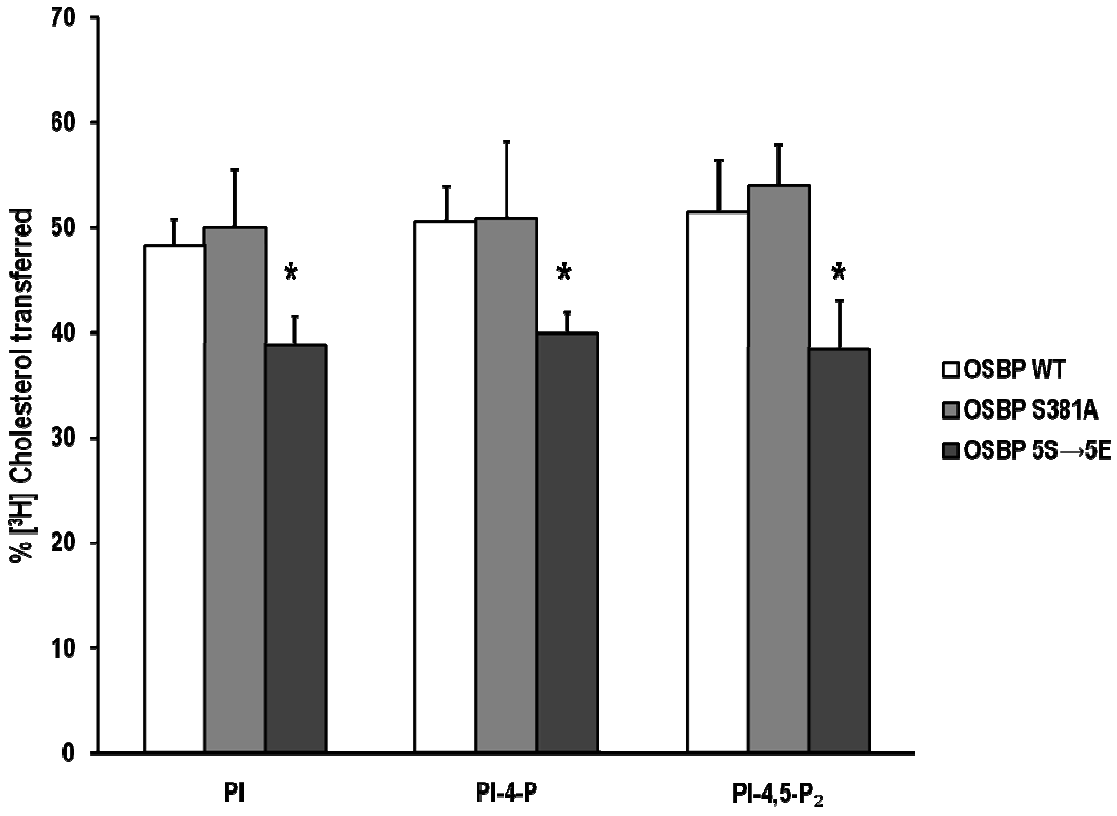


**Figure 3.16. OSBP 5S→5E has reduced transfer of cholesterol to liposomes.** Purified OSBP, OSBP S381A, and OSBP 5S→5E were incubated with [$^3$H]cholesterol for 2 h at 20°C. Protein was bound to Talon resin, eluted with 150 mM imidazole and incubated with liposomes containing 10 mol% PI, PI-4-P, or PI-4,5$P_2$ for 5 min at 25°C. Liposomes were incubated with 1 µg of lectin for 15 min at 4°C, centrifuged at 13,000 rpm for 10 min at 4°C and the radioactivity of the supernatant and pellet fractions was measured. The percentage of transfer was calculated as the amount of radioactivity in the pellet compared to the total input. Data is presented the mean and SEM of three independent experiments. *P<0.01, compared to OSBP (two-tailed t-test).

100 and incubated with VAP polyclonal antibody. Protein bound to VAP was precipitated using protein A Sepharose beads, washed with PBS with Triton X-100, resuspended, resolved by 10%-SDS-PAGE and visualized by immunoblotting with an OSBP monoclonal antibody (Figure 3.17A). Immunoprecipitation was quantified by measuring the fluorescence of each of the bands and calculating the percentage of OSBP precipitated in comparison to the total input (Figure 3.17B). VAP precipitated approximately six-fold more OSBP 5S→5E than OSBP and OSBP S381A indicating that the negative charge of OSBP increases its association with VAP.

### 3.15 GST-VAP pulls down more OSBP 5S→5E than wild-type OSBP

GST-tagged VAP was used to pull down overexpressed OSBP to confirm that OSBP 5S→5E has increased association with VAP in comparison to OSBP. CHO shOSBP cells were transfected with plasmids encoding OSBP, OSBP S381A, or OSBP 5S→5E for 24 h. Cells were harvested, extracted with Triton X-100 and incubated with GST-VAP or GST for 30 min at 20°C. Samples were incubated with glutathione Sepharose beads, washed with PBS with Triton X-100, resuspended, resolved by 10%-SDS-PAGE and visualized by immunoblotting with an OSBP monoclonal antibody (Figure 3.18A). Pull-down was quantified by measuring the fluorescence of each of the bands and calculating the percentage of protein pulled down in comparison to the total input (Figure 3.18B). GST-VAP pulled down three-fold more OSBP 5S→5E than OSBP and two-fold more than OSBP S381A. The GST-VAP pulldown in combination with the VAP immunoprecipitation (Figure 3.17A and B) show that OSBP 5S→5E has an increased association with VAP.

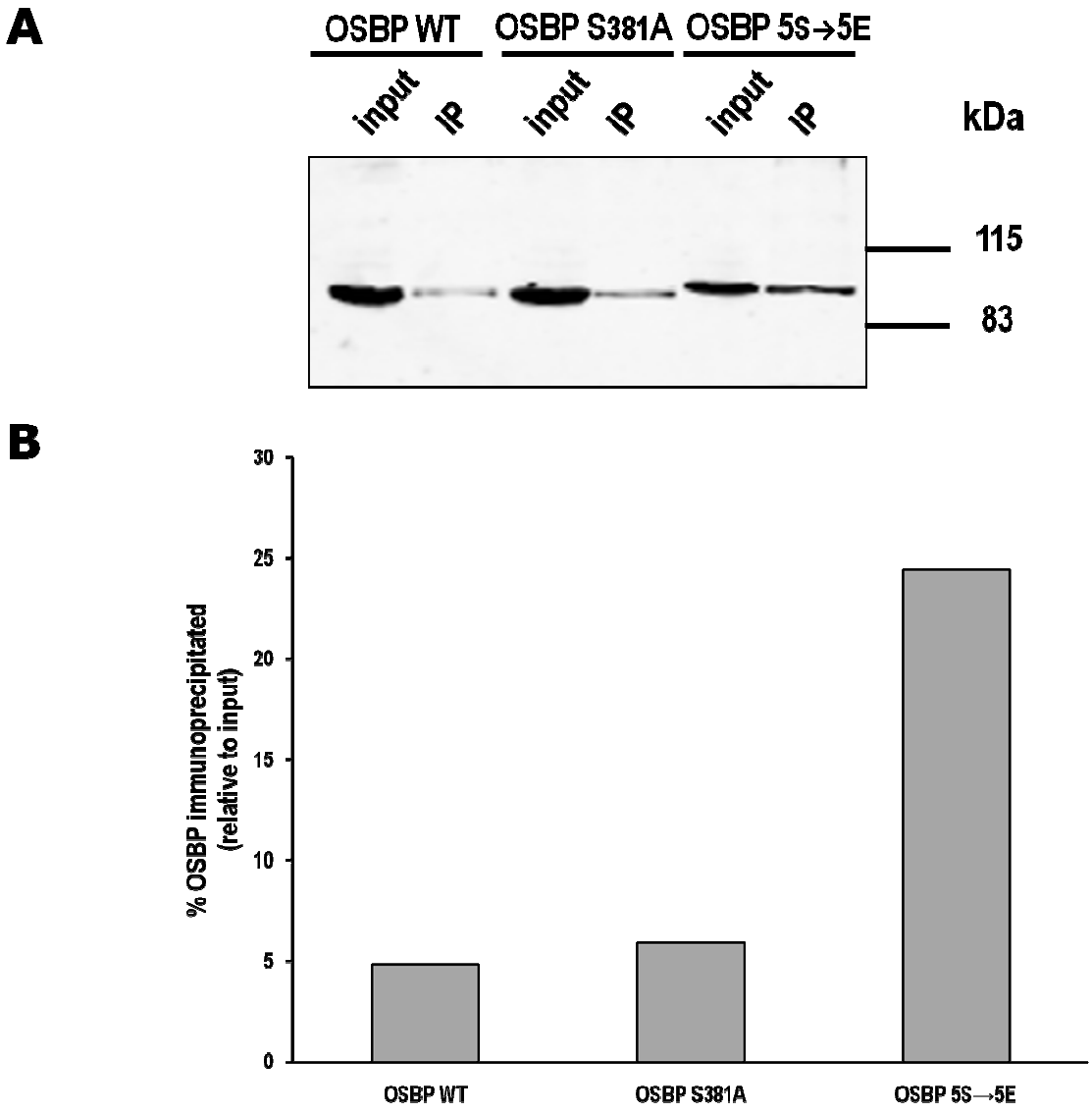


**Figure 3.17. Co-immunoprecipitation of OSBP phosphorylation mutants with VAP.** CHO shOSBP cells were transfected with plasmids encoding OSBP, OSBP S381A, or OSBP 5S→5E for 24 h. Cells were harvested and extracted using 0.5% Triton X-100, the soluble fraction was incubated with a VAP polyclonal antibody for 16 h at 4°C. The antibody was precipitated using protein A Sepharose, beads were washed with PBS with 0.5% Triton X-100 and resuspended in SDS gel-loading buffer. (A) Samples were resolved by 10%-SDS-PAGE, transferred to NC, immunoblotted with OSBP monoclonal antibody and IRDye® conjugated GAM 580LT, and visualized using a LI-COR Odyssey. (B) Quantification of western blot analysis was performed using fluorescence intensity of each of the bands to calculate the percentage of OSBP immunoprecipitated of the total input.

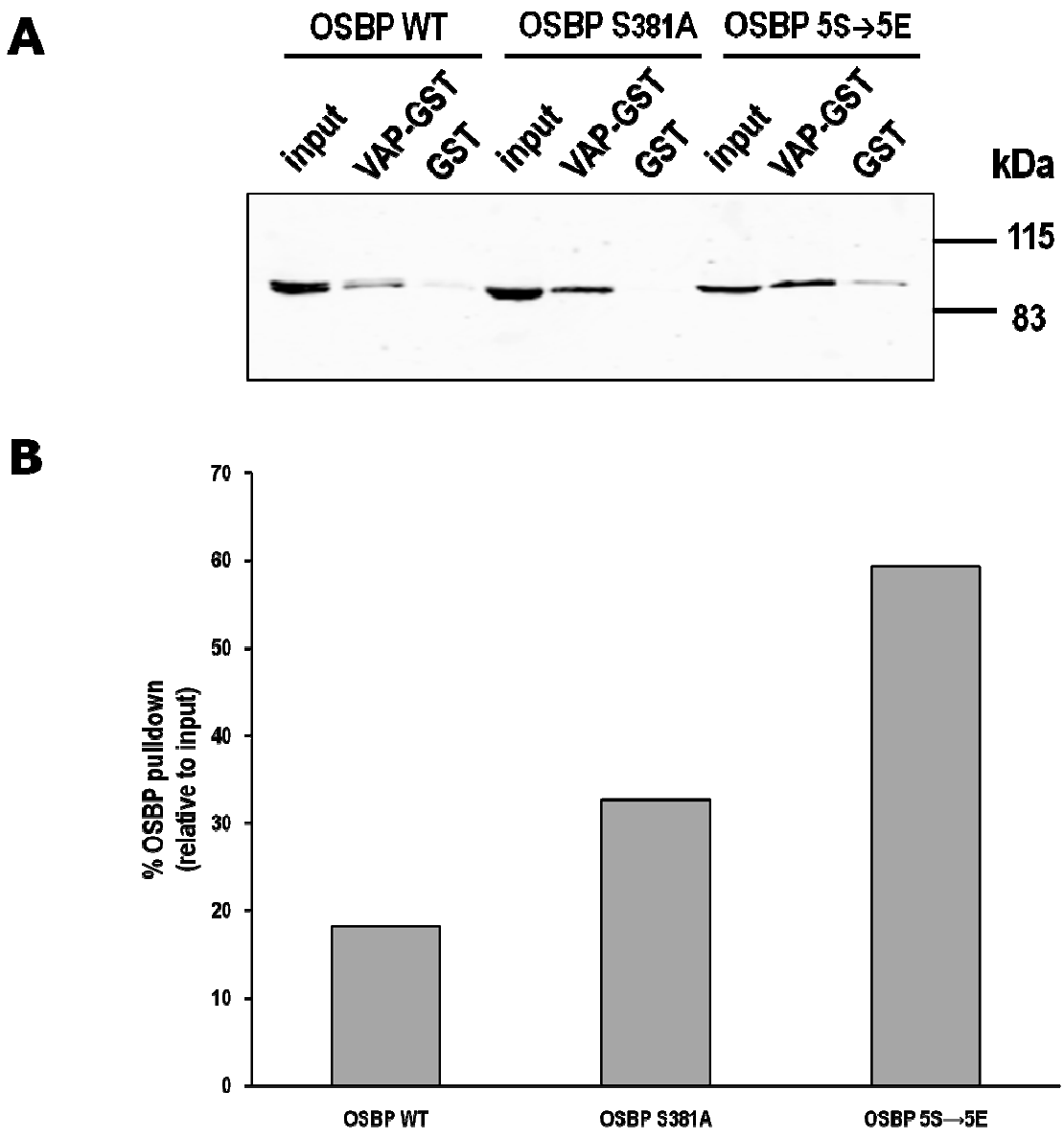


**Figure 3.18. Pulldown of OSBP phosphomutants with VAP-GST.** CHO shOSBP cells were transfected with plasmids encoding OSBP, OSBP S381A, or OSBP 5S→5E for 24 h. Cells were harvested and extracted with 0.5% Triton X-100, and the soluble fraction was incubated with either VAP-GST or GST for 30 min at 20°C. Samples were incubated while shaking with glutathione Sepharose beads for 30 min at 20°C, beads were washed with PBS with Triton X-100, resuspended in SDS gel-loading buffer and heated for 3 min at 90°C. (A) Samples were resolved by 10%-SDS-PAGE, transferred to NC, immunoblotted with OSBP monoclonal antibody and IRDye® conjugated GAM 580LT, and visualized using a LI-COR Odyssey. (B) Quantification of western blots was performed using fluorescence intensity of each of the bands to calculate the percentage of OSBP pulled down of the total input.

# CHAPTER 4 DISCUSSION

Intracellular cholesterol trafficking maintains the distribution of cholesterol within organelle membranes, thereby controlling cholesterol synthesis, uptake and membrane function. How cholesterol is transported inside the cell is still not understood due to the competing roles of vesicular and protein mediated lipid transfer, and the vast number of putative lipid transport proteins. The OSBP gene family of proteins is an excellent group of candidates for sterol transport proteins and was investigated in this study. OSBP and ORPs contain a sterol binding motif and the ability to target to different membranes. The PH domain of OSBP recognizes PI-4-P at the Golgi and the FFAT motif targets OSBP to the ER via an interaction with VAP. OSBP has been shown to extract and transfer cholesterol between liposomes containing PI-4-P [112]. Since cholesterol is synthesized in the cholesterol-poor ER, OSBP could be transferring cholesterol from the ER to the Golgi, from whence it could be distributed to other membranes by vesicular transport and/or other lipid transport proteins.

OSBP could transport sterols by shuttling between the ER and the Golgi apparatus by associating with one membrane at a time or at membrane contact sites (Figure 1.2). Either mode of transport would require some form of regulation to switch OSBP between the two membranes to influence sterol binding. The SRM located between the FFAT motif and the OH domain (Figure 2.1) could be acting in this regard. Originally, this site was identified as S381, 384, and 387 [111]. More recently other residues were identified to be part of this site: T379 and S388 and S391 [137]. A similar phosphorylation motif is found in CERT (Figure 1.4). Phosphorylated CERT localizes to the ER where it binds ceramide and the dephosphorylated form localizes to the Golgi apparatus where it

delivers ceramide [128]. Since OSBP is required for the stimulation of SM synthesis by CERT [116], it would seem likely that the localization of both proteins is controlled by a similar mechanism.

To determine whether phosphorylation of OSBP was affecting its functions, several mutant OSBPs were constructed by substituting glutamate as a phospho-mimic and alanine as a dephospho-mimic (Figure 2.1). Some of these mutants had previously been analyzed by migration on 6%-SDS-PAGE, showing that mutation of S381 to alanine caused an apparent decrease in mass while mutating S381 to glutamate increased apparent mass. Furthermore, mutating S381, 384, and 387 to glutamate residues resulted in the same migration as the S381 to glutamate mutant [111]. These differences in mobility on SDS-PAGE represent the phosphorylated state of OSBP at the SRM; the faster migration is non-phosphorylated OSBP and the slower migration is phosphorylated OSBP. The mutants I generated, OSBP T379A, OSBP 5S→5E and OSBP 6S/T→6E, confirmed these results (Figure 3.1). There was no additional decrease in migration with the OSBP 5S→5E or OSBP 6S/T→6E mutants, both migrated similar to OSBP 3S→3E indicating that they mimicked the phosphorylated protein. However, OSBP T379A did not migrate as one distinct band but instead had a dark lower band and a faint but present upper band (Figure 3.2). This would suggest that T379 phosphorylation is not required for phosphorylation of the SRM.

Similar to CERT there could be a priming phosphorylation site for the subsequent phosphorylation on the downstream CK1 sites. CK1 is thought to be the kinase involved in the phosphorylation of the remaining serine residues due to the sequence surrounding these residues. T379 is not involved in the downstream phosphorylation of serine

residues based on OA inhibition of PP2A (Figure 3.3). Inhibiting PP2A in cells expressing wild type OSBP results in a shift to the upper band of the doublet as the protein becomes progressively phosphorylated [135]. Inhibition of PP2A in cells expressing OSBP T379A shifted mobility to the upper band when analyzed by western blot. However, OSBP S381A remained as a single lower band of the doublet. Since OSBP S381A did not become phosphorylated upon PP2A inhibition, phosphorylation of S381, and not T379, is required to act as the priming phosphorylation site for the phosphorylation of the remaining serine residues by CK1.

When OSBP was analyzed by mass spectrometry it was important to excise the upper and lower bands separately to identify the phospho-peptides that exist in each of the bands. Mass spectrometry analysis revealed that only the non-phosphorylated form of the peptide (TGNSISGASSDVS) was present in the lower band and the phosphorylated forms of the peptide only appeared in the upper band analysis (Figure 3.4B and C). To determine which residues were phosphorylated within the phosphopeptides, MS/MS analysis was performed. The MS/MS spectrum obtained from the non-phosphorylated peptide (Figure 3.5A) was compared with the MS/MS spectrum obtained for the monophosphorylated peptide (Figure 3.5B). There were properties of the peptide that could be exploited in order to determine which residue was phosphorylated: identifying peptide fragments that had gained the mass of a phosphate moiety and examining peptides for the loss of phosphoric acid, known as a neutral loss [137]. Both of these instances were observed when analyzing the monophosphorylated peptide MS/MS spectrum and the fragmentation produced confirmed that S381 was one residue that was phosphorylated.

Unfortunately, the diphosphorylated peptide did not produce a MS/MS spectrum with sufficient resolution to determine the locations of the phosphate residues. There were three distinct peaks in the MS scan that appeared for the monophosphorylated peptide, two weaker peaks that eluted slightly earlier and one strong peak; however only the strong peak produced an MS/MS spectrum of high enough quality to determine the site of the phosphate moiety. These additional monophosphorylated peaks are probably caused by a single phosphate moiety on another residue within the peptide. Since the most intense peak was the one representing phosphorylation at S381 it is likely that it is the major monophosphorylated species within this sequence. Peptides containing more phosphate moieties were not detected by mass spectrometry analysis due to the need for optimization of the technique for these peptides, a different approach involving phospho-enrichment before mass spectrometry analysis or a more sensitive mass spectrometer. All five serine residues have been observed to be phosphorylated at the same time in another mass spectrometry study [138]; however T379 has not been observed to be simultaneously phosphorylated with the serine residues. The data obtained from the mass spectrometry analysis of OSBP supports S381 as the initiating phosphorylation site (Figure 3.3) and the concept that all of the serine residues are phosphorylated under the same conditions.

Since S381 is the first residue to become phosphorylated and is required for the phosphorylation of the downstream serine residues, identification of the kinase responsible for the phosphorylation of S381 was of interest. Using PHOSIDA, it was determined that PKA was a strong potential candidate for the kinase that was phosphorylating S381. The consensus sequence for PKA is RRXS/TY, where X is a

small residue and Y is a hydrophobic residue and arginine may be replaced by a lysine residue [141]. The sequence upstream of S381 fits these requirements with a lysine residue substituted for one of the arginine residues. When cells were treated with a specific PKA inhibitor, there was a decrease in OSBP phosphorylation over time (Figure 3.6 A and B). Since S381 phosphorylation is responsible for the band shift to the upper band of OSBP, these results suggest that PKA is directly or indirectly phosphorylating S381, and furthermore that PKA is the initiating kinase for the downstream phosphorylation activity of CK1.

The phosphorylation of CERT causes a change in its localization, acting as a switch between the Golgi apparatus and the ER. The phosphorylation of OSBP at the SRM could be acting to regulate the movement of OSBP between the Golgi and the ER similar to CERT phosphorylation. Using CERT as a model, the phospho-mimic of OSBP should be localized to the ER and cytoplasm while the dephospho-mimic of OSBP should be localized more to the Golgi. A change in OSBP localization was reported recently when the PKD phosphorylation site of OSBP was analyzed; phosphorylation of OSBP at this site caused a decrease in Golgi localization and fragmentation of the Golgi [133]. When OSBP, OSBP S381A, and OSBP 5S→5E localization were analyzed by immunofluorescence a change in localization of OSBP was not apparent, especially with the addition of 25OH to induce OSBP translocation to the Golgi [103]. This could mean that the phosphorylation of OSBP at the SRM is not affecting the distribution between the ER and Golgi or that phosphorylation of OSBP at other sites, such as the PKD site, is required for a more obvious phenotype. Furthermore, the addition of 25OH to the cell may be overriding any regulatory events induced by phosphorylation.

When OSBP is silenced there is no sterol-dependent stimulation of SM synthesis, which could be restored by expression of OSBP, but not PH, FFAT or OH domain mutants (Figure 3.9A) [116]. If phosphorylation affects OSBP localization there could also be a change in SM synthesis [116]. However, expression of OSBP 5S→5E in OSBP-depleted CHO cells stimulated SM synthesis upon treatment with 25OH. It could be argued that the values for the OSBP 5S→5E mutant and OSBP 6S/T→6E mutant looked slightly attenuated compared to the other mutants, but this was not significant compared to controls or other mutants. Glucosylceramide (Figure 3.9B), ceramide (Figure 3.9C), PS (Figure 3.10A) and PE (Figure 3.10B) were also unaffected by the expression of the different OSBP phosphomutants. Phosphorylation of OSBP at the SRM does not affect OSBP-stimulated SM synthesis and also does not seem to affect OSBP localization (Figure 3.8) with the caveat that 25OH could override phosphorylation-specific regulation.

Phosphorylation could have a role in regulating sterol binding by OSBP via its OH domain. When assayed for binding activity, OSBP 5S→5E had a greater binding capacity for both 25OH and cholesterol, and a greater binding affinity for cholesterol when compared to wild-type OSBP (Figure 3.12). Phosphorylation of OSBP may cause a conformational change to allow easier access of the ligand to the binding pocket of OSBP, specifically for cholesterol. Treatment with 25OH causes OSBP to translocate to the Golgi [103] and since OSBP 5S→5E has a higher binding capacity for 25OH, this could explain the translocation of OSBP seen with the immunofluorescence experiments (Figure 3.8) and the stimulation of SM synthesis (Figure 3.9A). However, cholesterol is the more prevalent molecule in the cell by approximately 1000-fold [8] meaning that

increased binding capacity and affinity for cholesterol by phosphorylated OSBP may be the more physiologically relevant result.

Phosphorylated OSBP binds more cholesterol with higher affinity and therefore could also be transporting more cholesterol between the ER and the Golgi. However, it was first important to determine whether phosphorylated OSBP extracted more cholesterol from liposomes *in vitro*. When assayed for cholesterol extraction from liposomes, OSBP 5S→5E extracted approximately two-fold more cholesterol than OSBP and OSBP S381A (Figure 3.13). Since phosphorylated OSBP has an increased affinity and capacity for cholesterol, the increase in extraction can be attributed to those factors (Figure 3.12). Phosphorylation of OSBP increases extraction of cholesterol from liposomes and therefore could be acting to promote the transfer of cholesterol by increasing loading at ER for transport to the Golgi apparatus.

If phosphorylation of OSBP is increasing cholesterol binding at the ER there may be decreased association of OSBP with the Golgi. This was not apparent with the immunofluorescence experiment (Figure 3.8). However, to test whether phosphorylation affected PH domain association with PI-4-P, the binding of OSBP and OSBP 5S→5E was assayed with liposomes containing PI, PI-4-P, or PI-4,5-$P_2$ (Figure 3.14). There was no difference in OSBP, OSBP S381A and OSBP 5S→5E meaning that SRM phosphorylation status is not affecting the association of the PH domain with PIPs. An increase in binding of the OSBPs occurred in the presence of PI-4-P and PI-4,5-$P_2$ compared to PI. The increase in association with PI-4-P and PI-4,5-$P_2$ was expected since the PH domain of OSBP associates with both PIPs [112] and further confirms that the phosphorylation of OSBP is not interfering with PH domain binding. These results

were supported by the phospholipid overlay assay (Figure 3.15) in which OSBP and OSBP 5S→5E showed similar binding to the immobilized PI-4-P. Binding to PI-4,5-$P_2$ was not observed with either OSBP or OSBP 5S→5E in this experiment, higher concentrations of PI-4,5-$P_2$ may be required to observe binding.

Regulating cholesterol binding to OSBP may be the sole role of phosphorylation of the SRM. However, it may still be playing a role in the regulation of cholesterol transport. To determine the cholesterol transport capacity of OSBP, OSBP S381A and OSBP 5S→5E while avoiding the problem of tethering between liposomes, previously reported with Osh4 [92], a new assay was developed. OSBP, OSBP S381A and OSBP 5S→5E were pre-loaded with [$^3$H]cholesterol and then incubated with liposomes containing PI, PI-4-P or PI-4,5-$P_2$. This ensured that cholesterol associated with the liposomes was not the result of OSBP tethering a cholesterol donating liposome to an acceptor liposome. OSBP 5S→5E transferred approximately 20% less cholesterol to the liposomes than OSBP and OSBP S381A (Figure 3.16). However, the transport observed for each of the OSBPs was the same when PI, PI-4-P and PI-4,5-$P_2$ were included in liposomes. One would expect a difference in transport between the PI liposomes and the PI-4-P and PI-4,5-$P_2$ liposomes since there was an increase in OSBP association with PI-4-P and PI-4,5-$P_2$ in the liposome pelleting assay (Figure 3.14). This change in association with PIPs may not have been observed due to the duration of the assay and the concentration of liposomes present. For OSBP and OSBP S381A, cholesterol transfer reached equilibrium, with approximately 50% of the cholesterol transferred from those OSBPs to the liposomes in 5 min. A shorter incubation time with the liposomes, a decrease in liposome concentration, or the addition of cholesterol to the acceptor

liposomes may be required to accurately assay these values. Moreover, the decrease in transfer of cholesterol by OSBP 5S→5E is independent of PIPs; therefore, phosphorylation of OSBP is affecting cholesterol transport in a PIP-independent manner *in vitro*.

Phosphorylation of OSBP does not affect PH domain association with PI-4-P but the phosphorylation motif is closer to the FFAT motif [111] and therefore could be influencing the association of OSBP with VAP. Phosphorylation of CERT causes it to localize more with the ER through its FFAT motif and VAP [128]; this could be similar to the effect of phosphorylation on OSBP. The interaction of OSBPs with VAP was assayed by two methods, immunoprecipitation (Figure 3.17) and GST-VAP pull-down assays (Figure 3.18). Both assays showed that OSBP 5S→5E was more strongly associated with VAP than OSBP or OSBP S381A. The increase in VAP association would mean that phosphorylated OSBP was more attracted to the ER than dephosphorylated OSBP.

The increased association of phosphorylated OSBP with VAP (Figure 3.17 and 3.18) in combination with its increased binding affinity and capacity (Figure 3.12), as well as its increased extraction (Figure 3.13), imply that phosphorylation of OSBP acts to localize OSBP to the ER for binding of cholesterol. The PIP-independent decrease in cholesterol transfer by OSBP 5S→5E (Figure 3.16) could be another way that the cell facilitates the association of OSBP at the ER and not the Golgi apparatus. Phosphorylation of the SRM of OSBP is catalyzed by PKA (Figure 3.6) and then is likely phosphorylated by CK1. Localization of OSBP is also influenced by phosphorylation by PKD at serine 238 in mouse OSBP [133]. Given this information a model of a role for

OSBP phosphorylation in intracellular cholesterol transport can be created (Figure 4.1). OSBP in a non-phosphorylated and ligand-free state could be localized to the Golgi apparatus where it would be phosphorylated by PKD at S238 and PKA at S381. CK1 would then phosphorylate the S384, 387, 388, and 391, and OSBP would translocate to the ER due to its increased affinity for VAP and the influence of the PKD phosphorylation site. At the ER, OSBP would bind newly synthesized cholesterol. Once cholesterol is bound, dephosphorylation by PP2A could be triggered at both the PKD site and the SRM. Dephosphorylated OSBP could then deliver cholesterol to the Golgi and become re-phosphorylated to return to the ER.

In conclusion, the phosphorylation of OSBP at the SRM is important for regulation of the sterol binding activity of OSBP. Phosphorylation at this site also decreased the release of cholesterol from OSBP *in vitro* and increased the binding of OSBP to VAP. Therefore phosphorylation could facilitate the localization of OSBP to the ER. Phosphorylation of OSBP could help co-ordinate SM and cholesterol levels at the *trans*-Golgi network and possibly cholesterol efflux by ABCA1. OSBP phosphorylation at the SRM and PKD motif provides a reversible control mechanism to facilitate the regulation of cholesterol extraction from the ER.

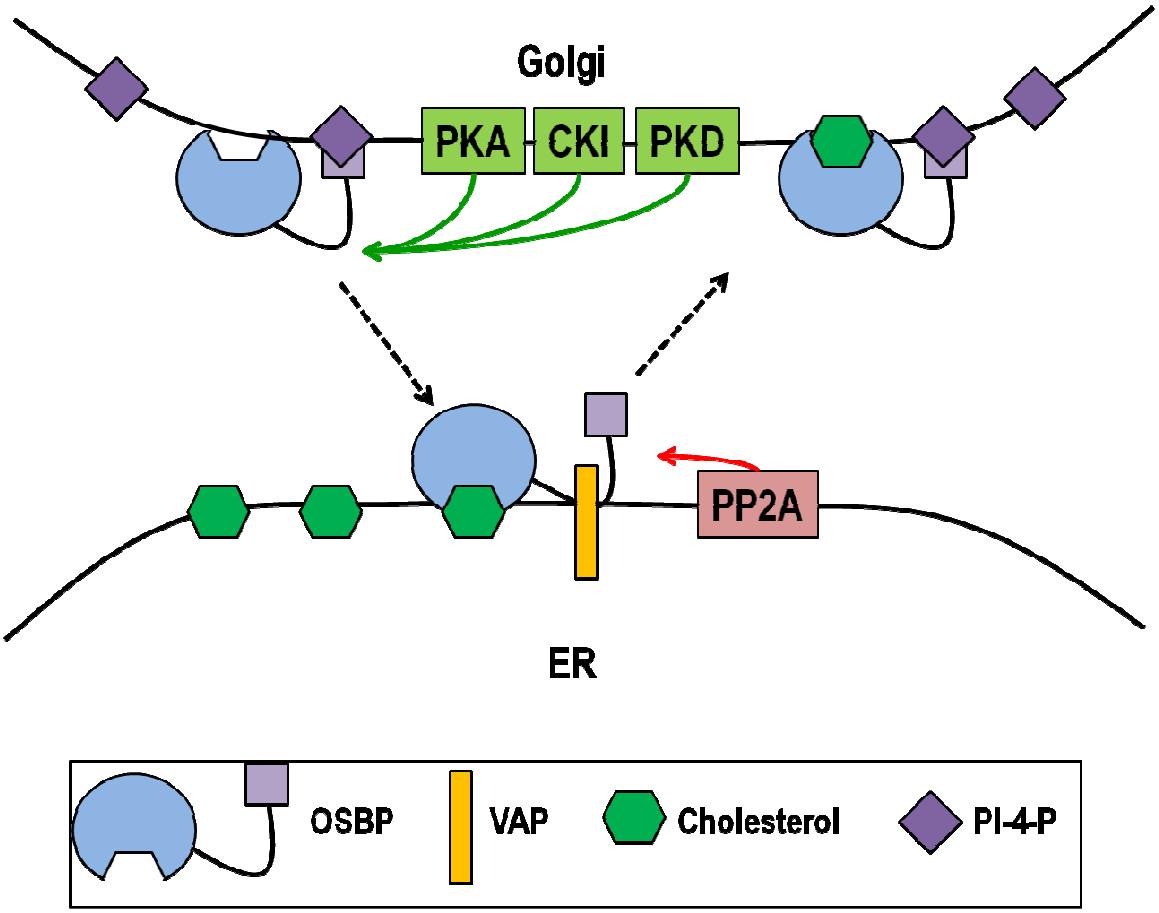


**Figure 4.1. A model for the role of OSBP in cholesterol trafficking.** Phosphorylation of OSBP (green arrows) occurs at the Golgi by PKA, CK1 and PKD. Once phosphorylated OSBP translocates (black arrows) to the ER via its FFAT motif and association with VAP, binds a molecule of cholesterol and is dephosphorylated (red arrow) by PP2A. Dephosphorylated OSBP translocates to the Golgi via its PH domain and association with PI-4-P to deliver cholesterol. There it would be phosphorylated to move back to the ER.

# REFERENCES


1 Maxfield, F. R. and Tabas, I. (2005) Role of cholesterol and lipid organization in disease. Nature. **438**, 612-621

2 Maxfield, F. R. and van Meer, G. (2010) Cholesterol, the central lipid of mammalian cells. Curr Opin Cell Biol. **22**, 422-429

3 Ikonen, E. (2006) Mechanisms for cellular cholesterol transport: Defects and human disease. Physiol Rev. **86**, 1237-1261

4 Mukherjee, S. and Maxfield, F. R. (2004) Membrane domains. Annu Rev Cell Dev Biol. **20**, 839-866

5 Resh, M. D. (1999) Fatty acylation of proteins: New insights into membrane targeting of myristoylated and palmitoylated proteins. Biochim Biophys Acta. **1451**, 1-16

6 Harris, J. R. and Milton, N. G. (2010) Cholesterol in alzheimer's disease and other amyloidogenic disorders. Subcell Biochem. **51**, 47-75

7 Bjorkhem, I. and Diczfalusy, U. (2002) Oxysterols: Friends, foes, or just fellow passengers? Arterioscler Thromb Vasc Biol. **22**, 734-742

8 Babiker, A. and Diczfalusy, U. (1998) Transport of side-chain oxidized oxysterols in the human circulation. Biochim Biophys Acta. **1392**, 333-339

9 Kandutsch, A. A. and Chen, H. W. (1974) Inhibition of sterol synthesis in cultured mouse cells by cholesterol derivatives oxygenated in the side chain. J Biol Chem. **249**, 6057-6061

10 Brown, M. S. and Goldstein, J. L. (1974) Suppression of 3-hydroxy-3-methylglutaryl coenzyme A reductase activity and inhibition of growth of human fibroblasts by 7-ketocholesterol. J Biol Chem. **249**, 7306-7314

11 Bjorkhem, I. (2007) Rediscovery of cerebrosterol. Lipids. **42**, 5-14

12 Danielsson, H., Kalles, I. and Wikvall, K. (1984) Regulation of hydroxylations in biosynthesis of bile acids. isolation of a protein from rat liver cytosol stimulating reconstituted cholesterol 7 alpha-hydroxylase activity. J Biol Chem. **259**, 4258-4262

13 Stiles, A. R., McDonald, J. G., Bauman, D. R. and Russell, D. W. (2009) CYP7B1: One cytochrome P450, two human genetic diseases, and multiple physiological functions. J Biol Chem. **284**, 28485-28489

14 Lund, E. G., Kerr, T. A., Sakai, J., Li, W. and Russell, D. W. (1998) cDNA cloning of mouse and human cholesterol 25-hydroxylases, polytopic membrane proteins that synthesize a potent oxysterol regulator of lipid metabolism. J Biol Chem. **273**, 34316-34327

15 Schwarz, M., Lund, E. G. and Russell, D. W. (1998) Two 7 alpha-hydroxylase enzymes in bile acid biosynthesis. Curr Opin Lipidol. **9**, 113-118

16 Chiang, J. Y. (2004) Regulation of bile acid synthesis: Pathways, nuclear receptors, and mechanisms. J Hepatol. **40**, 539-551

17 Lund, E. G., Guileyardo, J. M. and Russell, D. W. (1999) cDNA cloning of cholesterol 24-hydroxylase , a mediator of cholesterol homeostasis in the brain. Proc Natl Acad Sci USA. **96**, 7238-7243

18 Bjorkhem, I., Diczfalusy, U. and Lutjohann, D. (1999) Removal of cholesterol from extrahepatic sources by oxydative mechanisms. Curr Opin Lipidol. **10**, 161-165

19 McDonald, J. G. and Russell, D. W. (2010) Editorial: 25-hydroxycholesterol: A new life in immunology. J Leukoc Biol. **88**, 1071-1072

20 Faust, J. R., Luskey, K. L., Chin, D. J., Goldstein, J. L. and Brown, M. S. (1982) Regulation of synthesis and degradation of 3-hydroxy-3-methylglutaryl-coenzyme A reductase by low density lipoprotein and 25-hydroxycholesterol in UT-1 cells. Proc Natl Acad Sci USA. **79**, 5205-5209

21 Ecker, J., Liebisch, G., Englmaier, M., Grandl, M., Robenek, H. and Schmitz, G. (2010) Induction of fatty acid synthesis is a key requirement for phagocytic differentiation of human monocytes. Proc Natl Acad Sci USA. **107**, 7817-7822

22 Diczfalusy, U., Olofsson, K. E., Carlsson, A. M., Gong, M., Golenbock, D. T., Rooyackers, O., Flaring, U. and Bjorkbacka, H. (2009) Marked upregulation of cholesterol 25-hydroxylase expression by lipopolysaccharide. J Lipid Res. **50**, 2258-2264

23 Bauman, D. R., Bitmansour, A. D., McDonald, J. G., Thompson, B. M., Liang, G. and Russell, D. W. (2009) 25-hydroxycholesterol secreted by macrophages in response to toll-like receptor activation suppresses immunoglobulin A production. Proc Natl Acad Sci USA. **106**, 16764-16769

24 Park, K. and Scott, A. L. (2010) Cholesterol 25-hydroxylase production by dendritic cells and macrophages is regulated by type I interferons. J Leukoc Biol. **88**, 1081-1087

25 Honda, K. and Taniguchi, T. (2006) IRFs: Master regulators of signalling by toll-like receptors and cytosolic pattern-recognition receptors. Nat Rev Immunol. **6**, 644-658

26 Radhakrishnan, A., Goldstein, J. L., McDonald, J. G. and Brown, M. S. (2008) Switch-like control of SREBP-2 transport triggered by small changes in ER cholesterol: A delicate balance. Cell Metab. **8**, 512-521

27 Blanchette-Mackie, E. J. (2000) Intracellular cholesterol trafficking: Role of the NPC1 protein. Biochim Biophys Acta. **1486**, 171-183

28 Liscum, L. and Munn, N. J. (1999) Intracellular cholesterol transport. Biochim Biophys Acta. **1438**, 19-37

29 Yeagle, P. L. (1985) Cholesterol and the cell membrane Biochim Biophys Acta. **822**, 267-287

30 Hao, M., Lin, S. X., Karylowski, O. J., Wustner, D., McGraw, T. E. and Maxfield, F. R. (2002) Vesicular and non-vesicular sterol transport in living cells. the endocytic recycling compartment is a major sterol storage organelle. J Biol Chem. **277**, 609-617

31 Vainio, S. and Ikonen, E. (2003) Macrophage cholesterol transport: A critical player in foam cell formation. Ann Med. **35**, 146-155

32 Soccio, R. E. and Breslow, J. L. (2004) Intracellular cholesterol transport. Arterioscler Thromb Vasc Biol. **24**, 1150-1160

33 Yang, T., Espenshade, P. J., Wright, M. E., Yabe, D., Gong, Y., Aebersold, R., Goldstein, J. L. and Brown, M. S. (2002) Crucial step in cholesterol homeostasis: Sterols promote binding of SCAP to INSIG-1, a membrane protein that facilitates retention of SREBPs in ER. Cell. **110**, 489-500

34 Brown, A. J., Sun, L., Fermaisco, J. D., Brown, M. S. and Goldstein, J. L. (2002) Cholesterol addition to ER membranes alters conformation of SCAP, the SREBP escort protein that regulates cholesterol metabolism. Mol Cell. **10**, 237-245

35 Goldstein, J. L., DeBose-Boyd, R. A. and Brown, M. S. (2006) Protein sensors for membrane sterols. Cell. **124**, 35-46

36 Espenshade, P. J., Cheng, D., Goldstein, J. L. and Brown, M. S. (1999) Autocatalytic processing of site-1 protease removes propeptide and permits cleavage of sterol regulatory element-binding proteins. J Biol Chem. **274**, 22795-22804

37 Zelenski, N. G., Rawson, R. B., Brown, M. S. and Goldstein, J. L. (1999) Membrane topology of S2P, a protein required for intramembranous cleavage of sterol regulatory element-binding proteins. J Biol Chem. **274**, 21973-21980

38 Sato, R. (2010) Sterol metabolism and SREBP activation. Arch Biochem Biophys. **501**, 177-181

39 Sever, N., Yang, T., Brown, M. S., Goldstein, J. L. and DeBose-Boyd, R. A. (2003) Accelerated degradation of HMG CoA reductase mediated by binding of insig-1 to its sterol-sensing domain. Mol Cell. **11**, 25-33

40 Goldstein, J. L. and Brown, M. S. (2009) The LDL receptor. Arterioscler Thromb Vasc Biol. **29**, 431-438

41 Gil, G., Faust, J. R., Chin, D. J., Goldstein, J. L. and Brown, M. S. (1985) Membrane-bound domain of HMG CoA reductase is required for sterol-enhanced degradation of the enzyme. Cell. **41**, 249-258

42 Brown, M. S., Dana, S. E. and Goldstein, J. L. (1975) Cholesterol ester formation in cultured human fibroblasts. stimulation by oxygenated sterols. J Biol Chem. **250**, 4025-4027

43 Proctor, S. D., Vine, D. F. and Mamo, J. C. (2002) Arterial retention of apolipoprotein B(48)- and B(100)-containing lipoproteins in atherogenesis. Curr Opin Lipidol. **13**, 461-470

44 Qiao, J. H., Tripathi, J., Mishra, N. K., Cai, Y., Tripathi, S., Wang, X. P., Imes, S., Fishbein, M. C., Clinton, S. K., Libby, P., Lusis, A. J. and Rajavashisth, T. B. (1997) Role of macrophage colony-stimulating factor in atherosclerosis: Studies of osteopetrotic mice. Am J Pathol. **150**, 1687-1699

45 Glass, C. K. and Witztum, J. L. (2001) Atherosclerosis: the road ahead. Cell. **104**, 503-516

46 Goldstein, J. L., Ho, Y. K., Basu, S. K. and Brown, M. S. (1979) Binding site on macrophages that mediates uptake and degradation of acetylated low density lipoprotein, producing massive cholesterol deposition. Proc Natl Acad Sci USA. **76**, 333-337

47 Nicholson, A. C., Han, J., Febbraio, M., Silversterin, R. L. and Hajjar, D. P. (2001) Role of CD36, the macrophage class B scavenger receptor, in atherosclerosis. Ann NY Acad Sci. **947**, 224-228

48 Nicholls, S. J., Rye, K. A. and Barter, P. J. (2005) High-density lipoproteins as therapeutic targets. Curr Opin Lipidol. **16**, 345-349

49 Shamburek, R., Pentchev, P., Zech, L., Blanchette-Mackie, J., Carstea, E., VandenBroek, J., Cooper, P., Neufeld, E., Phair, R., Brewer, H.,Jr, Brady, R. and Schwartz, C. (1997) Intracellular trafficking of the free cholesterol derived from LDL cholesteryl ester is defective in vivo in Niemann-Pick C disease: Insights on normal metabolism of HDL and LDL gained from the NP-C mutation. J Lipid Res. **38**, 2422-2435

50 Ikonen, E. and Holtta-Vuori, M. (2004) Cellular pathology of Niemann-Pick type C disease. Semin Cell Dev Biol. **15**, 445-454

51 Maxfield, F. R. and Mondal, M. (2006) Sterol and lipid trafficking in mammalian cells. Biochem Soc Trans. **34**, 335-339

52 Brugger, B., Sandhoff, R., Wegehingel, S., Gorgas, K., Malsam, J. and Helms, J. B. (2000) Evidence for segregation of sphingomyelin and cholesterol during formation of COPI-coated vesicles. J Cell Biol. **151**, 507-518

53 Klemm, R. W., Ejsing, C. S., Surma, M. A., Kaiser, H. J., Gerl, M. J., Sampaio, J. L., de Robillard, Q., Ferguson, C., Proszynski, T. J., Shevchenko, A. and Simons, K. (2009) Segregation of sphingolipids and sterols during formation of secretory vesicles at the trans-Golgi network. J Cell Biol. **185**, 601-612

54 Heino, S., Lusa, S., Somerharju, P., Ehnholm, C., Olkkonen, V. and Ikonen, E. (2000) Dissecting the role of the Golgi complex and lipid rafts in biosynthetic transport of cholesterol to the cell surface. Proc Natl Acad Sci USA. **97**, 8375-8380

55 Hao, M., Lin, S. X., Karylowski, O. J., Wustner, D., McGraw, T. E. and Maxfield, F. R. (2002) Vesicular and non-vesicular sterol transport in living cells. The endocytic recycling compartment is a major sterol storage organelle. J Biol Chem. **277**, 609-617

56 Prinz, W. A. (2007) Non-vesicular sterol transport in cells. Prog Lipid Res. **46**, 297-314

57 Murphy, D. J. and Vance, J. (1999) Mechanisms of lipid-body formation. Trends Biochem Sci. **24**, 109-115

58 Wüstner, D., Mondal, M., Tabas, I. and Maxfield, F. R. (2005) Direct observation of rapid internalization and intracellular transport of sterol by macrophage foam cells. Traffic. **6**, 396-412

59 Levine, T. and Loewen, C. (2006) Inter-organelle membrane contact sites: Through a glass, darkly. Curr Opin Cell Biol. **18**, 371-378

60 Holthuis, J. C. and Levine, T. P. (2005) Lipid traffic: Floppy drives and a superhighway. Nat Rev Mol Cell Biol. **6**, 209-220

61 Filippin, L., Magalhaes, P. J., Di Benedetto, G., Colella, M. and Pozzan, T. (2003) Stable interactions between mitochondria and endoplasmic reticulum allow rapid accumulation of calcium in a subpopulation of mitochondria. J Biol Chem. **278**, 39224-39234

62 Pichler, H., Gaigg, B., Hrastnik, C., Achleitner, G., Kohlwein, S. D., Zellnig, G., Perktold, A. and Daum, G. (2001) A subfraction of the yeast endoplasmic reticulum associates with the plasma membrane and has a high capacity to synthesize lipids. Eur J Biochem. **268**, 2351-2361

63 Lavigne, P., Najmanivich, R. and Lehoux, J. G. (2010) Mammalian StAR-related lipid transfer (START) domains with specificity for cholesterol: Structural conservation and mechanism of reversible binding. Subcell Biochem. **51**, 425-437

64 Kallen, C. B., Billheimer, J. T., Summers, S. A., Stayrook, S. E., Lewis, M. and Strauss, J. F.,3rd. (1998) Steroidogenic acute regulatory protein (StAR) is a sterol transfer protein. J Biol Chem. **273**, 26285-26288

65 Tsujishita, Y. and Hurley, J. H. (2000) Structure and lipid transport mechanism of a StAR-related domain. Nat Struct Biol. **7**, 408-414

66 Zhang, M., Liu, P., Dwyer, N. K., Christenson, L. K., Fujimoto, T., Martinez, F., Comly, M., Hanover, J. A., Blanchette-Mackie, E. J. and Strauss, J. F.,3rd. (2002) MLN64 mediates mobilization of lysosomal cholesterol to steroidogenic mitochondria. J Biol Chem. **277**, 33300-33310

67 Kishida, T., Kostetskii, I., Zhang, Z., Martinez, F., Liu, P., Walkley, S. U., Dwyer, N. K., Blanchette-Mackie, E. J., Radice, G. L. and Strauss, J. F.,3rd. (2004) Targeted mutation of the MLN64 START domain causes only modest alterations in cellular sterol metabolism. J Biol Chem. **279**, 19276-19285

68 Hanada, K., Kumagai, K., Yasuda, S., Miura, Y., Kawano, M., Fukasawa, M. and Nishijima, M. (2003) Molecular machinery for non-vesicular trafficking of ceramide. Nature. **426**, 803-809

69 Levine, T. (2004) Short-range intracellular trafficking of small molecules across endoplasmic reticulum junctions. Trends Cell Biol. **14**, 483-490

70 Perry, R. J. and Ridgway, N. D. (2005) Molecular mechanisms and regulation of ceramide transport. Biochim Biophys Acta. **1734**, 220-234

71 Tall, A. R., Yvan-Charvet, L., Terasaka, N., Pagler, T. and Wang, N. (2008) HDL, ABC transporters, and cholesterol efflux: Implications for the treatment of atherosclerosis. Cell Metab. **7**, 365-375

72 Schmitz, G. and Buechler, C. (2002) ABCA1: Regulation, trafficking and association with heteromeric proteins. Ann Med. **34**, 334-347

73 Infante, R. E., Abi-Mosleh, L., Radhakrishnan, A., Dale, J. D., Brown, M. S. and Goldstein, J. L. (2008) Purified NPC1 protein. I. binding of cholesterol and oxysterols to a 1278-amino acid membrane protein. J Biol Chem. **283**, 1052-1063

74 Infante, R. E., Radhakrishnan, A., Abi-Mosleh, L., Kinch, L. N., Wang, M. L., Grishin, N. V., Goldstein, J. L. and Brown, M. S. (2008) Purified NPC1 protein: II. localization of sterol binding to a 240-amino acid soluble luminal loop. J Biol Chem. **283**, 1064-1075

75 Ohgami, N., Ko, D. C., Thomas, M., Scott, M. P., Chang, C. C. and Chang, T. Y. (2004) Binding between the Niemann-Pick C1 protein and a photoactivatable cholesterol analog requires a functional sterol-sensing domain. Proc Natl Acad Sci USA. **101**, 12473-12478

76 Xu, Z., Farver, W., Kodukula, S. and Storch, J. (2008) Regulation of sterol transport between membranes and NPC2. Biochemistry. **47**, 11134-11143

77 Kwon, H. J., Abi-Mosleh, L., Wang, M. L., Deisenhofer, J., Goldstein, J. L., Brown, M. S. and Infante, R. E. (2009) Structure of N-terminal domain of NPC1 reveals distinct subdomains for binding and transfer of cholesterol. Cell. **137**, 1213-1224

78 Xu, S., Benoff, B., Liou, H. L., Lobel, P. and Stock, A. M. (2007) Structural basis of sterol binding by NPC2, a lysosomal protein deficient in Niemann-Pick type C2 disease. J Biol Chem. **282**, 23525-23531

79 Gallegos, A. M., Atshaves, B. P., Storey, S. M., Starodub, O., Petrescu, A. D., Huang, H., McIntosh, A. L., Martin, G. G., Chao, H., Kier, A. B. and Schroeder, F. (2001) Gene structure, intracellular localization, and functional roles of sterol carrier protein-2. Prog Lipid Res. **40**, 498-563

80 Seedorf, U., Ellinghaus, P. and Roch Nofer, J. (2000) Sterol carrier protein-2. Biochim Biophys Acta. **1486**, 45-54

81 Keller, G. A., Scallen, T. J., Clarke, D., Maher, P. A., Krisans, S. K. and Singer, S. J. (1989) Subcellular localization of sterol carrier protein-2 in rat hepatocytes: Its primary localization to peroxisomes. J Cell Biol. **108**, 1353-1361

82 Puglielli, L., Rigotti, A., Amigo, L., Nunez, L., Greco, A. V., Santos, M. J. and Nervi, F. (1996) Modulation of intrahepatic cholesterol trafficking: Evidence by in vivo antisense treatment for the involvement of sterol carrier protein-2 in newly synthesized cholesterol transport into rat bile. Biochem. J. **317** ( Pt 3), 681-687

83 Lehto, M., Laitinen, S., Chinetti, G., Johansson, M., Ehnholm, C., Staels, B., Ikonen, E. and Olkkonen, V. M. (2001) The OSBP-related protein family in humans. J Lipid Res. **42**, 1203-1213

84 Ngo, M. H., Colbourne, T. R. and Ridgway, N. D. (2010) Functional implications of sterol transport by the oxysterol-binding protein gene family. Biochem J. **429**, 13-24

85 Laitinen, S., Olkkonen, V. M., Ehnholm, C. and Ikonen, E. (1999) Family of human oxysterol binding protein (OSBP) homologues. A novel member implicated in brain sterol metabolism. J Lipid Res. **40**, 2204-2211

86 Anniss, A. M., Apostolopoulos, J., Dworkin, S., Purton, L. E. and Sparrow, R. L. (2002) An oxysterol-binding protein family identified in the mouse DNA. Cell Biol. **21**, 571-580

87 Wang, C., JeBailey, L. and Ridgway, N. D. (2002) Oxysterol-binding-protein (OSBP)-related protein 4 binds 25-hydroxycholesterol and interacts with vimentin intermediate filaments. Biochem J. **361**, 461-472

88 Lehto, M., Tienari, J., Lehtonen, S., Lehtonen, E. and Olkkonen, V. M. (2004) Subfamily III of mammalian oxysterol-binding protein (OSBP) homologues: The expression and intracellular localization of ORP3, ORP6, and ORP7. Cell Tissue Res. **315**, 39-57

89 Beh, C. T., Cool, L., Phillips, J. and Rine, J. (2001) Overlapping functions of the yeast oxysterol-binding protein homologues. Genetics. **157**, 1117-1140

90 Im, Y. J., Raychaudhuri, S., Prinz, W. A. and Hurley, J. H. (2005) Structural mechanism for sterol sensing and transport by OSBP-related proteins. Nature. **437**, 154-158

91 Drin, G., Casella, J. F., Gautier, R., Boehmer, T., Schwartz, T. U. and Antonny, B. (2007) A general amphipathic alpha-helical motif for sensing membrane curvature. Nat Struct Mol Biol. **14**, 138-146

92 Schulz, T. A., Choi, M. G., Raychaudhuri, S., Mears, J. A., Ghirlando, R., Hinshaw, J. E. and Prinz, W. A. (2009) Lipid-regulated sterol transfer between closely apposed membranes by oxysterol-binding protein homologues. J Cell Biol. **187**, 889-903

93 Levine, T. P. and Munro, S. (2002) Targeting of Golgi-specific pleckstrin homology domains involves both PtdIns 4-kinase-dependent and -independent components. Curr Biol. **12**, 695-704

94 Levine, T. P. and Munro, S. (2001) Dual targeting of Osh1p, a yeast homologue of oxysterol-binding protein, to both the Golgi and the nucleus-vacuole junction. Mol Biol Cell. **12**, 1633-1644

95 Roy, A. and Levine, T. P. (2004) Multiple pools of phosphatidylinositol 4-phosphate detected using the pleckstrin homology domain of Osh2p. J Biol Chem. **279**, 44683-44689

96 Li, X., Rivas, M. P., Fang, M., Marchena, J., Mehrotra, B., Chaudhary, A., Feng, L., Prestwich, G. D. and Bankaitis, V. A. (2002) Analysis of oxysterol binding protein homologue Kes1p function in regulation of Sec14p-dependent protein transport from the yeast Golgi complex. J Cell Biol. **157**, 63-77

97 Raychaudhuri, S., Im, Y. J., Hurley, J. H. and Prinz, W. A. (2006) Nonvesicular sterol movement from plasma membrane to ER requires oxysterol-binding protein-related proteins and phosphoinositides. J Cell Biol. **173**, 107-119

98 Wang, P., Duan, W., Munn, A. L. and Yang, H. (2005) Molecular characterization of Osh6p, an oxysterol binding protein homolog in the yeast saccharomyces cerevisiae. FEBS J. **272**, 4703-4715

99 Loewen, C. J., Roy, A. and Levine, T. P. (2003) A conserved ER targeting motif in three families of lipid binding proteins and in Opi1p binds VAP. EMBO J. **22**, 2025-2035

100 Sullivan, D. P., Ohvo-Rekila, H., Baumann, N. A., Beh, C. T. and Menon, A. K. (2006) Sterol trafficking between the endoplasmic reticulum and plasma membrane in yeast. Biochem Soc Trans. **34**, 356-358

101 Beh, C. T., Alfaro, G., Duamel, G., Sullivan, D. P., Kersting, M. C., Dighe, S., Kozminski, K. G. and Menon, A. K. (2009) Yeast oxysterol-binding proteins: Sterol transporters or regulators of cell polarization? Mol Cell Biochem. **326**, 9-13

102 Dawson, P. A., Ridgway, N. D., Slaughter, C. A., Brown, M. S. and Goldstein, J. L. (1989) cDNA cloning and expression of oxysterol-binding protein, an oligomer with a potential leucine zipper. J Biol Chem. **264**, 16798-16803

103 Ridgway, N. D., Dawson, P. A., Ho, Y. K., Brown, M. S. and Goldstein, J. L. (1992) Translocation of oxysterol binding protein to Golgi apparatus triggered by ligand binding. J Cell Biol. **116**, 307-319

104 Wyles, J. P., Perry, R. J. and Ridgway, N. D. (2007) Characterization of the sterol-binding domain of oxysterol-binding protein (OSBP)-related protein 4 reveals a novel role in vimentin organization. Exp Cell Res. **313**, 1426-1437

105 Suchanek, M., Hynynen, R., Wohlfahrt, G., Lehto, M., Johansson, M., Saarinen, H., Radzikowska, A., Thiele, C. and Olkkonen, V. M. (2007) The mammalian oxysterol-binding protein-related proteins (ORPs) bind 25-hydroxycholesterol in an evolutionarily conserved pocket. Biochem J. **405**, 473-480

106 Hynynen, R., Suchanek, M., Spandl, J., Back, N., Thiele, C. and Olkkonen, V. M. (2009) OSBP-related protein 2 is a sterol receptor on lipid droplets that regulates the metabolism of neutral lipids. J Lipid Res. **50**, 1305-1315

107 Yan, D., Jauhiainen, M., Hildebrand, R. B., Willems van Dijk, K., Van Berkel, T. J., Ehnholm, C., Van Eck, M. and Olkkonen, V. M. (2007) Expression of human OSBP-related protein 1L in macrophages enhances atherosclerotic lesion development in LDL receptor-deficient mice. Arterioscler Thromb Vasc Biol. **27**, 1618-1624

108 Yan, D., Mayranpaa, M. I., Wong, J., Perttila, J., Lehto, M., Jauhiainen, M., Kovanen, P. T., Ehnholm, C., Brown, A. J. and Olkkonen, V. M. (2008) OSBP-related protein 8 (ORP8) suppresses ABCA1 expression and cholesterol efflux from macrophages. J Biol Chem. **283**, 332-340

109 Lehto, M., Hynynen, R., Karjalainen, K., Kuismanen, E., Hyvarinen, K. and Olkkonen, V. M. (2005) Targeting of OSBP-related protein 3 (ORP3) to endoplasmic reticulum and plasma membrane is controlled by multiple determinants. Exp Cell Res. **310**, 445-462

110 Johansson, M., Lehto, M., Tanhuanpaa, K., Cover, T. L. and Olkkonen, V. M. (2005) The oxysterol-binding protein homologue ORP1L interacts with Rab7 and alters functional properties of late endocytic compartments. Mol Biol Cell. **16**, 5480-5492

111 Mohammadi, A., Perry, R. J., Storey, M. K., Cook, H. W., Byers, D. M. and Ridgway, N. D. (2001) Golgi localization and phosphorylation of oxysterol binding protein in Niemann-Pick C and U18666A-treated cells. J Lipid Res. **42**, 1062-1071

112 Ngo, M. and Ridgway, N. D. (2009) Oxysterol binding protein-related protein 9 (ORP9) is a cholesterol transfer protein that regulates Golgi structure and function. Mol Biol Cell. **20**, 1388-1399

113 Laitinen, S., Lehto, M., Lehtonen, S., Hyvarinen, K., Heino, S., Lehtonen, E., Ehnholm, C., Ikonen, E. and Olkkonen, V. M. (2002) ORP2, a homolog of oxysterol binding protein, regulates cellular cholesterol metabolism. J Lipid Res. **43**, 245-255

114 Wang, P. Y., Weng, J. and Anderson, R. G. (2005) OSBP is a cholesterol-regulated scaffolding protein in control of ERK 1/2 activation. Science. **307**, 1472-1476

115 Wang, P. Y., Weng, J., Lee, S. and Anderson, R. G. (2008) The N terminus controls sterol binding while the C terminus regulates the scaffolding function of OSBP. J Biol Chem. **283**, 8034-8045

116 Perry, R. J. and Ridgway, N. D. (2006) Oxysterol-binding protein and vesicle-associated membrane protein-associated protein are required for sterol-dependent activation of the ceramide transport protein. Mol Biol Cell. **17**, 2604-2616

117 Lagace, T. A., Byers, D. M., Cook, H. W. and Ridgway, N. D. (1999) Chinese hamster ovary cells overexpressing the oxysterol binding protein (OSBP) display enhanced synthesis of sphingomyelin in response to 25-hydroxycholesterol. J Lipid Res. **40**, 109-116

118 Banerji, S., Ngo, M., Lane, C. F., Robinson, C. A., Minogue, S. and Ridgway, N. D. (2010) Oxysterol binding protein-dependent activation of sphingomyelin synthesis in the Golgi apparatus requires phosphatidylinositol 4-kinase IIalpha. Mol Biol Cell. **21**, 4141-4150

119 Bowden, K. and Ridgway, N. D. (2008) OSBP negatively regulates ABCA1 protein stability. J Biol Chem. **283**, 18210-18217

120 Tamehiro, N., Zhou, S., Okuhira, K., Benita, Y., Brown, C. E., Zhuang, D. Z., Latz, E., Hornemann, T., von Eckardstein, A., Xavier, R. J., Freeman, M. W. and Fitzgerald, M. L. (2008) SPTLC1 binds ABCA1 to negatively regulate trafficking and cholesterol efflux activity of the transporter. Biochemistry. **47**, 6138-6147

121 Lessmann, E., Ngo, M., Leitges, M., Minguet, S., Ridgway, N. D. and Huber, M. (2007) Oxysterol-binding protein-related protein (ORP) 9 is a PDK-2 substrate and regulates akt phosphorylation. Cell Signal. **19**, 384-392

122 Perttila, J., Merikanto, K., Naukkarinen, J., Surakka, I., Martin, N. W., Tanhuanpaa, K., Grimard, V., Taskinen, M. R., Thiele, C., Salomaa, V., Jula, A., Perola, M., Virtanen, I., Peltonen, L. and Olkkonen, V. M. (2009) OSBPL10, a novel candidate gene for high triglyceride trait in dyslipidemic finnish subjects, regulates cellular lipid metabolism. J Mol Med. **87**, 825-835

123 Evans, R. M. (1994) Intermediate filaments and lipoprotein cholesterol. Trends Cell Biol. **4**, 149-151

124 Sarria, A. J., Panini, S. R. and Evans, R. M. (1992) A functional role for vimentin intermediate filaments in the metabolism of lipoprotein-derived cholesterol in human SW-13 cells. J Biol Chem. **267**, 19455-19463

125 Johansson, M., Rocha, N., Zwart, W., Jordens, I., Janssen, L., Kuijl, C., Olkkonen, V. M. and Neefjes, J. (2007) Activation of endosomal dynein motors by stepwise assembly of Rab7-RILP-p150Glued, ORP1L, and the receptor betalll spectrin. J Cell Biol. **176**, 459-471

126 Rocha, N., Kuijl, C., van der Kant, R., Janssen, L., Houben, D., Janssen, H., Zwart, W. and Neefjes, J. (2009) Cholesterol sensor ORP1L contacts the ER protein VAP to control Rab7-RILP-p150 glued and late endosome positioning. J Cell Biol. **185**, 1209-1225

127 Lehto, M., Mayranpaa, M. I., Pellinen, T., Ihalmo, P., Lehtonen, S., Kovanen, P. T., Groop, P. H., Ivaska, J. and Olkkonen, V. M. (2008) The R-ras interaction partner ORP3 regulates cell adhesion. J Cell Sci. **121**, 695-705

128 Kumagai, K., Kawano, M., Shinkai-Ouchi, F., Nishijima, M. and Hanada, K. (2007) Interorganelle trafficking of ceramide is regulated by phosphorylation-dependent cooperativity between the PH and START domains of CERT. J Biol Chem. **282**, 17758-17766

129 Fugmann, T., Hausser, A., Schoffler, P., Schmid, S., Pfizenmaier, K. and Olayioye, M. A. (2007) Regulation of secretory transport by protein kinase D-mediated phosphorylation of the ceramide transfer protein. J Cell Biol. **178**, 15-22

130 Tomishige, N., Kumagai, K., Kusuda, J., Nishijima, M. and Hanada, K. (2009) Casein kinase I{gamma}2 down-regulates trafficking of ceramide in the synthesis of sphingomyelin. Mol Biol Cell. **20**, 348-357

131 Saito, S., Matsui, H., Kawano, M., Kumagai, K., Tomishige, N., Hanada, K., Echigo, S., Tamura, S. and Kobayashi, T. (2008) Protein phosphatase 2Cepsilon is an endoplasmic reticulum integral membrane protein that dephosphorylates the ceramide transport protein CERT to enhance its association with organelle membranes. J Biol Chem. **283**, 6584-6593

132 Choudhary, C., Kumar, C., Gnad, F., Nielsen, M. L., Rehman, M., Walther, T. C., Olsen, J. V. and Mann, M. (2009) Lysine acetylation targets protein complexes and co-regulates major cellular functions. Science. **325**, 834-840

133 Nhek, S., Ngo, M., Yang, X., Ng, M. M., Field, S. J., Asara, J. M., Ridgway, N. D. and Toker, A. (2010) Regulation of oxysterol-binding protein Golgi localization through protein kinase D-mediated phosphorylation. Mol Biol Cell. **21**, 2327-2337

134 Ridgway, N. D., Lagace, T. A., Cook, H. W. and Byers, D. M. (1998) Differential effects of sphingomyelin hydrolysis and cholesterol transport on oxysterol-binding protein phosphorylation and Golgi localization. J Biol Chem. **273**, 31621-31628

135 Ridgway, N. D., Badiani, K., Byers, D. M. and Cook, H. W. (1998) Inhibition of phosphorylation of the oxysterol binding protein by brefeldin A. Biochim Biophys Acta. **1390**, 37-51

136 Dephoure, N., Zhou, C., Villen, J., Beausoleil, S. A., Bakalarski, C. E., Elledge, S. J. and Gygi, S. P. (2008) A quantitative atlas of mitotic phosphorylation. Proc Natl Acad Sci USA. **105**, 10762-10767

137 Gauci, S., Helbig, A. O., Slijper, M., Krijgsveld, J., Heck, A. J. and Mohammed, S. (2009) Lys-N and trypsin cover complementary parts of the phosphoproteome in a refined SCX-based approach. Anal Chem. **81**, 4493-4501

138 Zahedi, R. P., Lewandrowski, U., Wiesner, J., Wortelkamp, S., Moebius, J., Schutz, C., Walter, U., Gambaryan, S. and Sickmann, A. (2008) Phosphoproteome of resting human platelets. J Proteome Res. **7**, 526-534

139 Gnad, F., Ren, S., Cox, J., Olsen, J. V., Macek, B., Oroshi, M. and Mann, M. (2007) PHOSIDA (phosphorylation site database): Management, structural and evolutionary investigation, and prediction of phosphosites. Genome Biol. **8**, R250

140 Zhou, Y., Li, S., Mayranpaa, M. I., Zhong, W., Back, N., Yan, D. and Olkkonen, V. M. (2010) OSBP-related protein 11 (ORP11) dimerizes with ORP9 and localizes at the Golgi-late endosome interface. Exp Cell Res. **316**, 3304-3316

141 Griffioen, G. and Thevelein, J. M. (2002) Molecular mechanisms controlling the localisation of protein kinase A. Curr Genet. **41**, 199-207

142 Lowry, O. H., Rosebrough, N. J., Farr, A. L. and Randall, R. J. (1951) Protein measurement with the folin phenol reagent. J Biol Chem. **193**, 265-275

143 Perry, R. J. and Ridgway, N. D. (2004) The role of de novo ceramide synthesis in the mechanism of action of the tricyclic xanthate D609. J Lipid Res. **45**, 164-173

144 Kandutsch, A. A. and Shown, E. P. (1981) Assay of oxysterol-binding protein in a mouse fibroblast, cell-free system. dissociation constant and other properties of the system. J Biol Chem. **256**, 13068-13073

145 Datta, S. and Desarnaud, F. (2010) Protein kinase A in the pedunculopontine tegmental nucleus of rat contributes to regulation of rapid eye movement sleep. J Neurosci. **30**, 12263-12273

146 Wyles, J. P., McMaster, C. R. and Ridgway, N. D. (2002) Vesicle-associated membrane protein-associated protein-A (VAP-A) interacts with the oxysterol-binding protein to modify export from the endoplasmic reticulum. J Biol Chem. **277**, 29908-29918